Propylene Polymerization in a Circulating Slugging Fluidized Bed Reactor

Inge van Putten

PROPYLENE POLYMERIZATION IN A CIRCULATING SLUGGING FLUIDIZED BED REACTOR

PROEFSCHRIFT

ter verkrijging van
de graad van doctor aan de Universiteit Twente,
op gezag van de rector magnificus,
prof. dr. F.A. van Vught,
volgens besluit van het College voor Promoties
in het openbaar te verdedigen
op donderdag 10 juni 2004 om 15.00 uur

door

Inge Cornelia van Putten

geboren op 6 januari 1975
te Medemblik

Dit proefschrift is goedgekeurd door de promotor

Prof. dr. –ing. habil. G. Weickert

Contents

Summary

Polyolefins have become one of the most important plastics in the world. Continuous improvement of catalysts and processes caused the variety of different grades of polyolefins produced and with that the variety of possible applications to increase largely. Together with the low prices of these polymers it has led to a huge growth rate of the annual worldwide production capacity for polyolefins. The most important polypropylene polymerization processes are nowadays executed in liquid or in gas phase or a combination of both. Only few experimentally verified studies on these liquid and gas phase processes have however been published.

One of the newest developments in gas phase processes is the Basell multizone reactor, comprising of a riser and a downcomer tube, thereby creating a circulating fluidized bed, or multiple tubes. Powder is transported through the different tubes by a transporting fluidization regime (the gas blows out the particles) or for instance by gravity in a moving bed. In each tube reaction conditions can be different, offering an even wider variety of products to be produced. Products can be a mixture of different polypropylene grades within one product particle. No experimental data are available in the open literature about the polymerization in these different reaction zones.

The work presented in this thesis is concerned with research on the riser of a circulating fluidized bed system for olefin polymerization. In the riser section, fluidization takes place in the transporting slugging mode and polymer particles are produced in the riser in a non-isothermal way. Properties of the polymerization reaction and of the hydrodynamics were studied and their behavior with respect to conditions in the reactor were described. A reactor model was constructed that accurately describes the polymerization process in the circulating slugging fluidized bed. Elements in the reactor model are fluidization, heat transfer and kinetics of the used catalyst system. For heat transfer relations from the open literature are taken. Sorption of monomer into the polypropylene is not considered in the reactor model.

Fluidization behavior

The slugging fluidization regime ($0.6 < u_g < 1.0$ m/s) in a bed of particles with a very wide size distribution was studied intensively. Residence time and residence time distribution of particles in the riser, as well as segregation and raining of particles were studied to gain insight into the mixing behavior in the riser of a circulating fluidized bed. The mixing of solids could be varied from that of a well-mixed system to plug flow by changing the solids flux and the gas velocity. This feature of the slugging fluidization regime offers a potentially large window of operation for the polymerization reactor.
Segregation of particles according to size difference was found to be able to partly explain the broadness of the distribution. A difference in relative velocity through the bed between large and small particles could be measured. In this way, relatively easy segregation experiments can be used as a tool to estimate the broadness of the residence time distribution.

Plug velocities and plug lengths were determined as function of riser diameter, particle size distribution, gas velocity and solids flux. Plug lengths are dependent on the riser diameter and the gas velocity. A new relation was derived for the calculation of plug velocities in which the plug length is an important parameter, in contrast to relations presented in the open literature. With the new relation plug velocities can be calculated for a wide variety of process conditions.

Propylene polymerization

An experimental program to study kinetics of the gas phase propylene polymerization was performed. Polymerization in gas phase was preceded by a prepolymerization step in liquid phase. The step from liquid phase prepolymerization to gas phase main polymerization was studied for its effects on the polymerization in the gas phase. The reaction rate in the gas phase polymerization after a depressurization of the reactor at the end of prepolymerization was found to be only 50% of the reaction rate in the gas phase polymerization after a prepolymerization without depressurization. Several possible explanations such as poisoning of the catalyst, natural deactivation of the catalyst in time, change in concentration of cocatalyst or external donor were experimentally investigated. They could not explain the phenomenon. It was suggested that crystallization of the polymer might play a role in the lowering of the activity.

After prepolymerization in liquid phase propylene, the reactive bed preparation, the gas phase polymerization or main polymerization takes place. Kinetics of the polymerization reaction were studied in the gas phase with propylene and hydrogen. A relation between initial activity in the gas phase and hydrogen concentration was determined. The initial activity with 1.1 mol% hydrogen in the gas phase was 3 times higher (Rp_0' = 45 kg/g_{cat}hr) than the initial activity without hydrogen present (Rp_0' = 14 kg/g_{cat}hr). GPC analysis was performed on the polymer, as well as viscosimetry. The obtained MW and MWD, ranging from $1.1*10^6$ to $1*10^5$ and polydispersity between 5 and 3 was used to construct a kinetic model to describe reaction rate and molecular weight as a function of hydrogen concentration. The model was based on the quasi steady state assumption and accurately describes the initial reaction rate in the gas phase as function of hydrogen concentration and the resulting MW.

Combining fluidization and polymerization: towards a reactor model

A pilot plant was constructed for the polymerization of propylene in a circulating fluidized bed. The pilot plant can be used for polymerizations up to 30 bar and 120 °C, in risers of 102 and 55 mm. Gases are recycled and a centrifugal blower is placed in the recycle stream. Gas velocities up to 3 m/s can be applied in the 102 mm tube. Catalyst can be added to the reactor and product can be removed during operation. Several gases such as propylene, hydrogen and nitrogen can be fed to the system by using mass flow controllers or by hand. The reactor is fitted with cooling jackets for control of the temperature.
Pressure difference measurements over the riser help identify the fluidization regime in the riser. Analysis of the pressure difference over the riser is used as a tool to determine the actual hold up of solids in the riser. Also circulation of solids through the reactor is visible in the pressure difference measurements.

A reactor model was created that could describe the polymerization of propylene in the riser of a circulating slugging fluidized bed reactor using the hydrogen response model and the data from the fluidization studies. The model was constructed as a cell model. The number of cells was determined by the mixing degree and thus a function of the gas velocity and the solids flux. Results show a realistic behavior and give the possibility to compare operation of the reactor with different gas velocity and solids flux and different production rates.

Samenvatting

Polyolefinen zijn een van de meest belangrijke plastics in de wereld geworden. Verbeteringen aan produktieprocessen en steeds betere katalysatoren hebben gezorgd voor een steeds grotere variatie in polyolefinen produkten. Met deze grote verscheidenheid aan verschillende produkten is het aantal mogelijke toepassingen ook enorm toegenomen. Het brede aanbod heeft er samen met de lage prijzen van deze polymeren toe geleid dat er een enorme jaarlijkse groei in produktiecapaciteit voor polyolefinen kan worden gerealiseerd. De meest belangrijke polymerisatieprocessen voor polypropyleen tegenwoordig zijn vloeistoffase of gasfase processen of een combinatie van beiden. Er is echter nog maar weinig over dergelijke processen gepubliceerd in de open literatuur.
Een van de nieuwste ontwikkelingen in gasfase processen is de ‘multizone’ reactor die bestaat uit een stijgbuis en een valbuis waarmee een circulerend wervelbed of een combinatie van meerdere buizen kan worden gecreeerd. Polymeerpoeder wordt door de buizen omhoog geblazen met behulp van gas of valt naar beneden onder invloed van de zwaartekracht. In iedere buis kunnen de reactieomstandigheden verschillend zijn waardoor nog meer produktkwaliteiten kunnen worden geproduceerd. Verschillende produktkwaliteiten kunnen op deze manier op microschaal in een poederdeeltje aanwezig zijn. In de open literatuur is niets gepubliceerd over polymerisatie in deze verschillende reactiezones.

Dit proefschrift beschrijft onderzoek naar de stijgbuis van een circulerend wervelbed voor olefine polymerisatie. In de stijgbuis vindt fluidisatie plaats in het slugging regime waarbij poeder over de top van de buis wordt getransporteerd. Polymerisatie vindt plaats onder niet-isotherme omstandigheden. Verschillende eigenschappen van het fluidisatiegedrag en de polymerisatiereactie zijn onderzocht als functie van de reactiecondities in de reaktor. Er is een mathematisch model gemaakt dat het polymerisatieproces in de stijgbuis accuraat beschrijft. Onderdelen in dit model zijn fluidisatiegedrag, warmteoverdracht, kinetiek van de

polymerisatie met behulp van het gekozen katalysatorsysteem en sorptie van propyleen in het polypropyleen.

Fluidisatie gedrag

Het slugging fluidisatie regime ($0.6 < u_g < 1.0$ m/s) was nauwkeurig onderzocht in een poederbed met een brede deeltjesgrootteverdeling. Verblijftijd en verblijftijdsspreiding van deeltjes in de stijgbuis was onderzocht, samen met segregatie en afregening van deeltjes. Doel was om het menggedrag in de stijgbuis te kunnen begrijpen en verklaren. Het systeem in de stijgbuis kon worden gevarieerd van een goed gemengd systeem tot een 'plug flow' systeem door de doorvoer van deeltjes of de gassnelheid te veranderen. Hierdoor ontstaat een groot operatiegebied voor de reaktor.
Het bleek dat segregatie van deeltjes op deeltjesgrootte de breedte van de verblijftijdsspreiding gedeeltelijk kan verklaren. Het verschil in relatieve snelheid van grote en kleine deeltjes ten opzichte van het gemiddelde kon worden gemeten. Met behulp van deze eenvoudige experimenten kan simpel een schatting worden gemaakt van de breedte van de verblijftijdsspreiding.

Plug snelheden en plug lengtes zijn bepaald als functie van de buisdiameter, deeltjesgrootteverdeling, gassnelheid en deeltjesdoorvoer. Plug lengtes blijken afhankelijk te zijn van de buisdiameter en de gassnelheid. Een nieuwe relatie was afgeleid voor de berekening van de plug snelheid. In deze relatie speelt de plug lengte een belangrijke rol in tegenstelling tot relaties die in de literatuur zijn gegeven. Met deze nieuwe relatie kunnen plug snelheden voor uiteenlopende procescondities worden berekend.

Propyleen polymerisatie

Kinetiek voor de gas fase polymerisatie was bestudeerd. Polymerisatie in de gasfase werd voorafgegaan door een zogeheten prepolymerisatie in de vloeistoffase. De effecten van de overstap van vloeistoffase naar gasfase polymerisatie op de polymerisatie in de gasfase zijn bestudeerd. De reactiesnelheid in de gasfase na een drukverlaging tijdens de overstap was circa 50 % lager dan wanneer deze drukverlaging niet werd toegepast. Verschillende mogelijke oorzaken voor deze lagere reactiesnelheid zijn onderzocht, zoals vervuiling van de katalysator, natuurlijke deactivatie in de tijd en verandering van de concentratie van

cokatalysator of externe donor. Geen van deze mogelijke oorzaken zorgde voor de vastgestelde verlaging in activiteit. Gesuggereerd wordt dat kristallisatie van het polymeer een rol speelt in de verlaging van de activiteit.

Na de prepolymerisatie in de vloeistoffase vindt de gasfase polymerisatie of hoofdpolymerisatie plaats. De kinetiek van deze reactie onder invloed van propyleen en waterstof is onderzocht. Er is een relatie tussen initiële reactiesnelheid in de gas fase en waterstofconcentratie vastgesteld. De initiële reactiesnelheid bij een waterstofconcentratie van 1.1 mol% is 3 maal zo hoog (R_p = 45 kg/g_{cat}.hr) als de reactiesnelheid in afwezigheid van waterstof (R_p = 14 kg/g_{cat}.hr). Ter vaststelling van het molecuulgewicht zijn GPC metingen en viscosimetrie metingen uitgevoerd. Het molecuulgewicht en het gemiddelde molecuulgewicht die op deze manier zijn gevonden, van $1.1*10^6$ tot $1*10^5$ en een polydispersiteit tussen 5 en 3, zijn gebruikt in een model dat de reactiesnelheid en het molecuulgewicht berekent als functie van de waterstofconcentratie. Het model was gebaseerd op de ‘quasi steady state assumption’.

Combinatie van fluidisatie en polymerisatie: naar een reactormodel

Voor de polymerisatie van propylenen in een circulerend gefluidiseerd bed is een pilot plant gebouwd. De opstelling kan worden gebruikt voor polymerisatiereacties tot 30 bar en 120 °C, in stijgbuizen van 102 en 55 mm. Gassen worden gerecycled en in de recyclestroom is een centrifugaalpomp geplaatst. In de 102 mm buis kunnen snelheden tot 3 m/s worden gegenereerd.
Faciliteiten voor het toevoegen van katalysator en voor het verwijderen van produkt tijdens operatie van de opstelling zijn in het systeem opgenomen. Verschillende gassen zoals propyleen, waterstof en stikstof kunnen worden gevoed aan het systeem met behulp van mass flow controllers of met de hand. De reactor zelf is uitgevoerd met koelmantels voor temperatuurscontrole.
Met behulp van drukverschilmetingen over de stijgbuis kan het heersende fluidisatie regime in de buis worden herkend. Analyse van de drukverschilmetingen over de buis wordt gebruikt om de hoeveelheid deeltjes in de buis te bepalen. Ook is in de metingen de circulatie van poeder te zien.

Er is een reactor model opgezet waarmee de polymerisatie van propyleen in een circulerend sluggend wervelbed wordt beschreven, gebruikmakend van het waterstof respons model en de

data uit de fluidisatiestudies. Het model was opgezet als een cel model. Het aantal cellen was bepaald aan de hand van de mate van menging en was dus een functie van de gassnelheid en de doorvoer van deeltjes. Met behulp van een circulerende stroom kon terugmenging van deeltjes worden gesimuleerd. Resultaten zijn realistisch en geven de mogelijkheid om operaties van de reactor bij verschillende gassnelheden en doorvoeren van deeltjes en bij verschillende produktiesnelheden met elkaar te vergelijken.

Chapter 1

General introduction

General introduction

Before the 1950s of the last century propylene could hardly be polymerized. Only low molecular weight product with no regularity in the chain and often highly branched polymers resulted. The polypropylene was a product of low interest. The interest in polyolefins was mainly on crystalline polymers like crystalline polyethylene.
This changed in the 1950s with the discovery of chromium, zirconium and especially titanium catalysts by Ziegler who was doing research on the 'Aufbau' reaction: growing alkyl chains by insertion of ethylene on a Al-C bond of a tri-alkyl aluminum. He discovered that the presence of nickel was slowing down the Aufbau reaction. He started varying the metal components involved in the reaction and found that in the presence of titanium the reaction became very rapid. After lowering of the reaction temperature and pressure the reaction became controllable and high molecular polymer was made.
Natta heard from these successes from his assistants who were sent to Ziegler to learn on these systems. Zieglers group did not continue on propylene polymerization and Natta started trying to polymerize propylene. He was convinced he would succeed in making polypropylene and he finally produced semi-crystalline polypropylene in March 1954.

From that time on polypropylene became a valuable product with an exploding new market and with numerous practical applications. Already in 1960 there were several commercial polypropylene producers making more than 50000 tons of product.
The results of these efforts are visible around us every day. From the cans from which we eat our dairy products, the Tupperware in which we keep our food, all the way to our cars in which an increasing portion of the plastics is made of polypropylene and numerous applications in between.

Since the discovery of these catalysts highly active and stereo-selective catalysts have been developed. The high activity of the catalysts account for low amounts of catalyst present in the polymer that even can be left in the final product. Modern polymerization processes require heterogeneous catalysts to control the morphology of the polymer powder and to reduce the required amounts of cocatalyst. Thanks to the ongoing development of new catalysts and processes, new polypropylene materials and their applications have been introduced to the market thereby expanding the market share of polyolefins.

In the development of new processes, a clear trend can be identified towards gas phase processes in which solvent recycling is not required and a larger variety of products an be produced. One of these developments is the fluidized multizone reactor from Basell, in which fluidization of a riser tube is combined with a moving bed of powder in a downer tube. The powder is circulated between the riser and the downer. A combination of more tubes in which the powder is transported is imaginable, therefore the name ‘multizone’.
This type of reactor offers the opportunity to have two or more different reaction zones in the system and thereby the ability to produce different qualities of polymer within one reactor and even within one product particle. The reaction gases that are used to fluidize the powder bed is being recycled with conversion rates of 1-3 % of conversion per pass through the reactor. The heat of reaction is removed by cooling the circulating gas and sometimes by partial condensation of the gas to use the heat of evaporation of the re-injected condensates. The reactor is operated at constant pressure, in general between 10 and 30 bar.
The type of catalyst, temperature, monomer concentration and hydrogen concentration influence polymer properties like the molecular weight distribution of the polymer. Temperature and concentration gradients are a function of the solids mixing and segregation rates of the particles.

The concept of the multizone reactor is relatively new, with a first patent issued in 1997 (Govoni et al. (1997)). In the open literature on olefin polymerization no experimental data is available on the multizone reactor. To know more about the range of applications of such multizone reactors study of the type of reactor is required. Moreover, the investment and operation costs for a pressurized experimental facility of acceptable size are high. A reactor model based on experiments at relevant process conditions, i.e. same pressure and temperature range and same fluidization conditions, is crucial for the study of a multizone reactor.

1 Outline of the thesis

The objective of the work presented in this booklet is to study the polymerization of propylene with a Ziegler-Natta catalyst in the riser of a multizone reactor, using the slugging fluidization regime (Weickert (2000)). Key aspects in the research are the applicability of models that describe the polymerization reaction in the gas phase at possible conditions applied in the multizone reactor, that describe the hydrodynamic behavior of the fluidization

in the riser, that describe heat production and heat removal of the production heat and these aspects should be studied in a down-scaled reactor for olefin polymerization.
The research is split up in separate study of the polymerization reaction under conditions comparable to those in industry and a study of the hydrodynamics of the slugging fluidization regime that can be applied in the riser of the multizone reactor and that was chosen for this research. Several different set-ups are used to study the two separated subjects. A small-scale pilot plant resembling the concept of the multizone reactor was built to combine both subjects again and study the effects of them on the polymerization reaction. Time however was limited in the project and no actual polymerization experiments were done in the pilot plant.

The catalyst system used in the present work is a Ziegler-Natta catalyst with a phtalate as internal donor, a silane as external donor and tri ethyl aluminum as cocatalyst. The use of this catalyst was offered by Nippon Polychem. This catalyst produces polymer with a comparable narrow molecular weight distribution and molecular weights that range from 1.000.000 to 100.000 g/mol.

In chapter 2 residence time and residence time distribution of particles in the riser of a circulating fluidized bed resembling the configuration of a multizone reactor was studied. Influence of gas velocity, solids flux through the riser and particle size and particle size distribution on the residence time was investigated. Hold up in the riser as well as segregation of particles was studied into detail to find an explanation of the mixing behavior and to describe it.

In chapter 3 characteristics of plugs, the dense packets of solids in a slugging fluidized bed, were studied to further deepen the understanding of the mixing behavior. Influences of gas velocity, solids flux, particle size and particle size distribution as well as raining of particles through slugs on plug velocity and plug length were studied. The results were used to describe the plug length and the plug velocity.

In chapter 4 the influence of the step between prepolymerization and main polymerization on the polymerization rate in the gas phase main polymerization was investigated. Different procedures were applied for this change from liquid phase polymerization to gas phase polymerization. An attempt to find an explanation was done. Liquid phase

'prepolymerization' is required with the catalyst used in this work, because the fresh catalyst particles are too small to be used directly in a gas phase process without using an inert bed.

In chapter 5 the hydrogen concentration was varied systematically to study the influence of hydrogen on the reaction rate of the polymerization reaction in the gas phase. A kinetic model is constructed that predicts both the reaction rate and the average molecular weight of the product as a function of the hydrogen concentration, based on the extended dormant site theory, first proposed in this work. Such a model is unprecedented in the open literature: the prediction of the combination of these two parameters was never done before.

In chapter 6 a description of the construction of a pilot plant for olefin polymerization in a circulating fluidized bed reactor or riser downcomer reactor is given. A short study of the hydrodynamics of the pilot plant in terms of hydrodynamics is done and tools are offered to control the pilot plant and interpret its results.

In chapter 7 a reactor model is presented that combines the model results from the polymerization study and the hydrodynamic study. With the reactor model polymer production in a pilot plant scale circulating fluidized bed reactor is predicted. Again, gas velocity and solids flux are varied to study their combined influence on the production.

Chapters 2, 3, 4, 5 and 7 are to be submitted for publication and were therefore written in such a way that they can be read independently from the other chapters.

2 References

Govoni, G., Rinaldi, R., Covezzi, M., Galli, P. (1997). "Process and apparatus for the gasphase polymerization of alpha-olefins". United States Patent, nr. US005,698,642A.

Weickert, G. (2000). Deutsches Patent- und Markenamt, DE 199 07 021 A1

Chapter 2

Fluidization behavior in a circulating fluidized bed reactor for olefin polymerization operated in the slugging regime. Part I: residence time and residence time distribution of solids

---

Abstract

Square nosed slugging fluidization in a circulating fluidized bed riser with a polyethylene powder with a very wide particle size distribution was studied. In square nosed slugging fluidization the extent of mixing of particles of different size depends on the riser diameter, gas velocity, hold up and solids flux in the riser. Depending on the operating conditions the particle residence time distribution of a riser in the slugging fluidization regime can vary from that of a plug flow reactor to that of a well-mixed system.

Higher gas velocities cause shorter particle residence times because of a significant decrease in the hold-up of particles in the riser at higher gas velocities. A higher solids flux also shortens the average residence time. Both influences have been quantified for a given polyethylene-air system.

Residence time and residence time distribution were determined for different particle size ranges and the influence of gas velocity, solids flux, hold up and riser diameter was studied. When comparing data from segregation experiments and residence time experiments it is clear that segregation data can predict the spread in residence time as a function of overall residence time, particle size and gas velocity. The differential velocity between small and large particles found in the segregation experiments can predict the spread in residence time as found in the residence time distribution experiments with a powder with a broad particle size distribution. Raining of particles through the slugs was studied as a function of plug length, gas velocity and pulse length. It was found that raining is not the determining mechanism for segregation of particles.

1 Introduction

For polyolefin production several types of processes, mainly based on catalytic polymerization have been developed. The oldest types of catalytic processes are diluent slurry processes (Hercules, Montedison) and solution processes (Eastman). Improvements in polyolefin production were achieved with the introduction of the second type of processes, bulk or liquid polymerization processes which can be classified into two categories: those using loop reactors (Phillips, Fina, Solvay) and those using continuous stirred reactors (Rexall, Lippshac, Exxon). The third and newest type of processes is gas phase processes which can be divided again into two categories: processes using a mechanically stirred bed (Novolen, Amoco) and processes using a fluidized bed reactor (Unipol). Finally there are hybrid processes that combine several reactor types. Examples are the combination of a liquid loop reactor with a gas phase fluidized bed reactor (Spheripol, Borstar) or the combination of two gas phase fluidized bed reactors (Unipol).

The fluidized bed reactors are simple in design and construction because they have no mechanical agitators. However a blower is required, which uses about 20 % of the total unit energy costs. Compared to bulk processes like the Spheripol process, elimination of the liquid-solid separation further simplifies the equipment and reduces the energy costs associated with monomer recovery, purification and recirculation. Another advantage of gas phase operation is the possibility to increase the heat removal capacity by making use of the heat of vaporization when the recycle flow is introduced below the dew point of the gas.

In the present study, a circulating gas phase fluidized bed in the slugging regime for olefin polymerization is studied. In slugging fluidization gas velocities are higher than in bubbling fluidization. Gas bubbles grow to the diameter of the tube. These large bubbles are called slugs. Depending on the properties of the fluidized particles these slugs are either ‘round nosed’ or ‘square nosed’. With round nosed slugs the gas-particle interface on top of the slug is round as in bubbles. Slugs migrate through the bed of particles by means of particles flowing down along the sides of the slug. In square nosed slugging the gas-particle interface at the top of the slugs is flat. The slug moves through the particle bed by means of particles raining down through the slug over the whole diameter of the tube. The bed can be extended by slugs pushing up the plugs while raining of particles takes place.

The slugging regime in the riser tube of a circulating fluidized bed has not been used commercially before, because of a more difficult heat removal in the dense phase plugs and a

more difficult control of the gas phase composition. However, the slugging regime also gives a number of advantages: entrainment of fines is minimal because of the presence of the dense plugs and the solids move in a more plug flow like behavior through the riser. Furthermore, particles produced during polymerization in a fluidized bed tend to stick to the wall, which is prevented in the slugging bed by dense plugs continuously cleaning the wall. Also the particle residence time and its distribution may possibly be controlled more properly in the slugging regime and an axial temperature profile can be imposed on the system.

In contrast to many other fluid bed conversion processes for the slugging fluidized bed, an accurate understanding of the phenomena occurring in the particle phase is very important. In the polymerization process the particles are both the catalyst and the product. Therefore the residence time of the particles is crucial; the residence time of the particles influences the product properties.

Polymerization takes place inside the polymer particles. A particle is formed around a catalyst often supported on a mineral support, at which active sites polymer chains are formed. The time of formation of a polymer chain inside a growing particle is typically only a fraction of a second and is very short compared to the residence time of a particle in the reactor. When a grown polymer chain is detached from the active site, it will stick around the catalyst particle because of entanglement with other formed polymer chains. A growing layer of polymer is thus being formed around and inside the catalyst particle that even causes fragmentation of the catalyst particle, ultimately resulting in particles consisting of polymer containing traces of catalyst fragments. Fresh catalyst particles are extremely active and have a high heat generation rate. To prevent overheating of the particle the reaction heat has to be removed sufficiently rapidly. With the modern highly active catalysts the catalyst traces are not removed from the polymer.

As the resulting reaction rate, sorption and heat transfer strongly depend on the fluidization behavior in the riser of the circulating fluidized bed, the first step is to describe the fluidization behavior of a slugging fluidized bed. Characteristics as residence time and residence time distribution of the solids, axial mixing of the solids and slugging characteristics need to be described.

In this work residence time and mixing of solids was studied, and the influences of gas velocity and solids flux on the residence time of the solids in the riser of the circulating

fluidized were investigated. To quantify the mixing effects in the slugging regime, demixing or segregation and raining of solids through slugs was studied experimentally.

1.1 Segregation

In literature, in the study of mixing effects in fluidized beds in general, segregation of solids plays an important role. Studies of mixing and segregation however have mainly been confined to binary mixtures of different particle size or density (e.g. Gibilaro and Rowe (1974), Nienow et al. (1978), Daw and Frazier (1988), Nakagawa et al. (1994), Beeckmanns and Agrawal (1994), Sciazko and Bandrowski (1995), Wu and Baeyens (1998), Hirschberg and Werther (1998)) or other 'ideal' mixtures of monosized particle fractions with also ternary or quarternary systems (Nienow et al. (1987)), whereas in the current research a powder with equal density and continuous particle size distribution is used. Segregation in different fluidization regimes from bubbling fluidization to fast fluidization was studied, but only for binary mixtures.

Segregation behavior of a powder with a continuous size distribution has hardly been studied. Hoffmann and Romp (1991) did experiments with sand with a continuous size distribution in the bubbling fluidization regime. The particle size distribution of each layer was determined by sieve analysis. Matthiesen et al. (1999) used a powder with a continuous particle size distribution to model gas/particle flow in a CFB in a fast fluidized bed. In their work they mainly concentrated on radial profiles.

Also segregation or mixing effects in slugging fluidized beds have hardly been studied. Abanades et al. (1994) presented a mathematical model for the segregation of limestone-coal mixtures from a mechanistic point of view, they were considered binary mixtures. They stated that complete segregation will always occur when raining of particles prevails in the bed.

Schouten et al. (1988) studied systems of binary mixtures of relatively large particles with different sizes and densities. They proposed two models for the description of segregation in a slugging fluidized bed. Both models describe a downward flow of segregating particles in the slug and an upward flow of particles in a plug, where an upward buoyancy force due to density differences between the particles predominantly caused the upward flow of solids.

To the authors knowledge no research has been carried out on segregation in the slugging regime with a powder with a continuous size distribution.

1.2 Raining of solids

In the square nosed slugging regime slugs travel through the bed of solids by means of particles raining through the slugs. The occurrence of raining of particles was observed early. Yasui and Johanson (1958) composed a model that described bubble motion predominantly caused by particle rain. Square nosed slugging however was not considered in literature till Lim et al. (1997). They studied raining of solids from an emulsion gas interface such as the raining from the bottom of plugs in the square nosed slugging regime. They studied mainly velocities of slugs and bubbles as a function of the solids raining. They concluded that only solids raining causes movement of slugs and raining mainly occurs because of bridging of solids in the plug. Thiel and Potter (1977) stated that solids' raining only occurs when a plug gets stuck in the tube, caused by severe bridging.

The purpose of this research is to describe the particle mixing behavior in the circulating slugging fluidized bed for olefin polymerization. Properties such as residence time of the particles, gas solids contact and solids hold-up profiles as well as plug velocity and plug length are studied. Detailed knowledge on these fluid bed properties can eventually be combined with polymerization kinetics and sorption of monomer in the polymer particles as well as heat transfer properties to develop an integral reactor model of the polymerization process.

In part I of this work on slugging fluidization properties residence time and residence time distribution of the particles, segregation of particles and raining of particles through slugs is studied. First results on residence time and residence time distribution of the particles are given and discussed, after which results on segregation and raining are given. These results are compared with the results on residence time of the particles and explanations for the results on the residence time of the particles are proposed. In part II the plug velocity and the plug length are studied and quantified. Plug velocity and plug length can help understand the phenomena studied in part I.

2 Experimental

Three types of experiments have been carried out. The first type of experiments was used to determine the average residence times and the residence time distributions of particles in the riser of a circulating fluidized bed. In these experiments tracer particles were injected and followed. The second type of experiments was used to determine the segregation of particles of different size. Information on the segregation phenomenon may help explain and predict the residence time distribution. In these experiments the inflow of solids from the downer into the riser and the outflow from the riser to the downer were blocked. The third type of experiments was used to determine raining of solids through the slugs, to find an explanation of the segregation of particles. For these experiments the same type of set up was used as in the segregation experiments, and detectors were used to measure the raining of solids.

2.1 Residence time and -distribution measurements

Due to the intermittent nature of the slugging fluidization regime, it is difficult to measure the solids residence time in the riser of a circulating fluidized bed reactor operated in the slugging regime. Only at discrete intervals in time a plug travels over the top of the riser, resulting in discrete residence times. Therefore many experiments are required to determine the solids residence time within acceptable statistical limits. Nevertheless, residence time distribution experiments were performed and trends could be identified.

Two set ups with the same configuration were used (figure 1). Both set ups were constructed of clear Plexiglas tubes of 3 mm thickness. Set up A has a riser tube of 44 mm internal diameter and a length of 3.54 m. Set up B has a riser tube of 105.6 mm internal diameter and a length of 3.42 m. The top of both risers has a dead end and a downward inclined exit to prevent particles from settling on a horizontal surface. Part of a plug will enter the section to the cyclone; another part will fall back into the riser. To uncouple the riser and the downer with respect to gas flow, two ball valves were placed in the downer section of each set up. Particles will be transported through the downer of a set up by alternating opening and closing of both valves. In this way, no gas flows through the downer and the flow of powder is only dependent on the height of the powder bed in the section leading to the riser, the area of

opening in this section to the riser and the gas velocity. With the area of opening in the section to the riser the maximum flow of powder can be influenced.

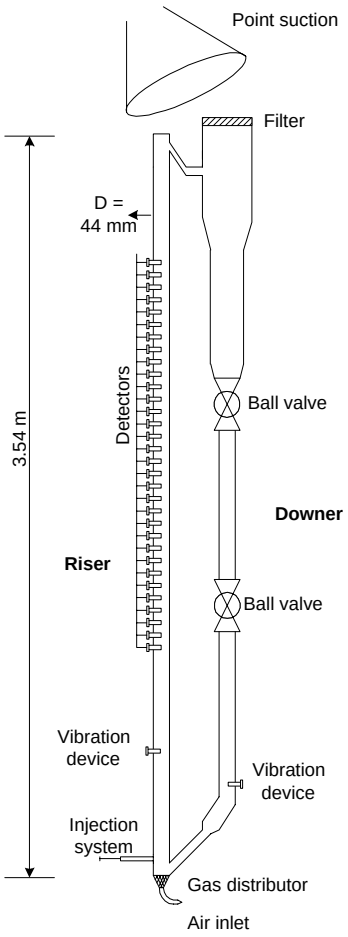

Figure 1: Experimental set up for residence time distribution experiments

A measured and calibrated air flow enters the bottom of the riser through a gas distributor consisting of a bed of glass beads below a grid to keep the bed in place and prevent polymer powder from entering the bed.

The residence time and its distribution for a single pass through the riser were determined using a tracer injection method. Particles of the different size ranges (table 1) were colored separately. A sample was made of the different size ranges according to the weight fractions of these different size ranges in the original (unsieved) powder, thus being representative for this powder. It was injected 100 mm above the distributor (figure 2) while the set up was being operated in the circulating slugging fluidization regime with the original unsieved powder. Plugs that traveled over the top of the riser were collected. By determining the

concentration of colored particles of each of the different particle size ranges in every collected plug it was possible to obtain the average residence time and the residence time distribution for the different size ranges.

Table 1: Model powder polyethylene details. Total powder refers to the unsieved complete particle size distribution; part of the total powder was sieved in four different size ranges

Fraction of powder	Particle size [μm]	Average bulk density [kg/m^3]	u_{mf} [m/s]
Total	70< d_p<1600	473	0.21
Large	d_p>1200	423	0.27
Average	800<d_p<1200	435	0.155
Small	420<d_p<800	450	0.08
very small	d_p<420	474	n/a

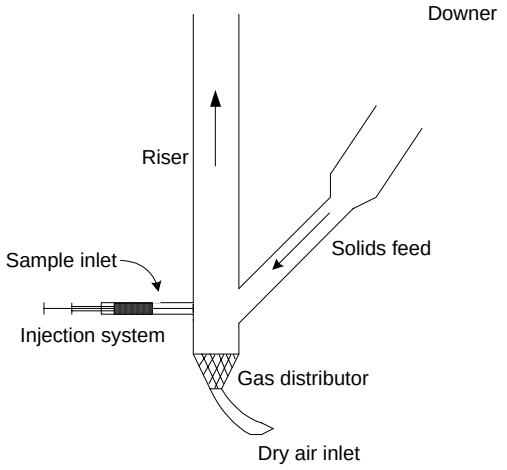

Figure 2: Injection section in riser

Since the tracer experiments are not very accurate, experiments were done to determine the average residence time of the polymer powder more accurately by measuring the hold-up of powder in the riser during operation, together with the solids flux into the riser.

The hold up was measured by suddenly stopping the gas flow during steady state operation. From the measured height of the bed of solids in the non-fluidized riser the hold up could be calculated. Since plugs travel over the top of the riser in discrete time intervals whereas the

solids are fed continuously at the bottom of the riser, the height of the bed can vary approximately with the length of a plug in an oscillating fashion. A large number of measurements taken at irregular intervals are necessary to prevent measuring the hold up always at the same interval in the oscillation.

The solids flux was determined by measuring the time needed for a specified amount of solids entering the riser via the section leading to the riser (figure 3). The height of the bed in this section and the standpipe above it should not vary much, because the changing weight of the bed may change the solids flux into the riser. Therefore the specified amount of solids was rather small, and a large number of measurements were needed to gain acceptable accuracy. The average residence time was determined in both the 44 mm and the 105.6 mm diameter riser.

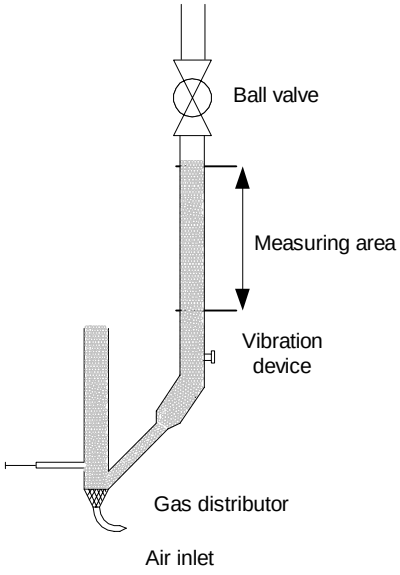

Figure 3: Measuring area for solids flux

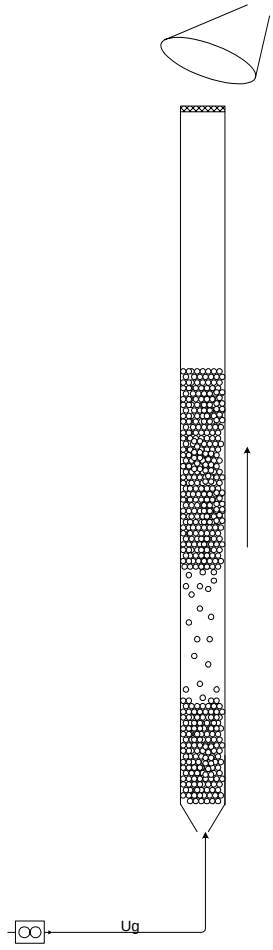

Figure 4: Experimental set up for segregation measurements

2.2 Segregation measurements

For the segregation experiments set up A and B were altered. The connections between the downer and the riser at the bottom and at the top of the riser were removed. A standpipe was thus created. The riser of set up B was shortened to 3.34 m by the decoupling (figure 4).

For an experiment the standpipe was filled with the required amount of mixed polymer powder. Then the gas flow through the standpipe was started and stopped after the required time for the experiment. The powder could then be taken out for analysis.

A vacuum technique was used to take out the bed of solids in layers of equal length (figure 4). After removal from the bed, the separate layers were mixed to avoid influences of particle size gradients within a single layer and their particle size distribution and average particle size were measured by means of laser diffraction.

2.3 Raining measurements

In the circulating slugging fluidization regime it is very difficult to determine the raining velocity or the degree of raining, due to the movement of the slugs. This would require a very exact actual measurement of the velocity of a slug with a measuring device that moves together with the slug. This device should start moving with a slug at a very precisely timed moment, which is very difficult. Therefore, a similar set up with a standpipe as in the segregation experiments was used.

A measuring method without having to move the measuring device with the moving bed is to measure the amount of powder that has fallen through a slug onto the successive plug or onto the dense bottom zone of the bed in a standpipe with an internal diameter of 105.6 mm and a length of 3.42 m (figure 5). In these experiments, the bed was operated at minimum fluidization velocity by a gas supply; pulses of gas, with a velocity that was used in experiments in a circulating fluidized bed were given through a second supply.

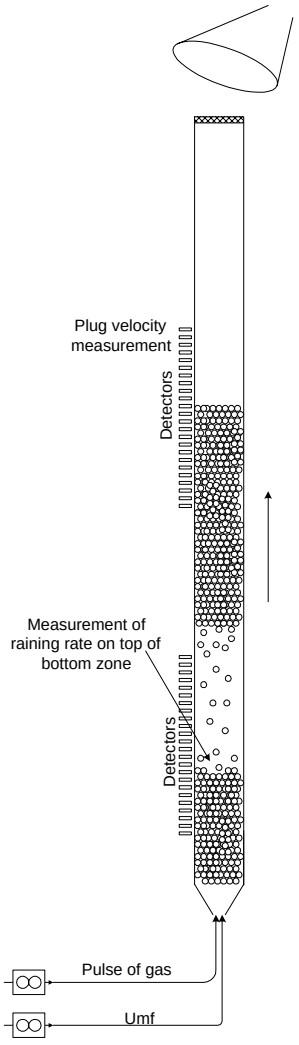

Figure 5: Experimental set up for raining measurements

A pulse of gas was given by switching valves in the gas supply system for the pulse gas from a bypass to the riser (figure 5), thus creating a constant gas velocity during the pulse. The valves were switched by a computer program, which controlled and recorded the time intervals the valves were switched to the riser and registered several measurements from the set up.

A pulse of gas needs to be given long enough for the system to reach a constant velocity of the formed slug. The slug will only start to move when it is large enough to accelerate itself and the plug above it. Only when both plug and slug reach a constant velocity measurements can be done. The dense part of the bed can be considered as the successive ‘plug’, solids raining through the slugs fall onto the growing bed. This means that measurements on slugging behavior in the standpipe when the velocity of the slug-and-plug combination has become constant will resemble slugging behavior in the circulating fluidized bed.
The height of the dense bed is measured during a pulse experiment by means of infrared detectors as well as the height that the solids on top of the slug reach in a pulse experiment. To avoid measurement errors caused by segregation, after 6 experiments the bed was removed from the standpipe, mixed and brought back in the standpipe.
When a pulse of gas is given, the bed is expanded and a slug is formed, pushing the part of the bed above it upward. When the bed height is approximately the height of the dense bed plus the average height of a plug in a circulating bed, the part of the bed above the slug will resemble the average plug length in a circulating bed.

During a pulse experiment 32 specially designed detectors were measuring constantly, with a frequency of 20 Hz, see figure 6. Detectors were placed 30 mm from each other in the lower zone of the standpipe and 19 mm in the upper zone of the standpipe.

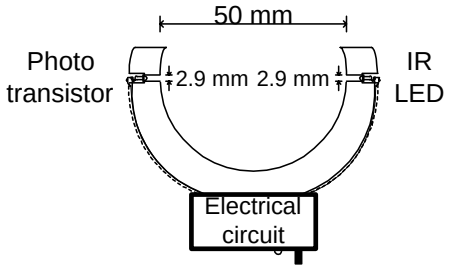

Figure 6: Schematic of IR-detectors

Every detector consisted of an infrared Light Emitting Diode (LED) (950 nm) and a phototransistor with a filter for visible light (400-700 nm). To prevent interference with daylight or IR-light scattering from neighboring detectors, the LED and the phototransistor were collimated. The signal from the phototransistor was treated in such a way that it gave a low signal (<0.7 V) when it detected IR-light from the LED, and a high signal (>2.3 V) when

no light from the LED was detected. The detectors were calibrated at the same output voltage of the phototransistor to swap from a low to a high signal. In this way a pseudo digital output was created, and processed by a data acquisition and control unit at high frequencies (20 Hz). Data interpretation was carried out on a separate computer after the experiments. The interpretation was based on recognition of a series of high voltage measurements in one time frame. When more than 2 detectors gave a high signal, this was recognized as a possible plug. When this pattern was also observed in neighboring time frames, a plug was detected. With monitoring sequences of high and low voltage measurements plugs and slugs could be followed. With this method also the growth of the dense bottom zone in the bed was followed.

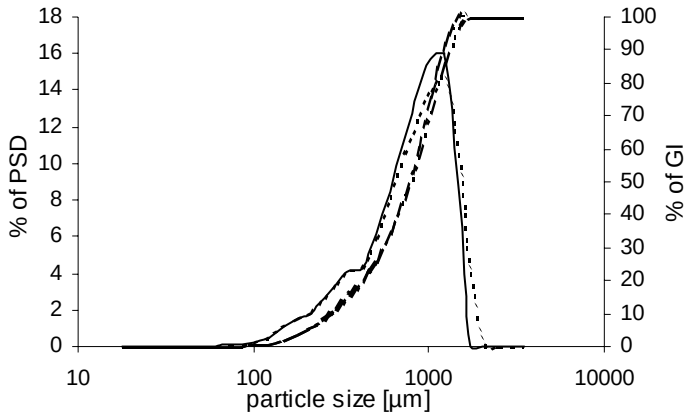

Figure 7: Particle size distribution of the polyethylene powder used in this work

The powder used in the experiments is a polyethylene powder with a particle size distribution of 70 µm < d_p < 1600 µm as given in figure 7. The bulk density is 470 kg/m^3 (polymer density 910 kg/m^3, porosity 47.5 %). The powder is easily fluidized but tends to suffer from static electricity. Therefore, the set up was grounded and the antistatic agent Larostat 519 was added. Without the use of Larostat bridging is severe in the bed and small particles stick to the wall showing a much longer residence time. Moreover, the solids flux is lowered by a factor of almost two because of bridging in the standpipe.

Part of the powder was sieved and split into four different particle size ranges (table 1) to determine the influence of the particle size range on the slugging phenomena. The minimum fluidization velocity for each of the fractions was determined.

3 Results

3.1 Residence time and - distribution

3.1.1 Residence time distribution

In the experiments, both the gas velocity and solids flux through the riser were varied (table 2). One experiment (experiment C) was repeated three times to studie the influence of the intermittent nature of the slugging fluidization. The results of the experiments were fitted with an axial dispersed plug flow model, giving average residence times and Peclet numbers that quantify the spread (figure 8).

Table 2: Overview of experimental results of the tracer injection experiments for the determination of the residence time distribution

Experiment	u_g [m/s]	G_s [kg/m^{2}s]	τ [s] (very small)	τ [s] (small)	τ [s] (average)	Pe (very small)	Pe (small)	Pe (average)
RTD-A	0.67	8.53	55.6	56.1	60.9	105.5	74.3	125
RTD-B	0.67	3.49	86.6	106	124.4	13.6	21.6	30.1
RTD-C1	0.53	4.7	111	139	148	39.7	118	207
RTD-C2	0.53	4.85	94.5	108	121	39.2	72.2	103
RTD-C3	0.53	4.69	136	151	149	33.9	65.3	327
RTD-D	0.81	5.53	49.5	60.3	65.1	15.9	20.8	23.2
RTD-E	0.67	5.28	64.7	81.0	89.6	30.4	42.5	52.3

The experiments show that fluctuations are indeed large because of the intermittent nature of the slugging fluidization. As can be seen with the repeated experiment C (i.e. experiments C1, C2 and C3), the intermittent nature causes rather large fluctuations in the hold up in the riser over longer time periods, thus causing differences in the residence time. However, trends can be discerned from the experimental results. In general it can be concluded that the results indicate that the slugging fluidization has a plug flow like behavior, based on the large Pe

numbers (most experiments have Peclet numbers above 40 for the larger particle size ranges). This is in strong contrast to bubbling fluidized beds, where the solids flow usually shows well-mixed behavior. Furthermore, the residence time distribution experiments show that larger particles have a somewhat larger average residence time, as was expected. The smallest particle size range, d_p< 420 μm, tends to be spread out more in time. This is probably due to static electricity effects that make the smallest particles tend to stick to the wall of the riser, causing a larger spread in residence time of this smallest fraction.

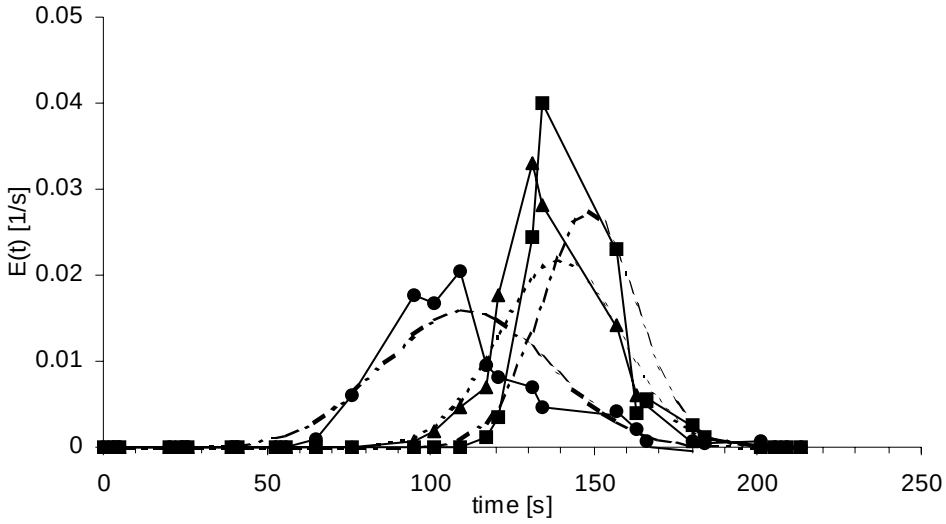

Figure 8: Example RTD fitting; experiment RTD-C1. u_g = 0.53 m/s, G_s = 4.7 kg/m^{2}s.
♦ = d_p < 420 μm; ■ = 420 < d_p < 800 μm; ▲ = d_p > 800 μm

3.1.2 Average residence time

Both hold up and solids flux were measured for different gas velocities and different areas of opening in the section leading to the riser (table 3). Thus, average residence times could be calculated. Results are given in figures 9 (hold up 44 mm riser), 10 (hold up 105.6 mm riser), 11 (residence time 44 mm riser) and 12 (residence time 105.6 mm riser). As can be observed, the hold up is influenced largely by the gas velocity, but the solids flux is hardly affected by the gas velocity. However a small variation is detected (figure 9). When the solids flux is higher at constant gas velocity, the hold up is larger. The accuracy of the measured residence times remains within statistical limits.

Table 3: Overview of the hold up experiments in the 44 mm riser and 105.6 mm riser. Hold up and solids flux were measured from which the average residence time was calculated. Results of these experiments are given in figures 9, 10, 11 and 12.

Tube diameter [mm]	Diameter solids flux limitation [mm]	lowest gas velocity measured [m/s]	highest gas velocity measured [m/s]
44	12	0.53	0.95
44	15	0.44	1.14
44	18	0.39	1.14
44	21	0.53	1.23
105.6	30	0.58	0.87
105.6	35	0.58	0.87
105.6	43	0.64	0.94
105.6	48	0.64	0.94

3.1.3 Influence of gas velocity

As can be seen from the comparison of tracer experiments C-1, D and E, in which the solids flux is kept constant and the gas velocity is varied, the gas velocity has a large influence on the residence time as well as the spread in residence time. With increasing gas velocity the residence time decreases (figure 13). Also the results from the experiments determining the average residence time show that the residence time is clearly dependent on the gas velocity (figure 11, 12). The gas velocity causes a shorter residence time by decreasing the hold-up in the column. The hold-up decreases enormously with increasing gas velocity (figures 9 and 10). The results from the tracer experiments are in good agreement with the average residence time measurements (figure 13).

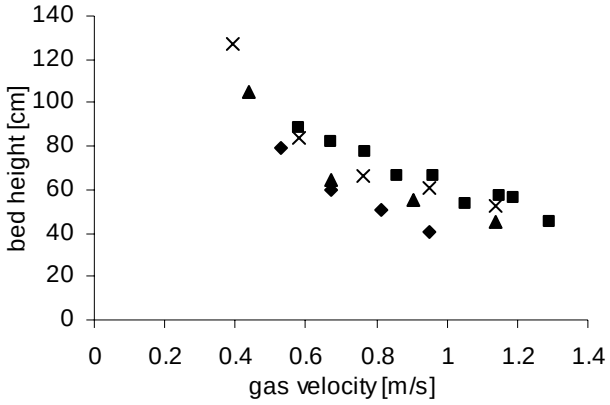

Figure 9: Hold up in cm bed height as function of gas velocity. (44 mm internal diameter riser); ◆: G_s=3.3 kg/m^{2}s; ▲: G_s=5.5 kg/m^{2}s; ×: G_s=8.3 kg/m^{2}s ;■: G_s=10.6 kg/m^{2}s

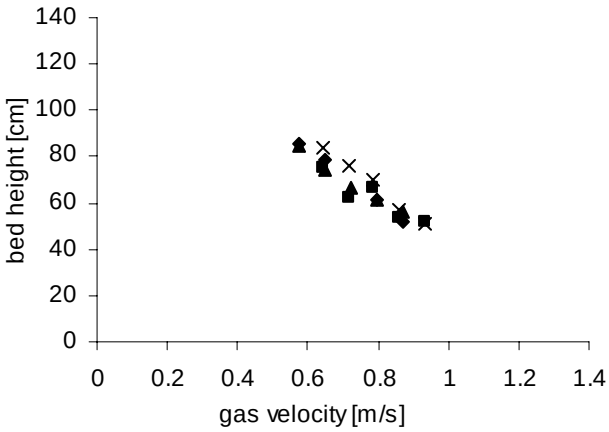

Figure 10: Hold up in cm bed height as function of gas velocity. (105.6 mm internal diameter riser); ◆: G_s=1.6 kg/m^{2}s; ▲: G_s=2.3 kg/m^{2}s; ×: G_s=4.9 kg/m^{2}s ;■: G_s=5.7 kg/m^{2}s

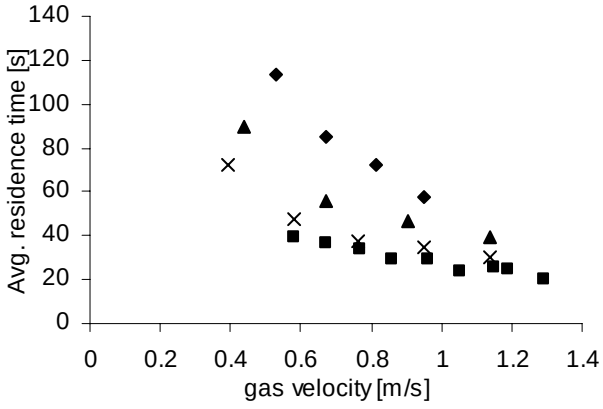

Figure 11: Calculated average residence time vs gas velocity in a 44 mm riser. 'total' powder used. ◆: G_s=3.3 kg/m^{2}s; ▲: G_s=5.5 kg/m^{2}s; ×: G_s=8.3 kg/m^{2}s ;■: G_s=10.6 kg/m^{2}s

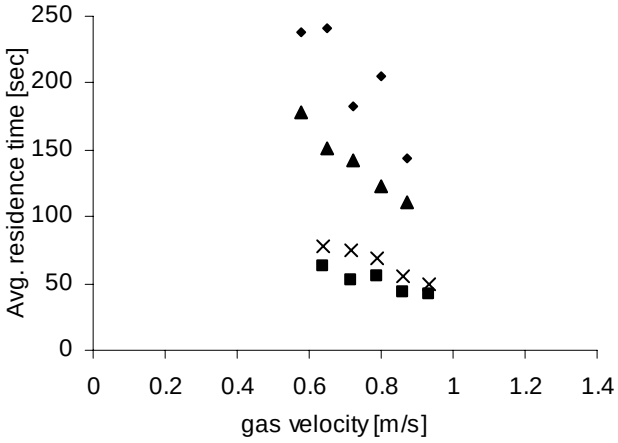

Figure 12: Calculated average residence time vs gas velocity in a 105.6 mm riser. 'total' powder used. ◆: G_s=1.6 kg/m^{2}s; ▲: G_s=2.3 kg/m^{2}s; ×: G_s=4.9 kg/m^{2}s ;■: G_s=5.7 kg/m^{2}s

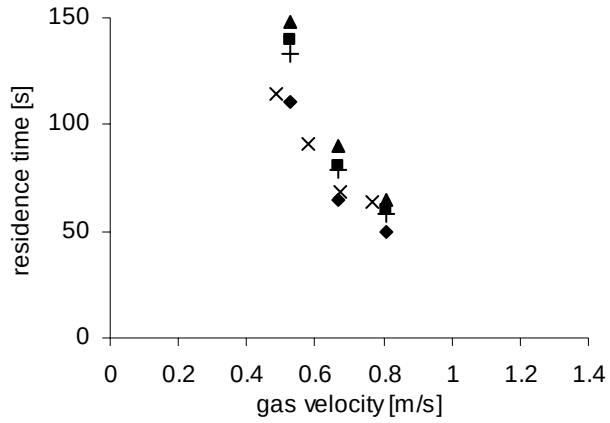

Figure 13: calculated average residence time from tracer experiments vs gas velocity. Comparison with hold up and solids flux measurements. ◆: d_p<420 μm; ■:420 <d_p<800 μm; ▲:d_p>800 μm; +: average of residence times particle size distributions; ×: average residence time of hold up experiments

The spread in residence time increases significantly with increasing gas velocity (figure 14). With higher gas velocities the system becomes better mixed with a shorter average solids residence time. A possible explanation for this observation is a change in mixing mechanism. A higher gas velocity causes more vigorous movement of the powder. With a lower hold-up the powder is more able to swirl and mix through the column, helped by the higher gas velocity. This causes a larger spread in residence time.

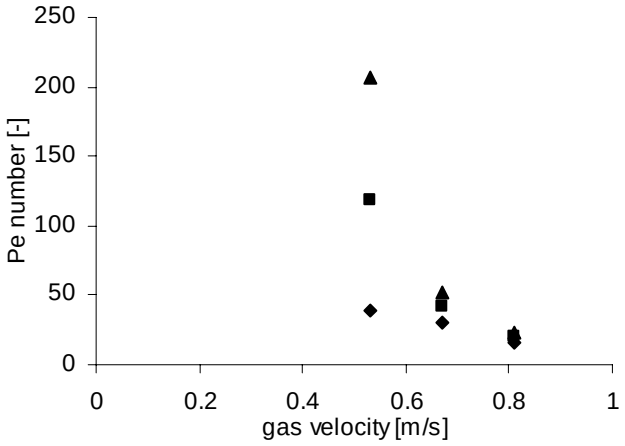

Figure 14: spread in residence time as function of gas velocity. Experiments done in a CFB with a 44 mm riser; ◆: Pe for d_p<420 μm; ■:Pe for 420 <d_p<800 μm;▲:Pe for d_p>800 μm.

3.1.4 Influence of solids flux

When comparing tracer experiments A, B and E in which the gas velocity was kept constant and the solids flux was varied, it is clear that also the solids flux through the riser influences the spread in residence time substantially. The effect however is contrary to the gas velocity effect; the spread becomes smaller at larger solids flux (figure 15), enabling a more plug flow like behavior at shorter residence times.

An explanation can be found in the decrease of the residence time with increasing solids flux while keeping the hold-up constant by applying the same gas velocity in every experiment. Since the extent of movement of the powder is similar when the gas velocity is kept constant and because the hold-up is almost exclusively dependent of the gas velocity (while the solids flux has no influence), the extent of mixing by the gas as explained above will not change. However, due to significant reduction in residence time at the same extent of mixing in the bed, the mixing and therefore spread in residence time will be less pronounced at shorter residence times.

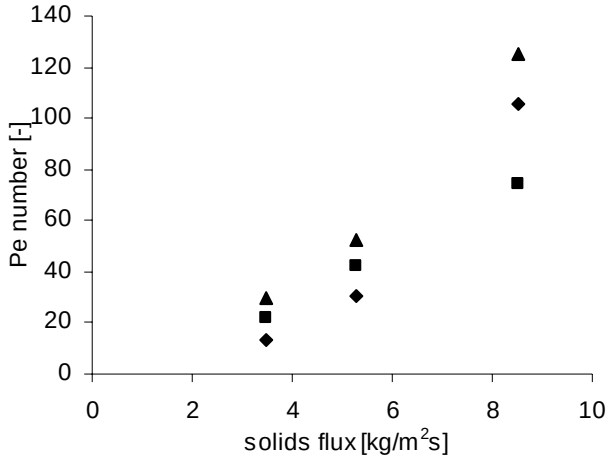

Figure 15: spread in residence time vs solids flux. Experimentnts done in a CFB with a 44 mm riser. ◆: Pe for d_p<420 μm; ■:Pe for 420 <d_p<800 μm; ▲:Pe for d_p>800 μm.

Comparing the two effects, it is clear that the gas velocity has a larger influence on both the residence time and the spread in residence time than the solids flux. The mixing caused by the mixing mechanism is influenced more by a change in the gas velocity than by a change in mixing time by changing the solids flux. Since these two adjustable parameters in the system

cause reverse effects in the spread of the residence time, the window of operation with the system with respect to residence time and residence time distribution is large.

3.2 Segregation

Not only a general spread in residence time was measured, but also a spread in average residence time of different particle size ranges (figure 11). This is caused by the particle size variation and thus by differences in terminal velocity or minimum fluidization velocity. With these phenomena however it is very difficult to quantify the differences in residence time. A different method is needed.
The average residence times of the different particle size ranges differ in general somewhat from the overall average residence time depending on the particle size (table 3). The extent of this deviation seems to be dependent on the particle size. This suggests a mixing mechanism that could be quantified. To investigate this spreading in residence time as function of particle size further, de-mixing or segregation of the powder was studied.

Segregation is caused by differences in particle density or particle size in a bed of solids that is being fluidized. The powder used in the present research has a uniform density but a broad particle size distribution and is therefore expected to suffer from segregation.
Segregation mainly occurs in a non-circulating fluidized bed. In a circulating fluidized bed the constant solids flux through the riser masks the effects of segregation, where it is expected that segregation between particles of different size entering the bed at the same moment in time does occur. The experiments done to determine the residence time distribution support this hypothesis. Thus, segregation measured in a non-circulating bed can be used to study segregation effects in a circulating fluidized bed.

The variation of the particle size as a function of bed height expresses the degree of segregation. Other characteristics that could be responsible for segregation such as density, sphericity and porosity are assumed to be equal for all particles in the used powder.
To be able to compare different beds a dimensionless particle diameter (Y) and a dimensionless bed height (Z) were used:

$$Y = \frac{d_p(h) - d_{p,average}}{d_{p,average}} \qquad (1)$$

$$Z = \frac{h}{H} \qquad (2)$$

The dimensionless particle diameter is plotted against the dimensionless bed height. This results in a straight line. The slope of this line is a measure for the degree of segregation in the bed. The absolute value will be defined as the segregation number (*S*). A steeper line has a larger segregation number and its corresponding bed is more segregated. The regression coefficient (R^2) of the line is an indication whether the segregation is constant throughout the bed. If the regression coefficient approaches 1 the fit is almost perfect so the particle diameter decreases constantly along the height without irregularities. If the regression constant is low variations occur in the particle diameter along the slope and segregation is not fully developed throughout the bed.

In the experiments, the rate of segregation is measured as well as influences of gas velocity, bed diameter and bed height on the rate of segregation (table 4). With the rate of segregation it was possible to calculate the relative velocity of particles of different size through the bed. On average the particles traveled maximum 80 cm through a bed with an initial bed height of 100 cm: from the center of the lowest/highest layer to the center of the highest/lowest layer, every layer that was analyzed for its particle size distribution being 20 cm.

3.2.1 The rate of segregation

To determine the rate of segregation, the bed height and gas velocity were kept constant while the fluidization time was varied. As can be seen in figure 16 segregation is fully developed within ten minutes, at a gas velocity of 0.45 m/s. The segregation becomes more constant throughout the bed after a longer fluidization time. Note that the powder already shows some segregation due to the filling of the bed from the top (at t = 0 s).

Table 4: Overview of the settings of the segregation experiments. Experiments were performed in two standpipes with 44 mm diameter and 105.6 mm diameter. 'Total' unsieved powder with complete particle size distribution was used in all experiments.

Experiment number	Fluidization time	Gas velocity	Bed height	Bed diameter
	[min]	[m/s]	[cm]	[mm]
1	0	-	100	44
2	2	0.45	100	44
3	3.5	0.45	100	44
4	5	0.45	100	44
5	7.5	0.45	100	44
6	10	0.45	100	44
7	40	0.45	100	44
8	5	0.28	100	44
9	5	0.34	100	44
10	5	0.56	100	44
11	5	0.44	50	44
12	5	0.44	75	44
13	5	0.44	125	44
14	5	0.28	100	105.6
15	10	0.28	100	105.6
16	10	0.28	125	105.6
17	10	0.4	100	105.6

Segregation was studied because it could lead to a quantitative calculation on the spread of particles with a different size. From segregation experiments a different overall velocity for small (<420 μm) and large (>1200 μm) particles can be calculated. Figure 16 shows that segregation is almost complete after 10 minutes. That means that after 10 minutes the small particles in the lowest layer traveled to the highest layer and large particles traveled from the highest layer to the lowest layer. This corresponds to an average velocity through the bed of 1.33 mm/s, in upward direction for the small particles and downwards for large particles.

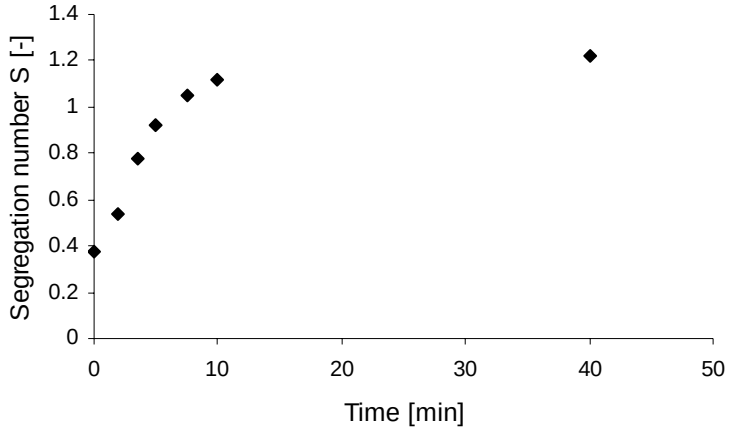

Figure 16: rate of segregation in a 44 mm riser. Bed height = 100 cm; u_0 = 0.45 m/s
. 'total' powder used.

Segregation was studied because it could lead to a quantitative calculation on the spread of particles with a different size. From segregation experiments a different overall velocity for small (<420 μm) and large (>1200 μm) particles can be calculated. Figure 16 shows that segregation is almost complete after 10 minutes. That means that after 10 minutes the small particles in the lowest layer traveled to the highest layer and large particles traveled from the highest layer to the lowest layer. This corresponds to an average velocity through the bed of 1.33 mm/s, in upward direction for the small particles and downwards for large particles.

When it is assumed that in a circulating fluidized bed the same velocity differences occur, differences in residence time between particles with different sizes can be calculated. With a solids flux of 4.2 kg/m^{2}s and an average solids hold up in the riser of 4.1 kg (corresponding to an initial bed height of 1 m in the 44 mm diameter riser), the average residence time is 112 s. On average particles will travel 0.9 cm/s through the bed in the riser, imposed by the solids flux. Small particles will travel faster through the bed than the average non-segregating particles and the average velocity difference is 0.13 cm/s. The smallest particles will have an average residence time of 97 s, 15 s shorter than the overall average and the largest particles will have a residence time of 130 s, 18 s longer than the overall average.

Because of a constant solids flux through the riser, segregation is masked when particles are not marked. The particle size distribution is about the same in every layer of the bed for different gas velocities and solids fluxes.

When looking at the results from the tracer experiments (table 2) the segregation effects can roughly account for the observed differences in residence times between the d_p< 420 μm and d_p> 800 μm for most experiments.

3.2.2 The influence of the gas velocity

The fluidization time was held constant at 5 minutes and the bed height was 100 cm. The influence of the gas velocity is shown in figure 17. At the lowest gas velocity the bed was not actually slugging. Some wall slugs could be observed but no steady slugging. This also explains the lower segregation number.

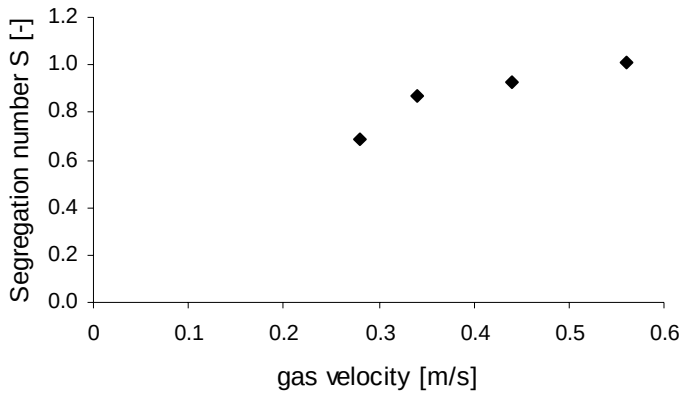

Figure 17: Influence of gas velocity on segregation in a 44 mm riser. Bed height = 100 cm; fluidization time = 5 min. 'total' powder used.

After 5 minutes the segregation process has not yet reached a state of maximum segregation for that gas velocity. At higher gas velocities the segregation process is further developed than at lower gas velocities so the segregation number will be higher. It may be concluded that at higher gas velocities the segregation process is faster than at low gas velocities.

From the results one could conclude that the segregation rate increases with increasing gas velocity. Different authors are not in agreement with each other on the phenomenon of the increase of segregation with an increase of the gas velocity. Abanades et al. (1994) stated that complete segregation will always occur in a bed operating in square nosed slugging when raining of particles occurs. However, Schouten et al. (1988) concluded that segregation decreases with increasing gas velocity in a slugging fluidized bed. Hoffmann and Romp

(1991) also stated that segregation is lower at higher gas velocities, but they measured only with a bed of 15 cm high. Daw and Frazier (1988) found that segregation is less pronounced at higher gas velocities, but suggested that segregation increases again above a certain gas velocity.

The results from the residence time distribution experiments, in which the spread in residence time is larger at higher gas velocities, support the findings in the current work. Because the spread in residence time is larger, it is expected that the injected particles be segregated more throughout the bed. Since the segregation process is faster at higher gas velocity, it may be expected that the relative velocity with which the particles travel through the bed is higher which is presented by the larger spread. Since the overall residence time is shorter than the time needed to complete segregation, only the rate of the segregation process is important.

3.2.3 The influence of the bed height

The influence of the bed height was studied while the gas velocity was held constant at 0.44 m/s, the segregation time was 5 minutes and the bed height was varied (figure 18). The degree of segregation was almost constant for bed heights of 50-100 cm. The degree of segregation drops significantly at a bed height of 125 cm.

According to Schouten et al. (1988) the extent of segregation should decrease with an increase in bed height. This can only be seen from the present experiments with a larger bed height where segregation drops. A possible explanation could be that in the lower bed heights the axial mixing is more profound and that the mixing is the same for all shallow beds at the specific gas velocity.

The results of the tracer experiments with a variation of the gas velocity show a similar trend as the current segregation experiments (figure 14). With increasing gas velocity the hold–up or measured bed height decreases and the spread in residence time becomes larger. At lower bed height the segregation increases. Both results are analogous: the larger segregation indicates that particles with different particle size travel with larger differential velocities through the bed, what is represented by the larger spread or the lower Pe number in the tracer experiments.

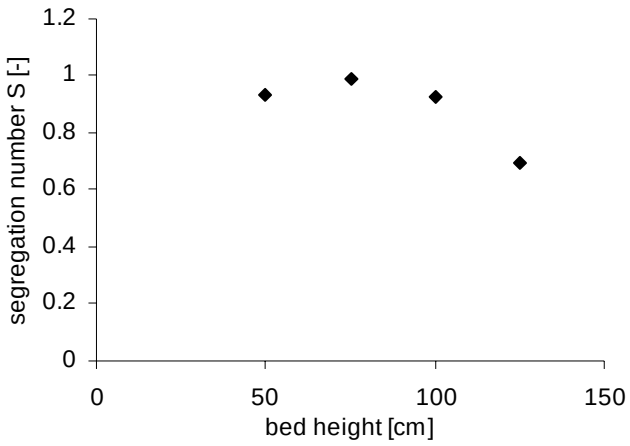

Figure 18: influence of bed height on segregation in a 44 mm riser. u_0 = 0.44 m/s, fluidization time = 5 min. 'total' powder used.

3.2.4 The influence of the bed diameter

To investigate the influence of the bed diameter on the segregation experiments were also performed in a 105.6 mm riser. The influence of the bed diameter on the segregation is studied by comparing experiments 8 (S = 0.689) and 14 (S = 0.448) (table 4).

From experiments 8 an 14 it can be concluded that the rate of segregation decreases with an increase in bed diameter. Another implication for the lower segregation rate in a bed with a larger diameter can be found by comparing the relative increase in segregation in the time. The segregation number after 10 minutes is divided by the segregation number after 5 minutes; for the 44 mm riser a value of 1.2 was obtained, but at a higher gas velocity (measurements at 0.45 m/s) and for the 105.6 mm riser a value of 1.8 (0.820/0.448). The lower value in the smaller diameter riser is an indication that the extent of segregation is larger after 5 minutes than in the larger diameter riser.

In the larger riser the segregation decreases with an increase in the bed height. This finding agrees with the earlier explanation on the influence of the bed height on segregation.

At high gas velocities the segregation decreases strongly. This is in agreement with earlier conclusions and literature findings (Daw and Frazier, Hoffmann and Romp, Schouten et al.).

In general the segregation in the tested system reacts in the same way to changes in gas velocity, bed height and riser diameter as was described by Schouten et al. (1988). In this work however the segregation behavior was not described in terms of jetsam and flotsam

particles as Schouten et al. did. They used a binary system whereas in this work a broad particle size distribution is used. The broad particle size distribution complicates the identification of flotsam and jetsam particles: the choice is somewhat arbitrary. In any case the behavior of these particles is an average behavior and cannot be compared to the work of Schouten et al.

Comparing results from the residence time distribution experiments and segregation experiments, it is clear that segregation experiments can predict the mixing process in a circulating fluidized bed in the slugging regime qualitatively. In some cases it can even give quantitative data on residence time distribution. These properties make segregation experiments a simple and valuable tool for exploring and even predicting axial dispersion and residence time distribution.

3.3 Raining

Abanades et al. (1994) stated that complete segregation will always occur when raining of particles prevails in the bed. If raining causes segregation, understanding of the phenomenon may help understand and describe segregation. Therefore the raining of particles was studied.
The velocity at which particles fall in the slug depends on the terminal velocity (Hirschberg and Werther, 1998). Small particles have a smaller terminal velocity so they will fall slower than larger particles. The larger particles will rain onto the top of the next plug before the small particles will. The process takes place continuously throughout the bed. This phenomenon could thus possibly explain the segregation in a slugging fluidized bed. To be able to understand, describe and possibly quantify the segregation as well as gas-solids contact, the rate of raining of particles was studied.

Experiments showed that if the pulse time of a pulse of gas was short, the plug above the slug that is pushed up by the pulse gas may not become stable and will disintegrate. The pulse gas velocity had to be somewhat higher than the gas velocity in the circulating fluidized bed to keep the amount of scatter low enough to be able to get results from the experiments. This higher gas velocity could lead to different results than in the circulating fluidized bed. A number of experiments were performed with a larger pulse time and a lower gas velocity to

compare the plug velocities with those found in the circulating fluidized bed. As can be seen in figure 19 plug velocities in the standpipe and in the CFB are comparable.

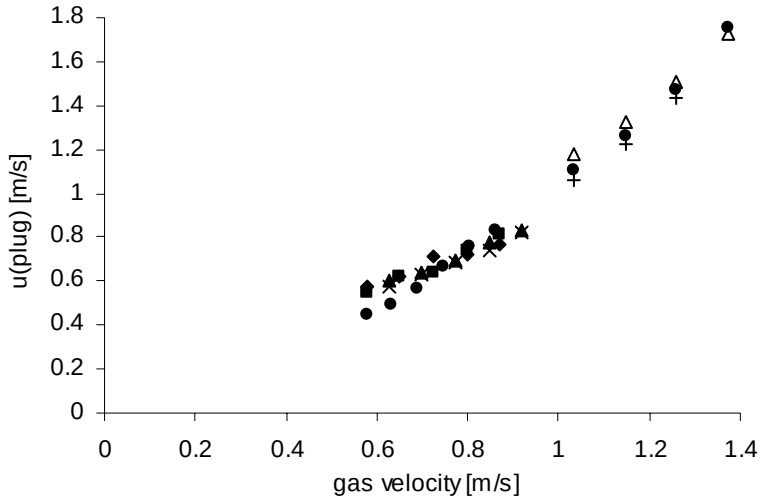

Figure 19: comparison between plug velocity in standpipe and CFB. Experiments done in a 44 mm riser; 'total' powder used. △: 70 cm bed; ●: 90 cm bed; +: 110 cm bed; ◆: G_s=2.9 kg/m^{2}s; ■: G_s=3.5 kg/m^{2}s; ▲: G_s=5.8 kg/m^{2}s; ×: G_s=6.5 kg/m^{2}s

Raining rates were measured for a combination of bed height, pulse gas velocity and pulse length. From the results of all experiments, no correlation between the raining rate and the gas velocity could be found. Therefore, it was concluded that the raining rate is independent of the gas velocity.

There is always a discontinuity in gas velocity at the interface at the bottom of a plug, as the interstitial gas velocity inside the plug is higher than u_0. Therefore, the solids at the interface experience a lower drag compared to the solids inside the plug, resulting in the raining of particles from the interface. It is believed that this difference in drag is not changed when the gas velocity is changed, since the plug as also pushed up faster when the gas velocity is higher.

Also, no correlation between raining rate and pulse length was found, so the raining rate was concluded to be also independent of the pulse length. Pulse length will not change the physical situation at the interface between plug and slug.

3.3.1 Influence of the bed height

A linear dependency of the raining rate on the bed height was found (figure 20). A possible explanation for the increase in the raining rate is that as the bed height increases, the amount of solids that is pushed up in the riser (i.e. plug length) increases. As the gas pushes up the plug through the riser, the bottom zone of the plug will be compressed slightly, thereby decreasing the porosity in the bottom zone of the plug. This effect will be larger for the longer plugs than for the shorter plugs. The explanation as to why this results in a higher raining rate lies in the nature of the raining phenomenon.

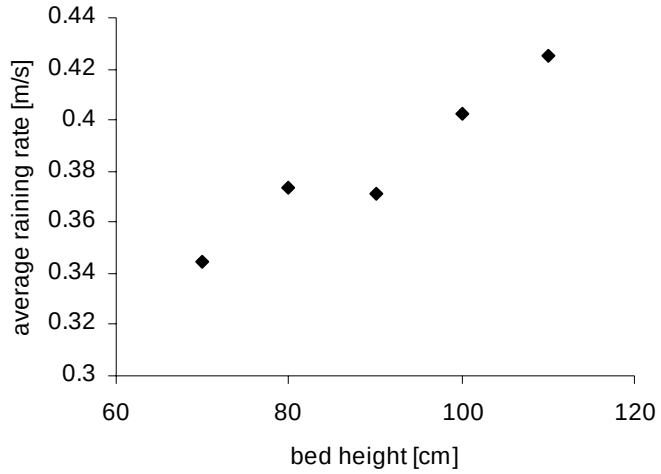

Figure 20: average raining rate vs bed height. Bed diameter 105.6 mm.
Measured with pulse length of 0.7 sec., 'total' powder used.

For the longer plugs the difference in drag between particles at the interface and particles in the plug will be more pronounced, as the gas porosity in the bottom zone of the plug is lower, resulting in a larger difference in gas velocities inside and outside the plug. Thus, the raining rate will be larger for longer plugs.

These results are in contrast with the results from the residence time distribution experiments and segregation data. Segregation is faster at higher gas velocities. The average bed height however is lower at higher gas velocities and it is expected that the plugs are then also shorter. Results show that the spread in residence time is larger at higher gas velocities. Also segregation is faster at higher gas velocities, whereas the raining is found to be less at lower bed heights.

The comparison of results leads to the conclusion that the raining of solids through slugs is not the responsible mechanism for segregation of solids. Most probably the mixing of solids in the dense plugs will be the dominant mechanism for segregation. More experiments need to be done to determine the responsible mechanism for the mixing of solids.

In part II of this work the plug velocity was studied. Also the plug length was measured with which the plug velocity could be described. In part II a mathematical description is given to describe the plug velocity as a function of gas velocity, solids flux, particle size and particle size distribution, bulk density and plug length.

4 Conclusions

Experiments were done to determine the average residence time and residence time distribution of particles of different size in a circulating fluidized bed operated in the slugging fluidization regime in the riser. Tracer particles were used to determine the residence time. Next to that, average hold up and solids flux was measured from which average residence time could be calculated.

To understand the spread in residence time, segregation of particles according to size was investigated. A polymer powder was fluidized for a certain time in a standpipe and the average particle size as function of the height in the column was measured.

Raining of particles through slugs was investigated to try to understand the mechanism responsible for segregation. The raining rate was determined as a function of time and of different process parameters such as gas velocity, solids flux and pulse time.

Summarizing the results presented in this work, it may be concluded that mixing effects play a major role in square nosed slugging fluidization; they tend to give a more plug flow like behavior than in bubbling or fast fluidization for the used polyethylene powder with a broad particle size distribution.

Mixing of particles of different size occurs in square nosed slugging fluidization, its extent depends on riser diameter, gas velocity, hold up and solids flux in the riser. The influence of these factors causes the slugging fluidization regime to have a broad operating range, from operating in the plug flow regime to a operating as a well-mixed system.

A higher gas velocity causes a shorter residence time. The gas velocity shortens the average residence time by causing a lower hold-up of particles in the riser. The hold-up is significantly lowered at higher gas velocities. A higher solids flux also shortens the average residence time. Both influences can be quantified for the used system and powder.

A higher solids flux causes a smaller spread in residence time, whereas the gas velocity broadens of the spread in residence time. A clear dependency between solids flux and spread in residence time was found, as well as a dependency between gas velocity and spread in residence time. The results however can only be used qualitatively because of the intermittent nature of the slugging fluidization, which requires many experiments to give acceptable accuracy.

When comparing data from segregation experiments and residence time experiments it is clear that segregation data can predict the spread in residence time as a function of overall residence time, particle size and gas velocity. The differential velocity between small and large particles found in the segregation experiments can account for the spread in residence time as found in the residence time distribution experiments with a powder with a broad particle size distribution. Also the larger spread in residence time at higher gas velocities can qualitatively be predicted by the segregation data. Thus, segregation experiments can be used as a simple tool to explore the mixing behavior in a gas solids fluidized system.

Raining of particles through slugs occurs in the square nosed slugging regime. Raining rates of particles can be determined. The raining of particles was expected to determine the difference in residence time between small and large particles because of the difference in terminal velocity of particles of different size. Experiments however prove this phenomenon not to be the determining factor in the mixing process for the solids in the fluidized bed. Data from raining experiments contradict earlier conclusions from residence time and segregation experiments and this contradiction leads to the conclusion that mixing of solids will mainly take place in the dense plugs.

5 Literature

Abanades, J.C., S. Kelly, G.P. Reed (1994). "A mathematical model for segregation of limestone-coal mixtures in slugging fluidised beds." Chemical Engineering Science **49**(23): 3943-3953.

Beeckmans, J.M. and Agrawal, R. (1994). "Studies on transport processes in a segregating fluidised bed." Powder Technology **80**: 17-23

Daw, C.S. and Frazier, G.C. (1988). "A quantitative analysis of binary solids segregation in large-particle gas-fluidized beds." Powder Technology **56**: 165-177

Gibilaro, L.G. and Rowe, P.N. (1974). “A model for a segregating gas fluidised bed.” Chem. Eng. Sci. **29**: 1403-1412

Hirschberg, B. and Werther, J. (1998). "Factors affecting solids segregation in circulating fluidized-bed riser." AIChE journal **44**(1): 25-34

Hoffmann, A.C. and Romp, E. J. (1991). "Segregation in a fluidised powder of a continuous size distribution." Powder Technology **66**: 119-126

Kunii, D. and Levenspiel, O. (1991). Fluidization Engineering, 2nd ed. Butterworth-Heinemann, Boston: 68-72

Lim, K.S., Khakhar, D.V., Chen, Z., Agarwal, P.K. (1997). "Raining of particles from an emulsion-gas interface in a fluidized bed." Chem. Eng. Comm **161**: 205-229

Nakagawa, N., Bai, D., Shibuya, E., Kinoshita, H., Takarada, T., Kato, K. (1994). "Segregation of particles in binary solids circulating fluidized beds." Journal of Chemical engineering of Japan **27**(2): 194-198

Nienow, A.W., Rowe, P.N., Chiba, T. (1978). A.I.Ch.E. Symp.Ser. **74**(176): 45-53

Nienow, A.W., Naimer, N.S., Chiba, T. (1987). Chem. Eng. Comm. **62**: 53

Schouten, J.C., Valkenburg, P.J.M., van den Bleek, C.M. (1988). "Segregation in a slugging FBC Large-particle system." Powder Technology **54**: 85-98

Sciazko, M. and Brandowski, J. (1995). "High-pressure segregation of solids with a wide particle size distribution when fluidized with a gas." The chemical engineering journal **60**: 89-95.

Thiel, W.J. and Potter, O.E. (1977). "Slugging in fluidized beds." Industrial & Engineering Chemistry Fundamentals **16**(2): 242-247

Yasui, G. and Johnson, L.N. (1958). AIChE Journal **4**: 445-452

Wu, S.Y. and Baeyens, J. (1998). "Segregation by size difference in gas fluidized beds." Powder Technology **98**: 139-150

Chapter 3

Fluidization behavior in a circulating fluidized bed reactor for olefin polymerization operated in the slugging regime. Part II: Plug characteristics

---

Abstract

In the transporting square nosed slugging fluidization regime ($0.4<u_0<1.0$ m/s) a bed of polyethylene powder with a low density (ρ = 900 kg/m^3) and a large particle size distribution ($70<d_p<1600$ μm) was operated in two circulating fluidized bed systems (riser diameters 0.044 m and 0.105 m). A relation was derived for the plug velocity as a function of the gas velocity, solids flux, riser diameter, particle size range and particle and powder properties.
The influence of the plug, the raining rate of solids onto and from the plugs and the of the particle size range on the plug velocity is accounted for.

1 Introduction

In chapter 2 it was explained that measurements on the hydrodynamics in a riser of a circulating fluidized bed reactor for olefin polymerization operated in the slugging regime (Weickert, 2000) were done to understand and describe the slugging fluidization regime. In chapter 2 the research was concentrated on the overall solids mixing expressed in the residence time and residence time distribution of solids in the riser of the circulating fluidized bed as well as segregation of particles of different size and raining of particles through slugs. In this chapter measurements on the hydrodynamics, the characteristics of plugs are done to further understand and interpret the overall solids mixing mechanisms in the slugging fluidization in terms of plug length and plug velocity and eventually be able to describe heat transfer in a model.

The fluidized bed reactor is operated in the square nosed slugging regime. With the polymer powder used in the current research square nosed slugging is observed. Square nosed slugging can occur with powders like coarse powders (group D powders). In contrast to round nosed slugging, in square nosed slugging particles do not flow along the side of the slug downward to mix up in the wake under the slug. In square nosed slugging particles rain down through the slug over the whole area of the slug. The velocities of slugs are influenced partly by the raining of particles through the slugs.

Square nosed slugging is studied only limited and further research is necessary for understanding and eventually modeling of the slugging behavior. In contrast to many other fluid bed conversion processes for the slugging fluidized bed, an accurate understanding of the phenomena occurring in the particle phase is very important. The particles are both the catalyst and the product. Therefore understanding of the plug characteristics is important; they are essential for correct description of local reaction rates and heat transfer to the wall.

Because the polymerization reaction is very exothermic, reaction temperatures can become very high. Heat is produced in the polymer particles in which catalyst is distributed. With fresh particles heat production is high and heat removal is difficult. The catalysts used in the polymerization process will be deactivated at higher temperatures, causing a lower production. Also the polymer can melt because of the higher temperatures, causing quality problems in the polymer and operational problems.

In this chapter attention is devoted to the actual velocity of solids in the riser. This velocity is necessary for description of the heat transfer in the riser column. Heat transfer in plugs and

slugs is different. Therefore the plug length and plug velocity are crucial for the product properties.

1.1 Plug velocity

In the slugging fluidization regime the gas slugs have velocities close to the gas velocity and will push the packets of solids or plugs above them up with about the same velocity. In square nosed slugging fluidization solids rain down from the plugs through the slugs on top of the plugs below them. This movement causes an oscillating velocity of solids in the riser. The actual velocity of solids in the riser column is therefore sometimes much higher and sometimes much lower than can be expected from the residence time of the solids and the length of the column.

Much attention is devoted to slug velocity in literature, but the interest of the current research is on the particles and thus on the plugs above the slugs as is explained in part I. The relations to describe the slug velocities can however also be used in the understanding of the mechanisms responsible for the velocities of the plugs. The plugs move through the column with about the same velocities as the slugs that push up the plugs. Therefore, the same relations might apply for the plugs although the basis for the expressions is different, as will be shown.

Most work done on the description of the slug velocity is focused on the velocity of round nosed slugs or wall slugs. Some research focused on slugs in liquid, for instance Ormiston (1965). Round nosed slugs were further studied by Stewart and Davidson (1967), Kehoe and Davidson (1971), Baeyens and Geldart (1974) Fan et al. (1983) and Lee et al. (2002). The expressions for slugs in liquid were also applied to slugs in fluidized beds of particles. However, for understanding of the slugging phenomena an overview of work on the velocity round nosed slugs is given.

Ormiston et al. (1965) gave an overview of workers who studied air slugs in water and defined the slug velocity to be

$$u_{sl} = k_2 \sqrt{gD} \tag{1}$$

with k_2 having various values around 0.35. This is the velocity of the slugs relative to the fluidized medium. This expression could be derived from analysis of streamlines around the nose of the slug, as was done by Davies and Taylor (1950) and Stewart and Davidson (1967).

For continuously generated slugs rising through a stagnant fluidized medium, the often used general description for the slug velocity reads:

$$u_{sl} = k_1\left(u_0 - u_{mf}\right) + k_2\sqrt{gD} \tag{2}$$

With k_1 = 1.2 (Davidson and Harrison, 1963) and k_2 = 0.361 as found by Ormiston et al. (1965) and Layzer (1955). More recently, Fan et al (1983) derived an expression for k_1. They found in their model I:

$$k_1 = 2.43\left(\frac{\overline{d_p}}{D}\right)^{-0.5}\left(\frac{\rho_s}{1000\rho_g}\right)^{-4.2} \tag{3}$$

by defining a dimensionless particle size and a dimensionless particle density. They suggested however that the slug rise velocity was not dependent on the volume of the slug. In their model II they assume that the behavior of slugs is influenced mostly by the characteristics of the column wall and is affected only slightly by the particle properties and the column size. This is not in agreement with the expression for k_1 in their model I. Lee and Kim (1989) followed this derivation but found a slightly different expression for k_1, based on a fit of experimental results.

Lee et al. (2002) found that the rise velocity of slugs was dependent on the bed height due to slug coalescence. They work with powders that cause square nosed slugging and report, in accordance with findings of Noordergraaf et al. (1987), that the velocity of square nosed slugs is lower than the superficial gas velocity. The slope of slug rise velocities, expressed in the constant k_1 for particles causing square nosed slugging is also lower than for beds with round nosed slugging.

1.2 Plug length

To further understand and describe the movement of solids in the riser, it is necessary to study the plug characteristics such as the plug length; the length of a plug will influence its velocity as will be shown. In most research more emphasis is put on the study of slugs than on the study of plugs. In fluidization research the slug length is well studied, whereas the plug length received less attention. A summary of research on slug length will be given for understanding. These relations might apply to describe plug length.

Kehoe and Davidson (1973) derived an equation for the slug length based on pressure fluctuations in an ideally slugging (single slug) fluidized bed:

$$\frac{L_{sl}}{D} - 0.495\left(\frac{L_{sl}}{D}\right)^{1/2}\left[1+\frac{u_0-u_{mf}}{0.35\sqrt{gD}}\right] + 0.061 - (T-0.061)\left[\frac{u_0-u_{mf}}{0.35\sqrt{gD}}\right] = 0 \quad (4)$$

For large particle systems the slug length is given by (De Luca et al. 1992):

$$\frac{L_{sl}}{\sqrt{DH_{mf}}} = 2.09\frac{u_0-u_{mf}}{\sqrt{gD}} - 0.37 \quad (5)$$

The angle of internal friction (φ) determines the maximum plug length possible (Gibilaro, 2001):

$$\tan\varphi = \frac{L_{\max}}{D} \quad (6)$$

This relation however is only of interest for single-slug systems. In multi slug systems this maximum plug length is never reached because of the contact forces between plugs and raining of particles. An average plug and slug length has to be used in multi-slug systems.
In this chapter it will be shown that the slug or plug velocity in square nosed slugging is described as a function of the slug or plug length. New results on plug velocity and plug length are presented.

1.3 Raining of solids

For the measurement of the raining rate the bed height is used as a measure for the plug length. A minimal amount of solids in the riser will however not be pushed up by the slug. This is the part of the bed that would be the dense bubbling zone at the bottom of the riser, where bubbles did not yet grow large enough to become slugs. So the plug length can be calculated from the used bed height and the height of the dense bed of solids at the bottom of the riser. The calculation of the height of the dense part of the bed might however not be very accurate. Only few authors have given an expression for the height of the dense bed. De Luca et al. (1992) gave an expression:

$$H_{bf} = 68.6\frac{(rD)^{1.235}}{(u_0-u_{mf})^{1.37}} \quad (7)$$

when the ratio between the bubble and bed diameter, r, is larger than 0.5 and when the bed height is higher than the limiting bed height H_L defined by:

$$H_L = 60D^{0.175} \quad (8)$$

2 Experimental

Two types of experiments were carried out. The first type of experiments was used for different studies. Gas velocity, solids flux, riser diameter and particle size range were varied. With the data from the detectors (chapter 2) the plug velocity and the plug length could be measured. The length of a plug can change during the lifetime of a plug and this can be followed in the measured data.

The second type of experiments was used to study raining of particles through slugs. The growing height of the dense bottom zone of the powder bed was measured. The dense zone grew because of particles raining onto the dense zone. The gas velocity was varied. From the measurements the raining rate as function of gas velocity could be determined.

2.1 Determination of plug characteristics

Two set ups (set up A and set up B) with the same configuration were used, as are described in chapter 2. With the detectors described in chapter 2 and analysis of the measurement data from the detectors plug velocities and plug lengths could be determined. In the 105 mm riser the array of detectors needed to be elongated (table 1) as compared to the 44 mm riser to be able to measure the larger plug lengths (table 2). The polyethylene powder as was described in chapter 2 was used.

Table 1: overview of vertical positions of detector array in the 105 mm riser experiments for measuring plug velocity and plug length. Heights above distributor plate.

Vertical position of array in riser	lowest detector [m]	highest detector [m]	length of array [m]	distance between detectors [m]
upper zone	1.810	2.795	0.985	0.003177
lower zone	0.695	1.795	1.100	0.003548

Table 2: overview of vertical positions of detector array in the 44 mm riser experiments for measuring plug velocity and plug length. Heights above distributor plate.

Vertical position of array in riser	lowest detector [m]	highest detector [m]	length of array [m]	distance between detectors [m]
upper zone	2.452	3.126	0.674	0.00217
middle zone	1.295	1.915	0.620	0.00220
lower zone	0.750	1.406	0.656	0.00212

2.1.1 Raining of solids

A standpipe was created by altering set up B as described in chapter 2. In the standpipe the growth of the height of the dense bottom zone of the bed was measured with detectors. This growth of the height of the dense bottom zone is a measure for the raining rate. The raining rate is expressed in meters of powder bed growth.

3 Results

3.1 Plug velocity

Different gas velocities were applied, with polymer beds of different particle size ranges. Influence of gas velocity on the plug velocity could be determined. Experiments were done in two different set-ups with risers with different diameters so that influence of riser diameter could be determined as well.

3.1.1 Influence of the gas velocity

Velocities of plugs, the dense phase packets of solids on top of gas slugs, were measured as a function of gas velocity, solids flux through the riser, riser diameter and height in the riser column.

The plug velocity is given as a function of $(u-u_{mf})$, in accordance with representation in literature (figure 1). The plug velocity seems to have a linear dependency on the gas velocity.

The diameter of the riser does not have a profound influence on the size of the plug velocity but more on the development of the plug velocity with increasing riser diameter. The plug rise velocities increase less with increasing gas velocity in the larger diameter than in the smaller diameter. The plug velocities are lower when measured at a higher position in the riser. This is most visible in the smaller diameter riser.

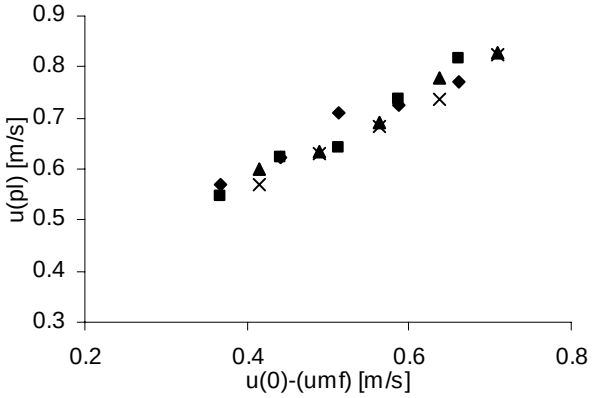

Figure 1a: plug velocity vs excess gas velocity in lower zone of 105 mm diameter riser. Comparison of plug velocities at different solids fluxes. ♦: G_s = 2.9 kg/m^{2}s; ■: G_s = 3.48 kg/m^{2}s; ▲: G_s = 5.84 kg/m^{2}s; ×: G_s = 6.45 kg/m^{2}s

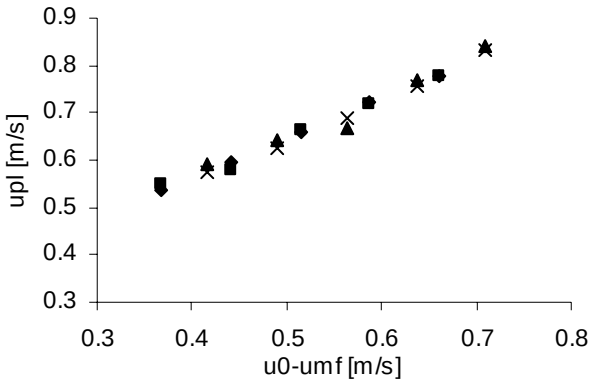

Figure 1b: plug velocity vs excess gas velocity in upper zone of 105 mm diameter riser. Comparison of plug velocities at different solids fluxes. ♦: G_s = 3.37 kg/m^{2}s; ■: G_s = 4.14 kg/m^{2}s; ▲: G_s = 7.38 kg/m^{2}s; ×: G_s = 8.08 kg/m^{2}s

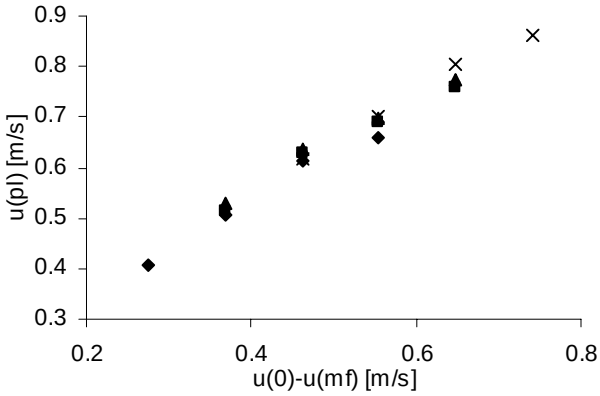

Figure 1c: plug velocity vs excess gas velocity in lower zone of 44 mm diameter riser. Comparison of plug velocities at different solids fluxes. ♦: G_s = 3.27 kg/m^{2}s; ■: G_s = 5.45 kg/m^{2}s; ▲: G_s = 8.3 kg/m^{2}s; ×: G_s = 10.52 kg/m^{2}s

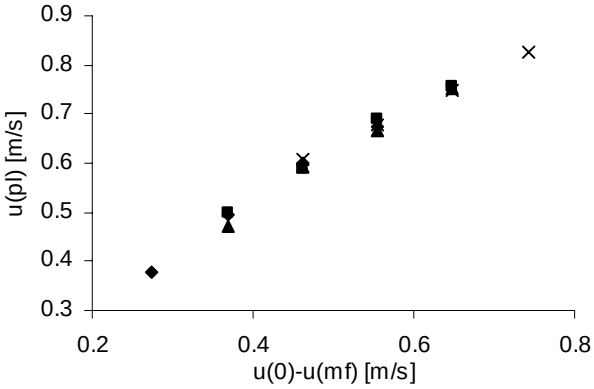

Figure 1d: plug velocity vs excess gas velocity in middle zone of 44 mm diameter riser. Comparison of plug velocities at different solids fluxes. ♦: G_s = 3.27 kg/m^{2}s; ■: G_s = 5.45 kg/m^{2}s; ▲: G_s = 8.3 kg/m^{2}s; ×: G_s = 10.52 kg/m^{2}s

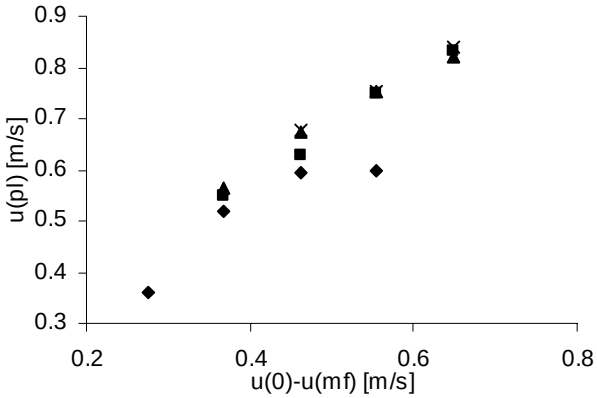

Figure 1e: plug velocity vs excess gas velocity in middle zone of 44 mm diameter riser. Comparison of plug velocities at different solids fluxes. ♦: G_s = 3.27 kg/m^{2}s; ■: G_s = 5.45 kg/m^{2}s; ▲: G_s = 8.3 kg/m^{2}s; ×: G_s = 10.52 kg/m^{2}s

3.1.2 Influence of the particle size

The different particle size fractions were fluidized separately to determine influence of the average particle size on the velocity of the plugs. The particle size fractions were fluidized in both the 44 mm and the 105 mm riser. Results (figure 2) show that the particle size range has a profound influence on the plug rise velocities.

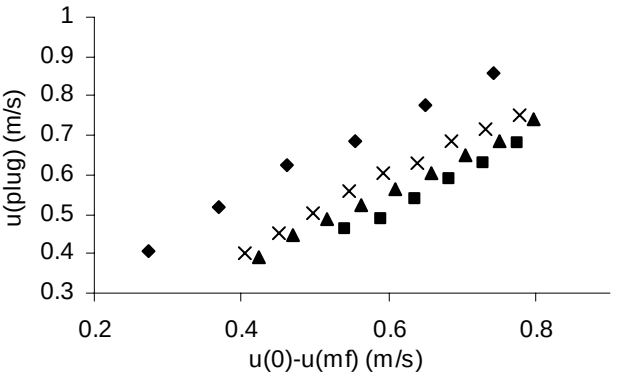

Figure 2a: plug velocity vs exces gas velocity. Plug velocities in lower part of 44 mm diameter riser (75 cm-141cm above distribution plate). ♦: 'total' powder; ×: 420 μm<dp<800 μm; ▲: 800 μm<dp<1200 μm; ■: dp>1200 μm.

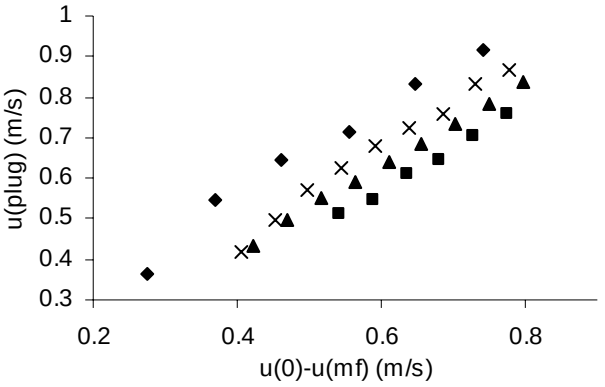

Figure 2b: plug velocity vs excess gas velocity. Plug velocities in higher part of 44 mm diameter riser (245cm-313cm above distribution plate). ♦: 'total' powder; ×: 420 μm<dp<800 μm; ▲: 800 μm<dp<1200 μm; ■: dp>1200 μm.

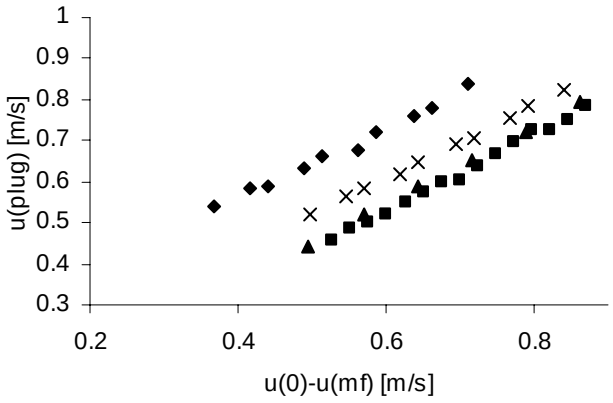

Figure 2c: plug velocity vs excess gas velocity. Plug velocities in higher part of 105 mm diameter riser (181cm-279cm above distribution plate). ♦: 'total' powder; ×: 420 μm<dp<800 μm; ▲: 800 μm<dp<1200 μm; ■: dp>1200 μm.

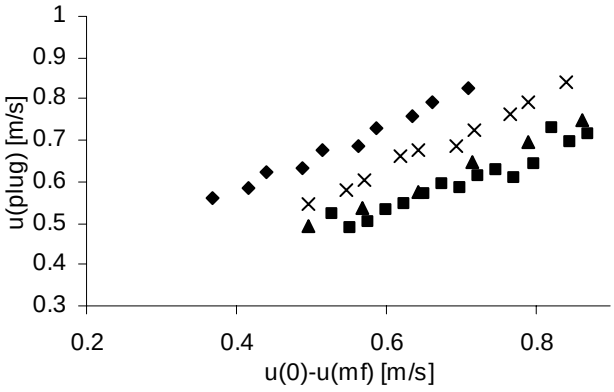

Figure 2d: plug velocity vs excess gas velocity. Plug velocities in lower part of 105 mm diameter riser (69cm-179cm above distribution plate). ♦: 'total' powder; ×: 420 μm<dp<800 μm; ▲: 800 μm<dp<1200 μm; ■: dp>1200 μm.

For larger particle diameters the plug velocities are lower at a given gas velocity. For the different ranges this trend is clearly visible. However the 'total' powder shows significantly larger plug velocities although the average particle diameter is smaller than for the 'large' particle range.

The trends in the plug velocities for the different particle size ranges are the same for both riser diameters, although in the 105 mm riser almost no distinction can be made between the plug velocities of the 'average' size fraction and the 'large' size fraction.

3.2 Plug length

The plug lengths were measured for different gas velocities and different particle size ranges in both the 44 mm riser and the 105 mm riser. Results are shown in figure 3. The plug lengths

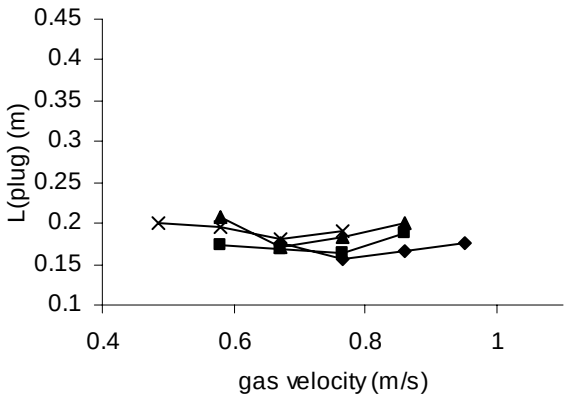

Figure 3a: plug length vs gas velocity, in lower part of 44 mm riser (75cm-141cm above distribution plate), 'total' particle size distribution. ♦: G_s= 10.52 kg/m^{2}s; ■: G_s= 8.3 kg/m^{2}s; ▲: G_s= 5.45 kg/m^{2}s; ×: G_s= 3.27 kg/m^{2}s

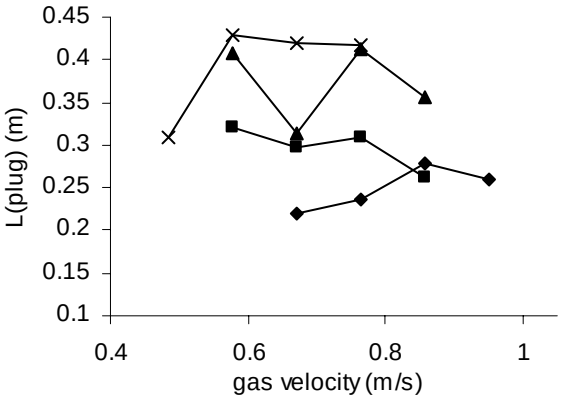

Figure 3b: plug length vs gas velocity, in middle part of 44 mm riser (129cm-191cm above distribution plate), 'total' particle size distribution. ♦: G_s= 10.52 kg/m^{2}s; ■: G_s= 8.3 kg/m^{2}s; ▲: G_s= 5.45 kg/m^{2}s; ×: G_s= 3.27 kg/m^{2}s

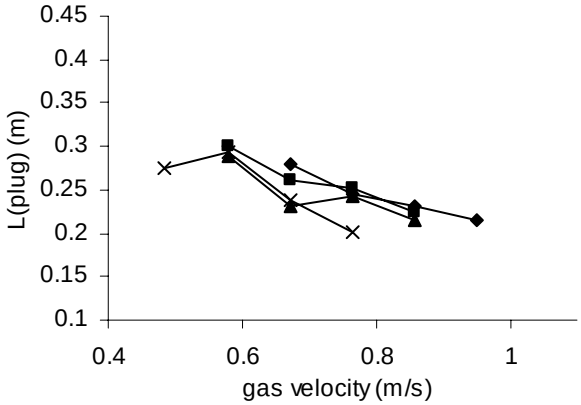

Figure 3c: plug length vs gas velocity, in upper part of 44 mm riser (245cm-313cm above distribution plate), 'total' particle size distribution. ♦: G_s= 10.52 kg/m^{2}s; ■: G_s= 8.3 kg/m^{2}s; ▲: G_s= 5.45 kg/m^{2}s; ×: G_s= 3.27 kg/m^{2}s

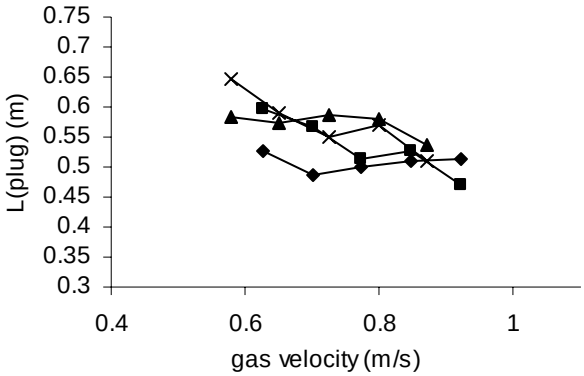

Figure 3d: plug length vs gas velocity, in lower part of 105 mm riser (70cm-180cm above distribution plate), 'total' particle size distribution. ♦: G_s= 6.45 kg/m^{2}s; ■: G_s= 5.84 kg/m^{2}s; ▲: G_s= 3.48 kg/m^{2}s; ×: G_s= 2.9 kg/m^{2}s

given are average plug lengths of a number of measurements.

As can be seen, the height at which the plug length is measured is of influence on the results. This can be explained from the slugging fluidization itself. At lower height in the bed the plugs are still being formed, resulting in rather short plugs. In the middle zone of the riser plugs are increasing and decreasing in length because of raining of solids onto and from them. They are completely developed, having a large average length. In the upper zone of the riser the plugs only loose solids because of raining and are therefore shorter again than in the middle zone.

The plug length in the middle zone is most important, since only the middle zone will increase when scaling up whereas the lower zone and the upper zone will remain the same. Exit effects affect the upper zone of the riser and the lower zone is affected by the creation of plugs from the dense bottom zone of the powder bed. Only the riser diameter has influence on the heights of these zones.

The solids flux does not have a large influence on the length of the plugs in the lower and upper zones of both risers: the results for the measurements with different solids fluxes are approximately the same. But the solids flux causes a spread in plug length in the middle zone, where raining onto and from the plugs takes place. The plug length is largest at the lowest solids flux and is smallest at the highest solids flux. The trend in plug length seems to be linear with the solids flux (figure 4). The results however show a fairly large scatter. Also this dependency is not found in the results for the lower and the upper part of the riser.

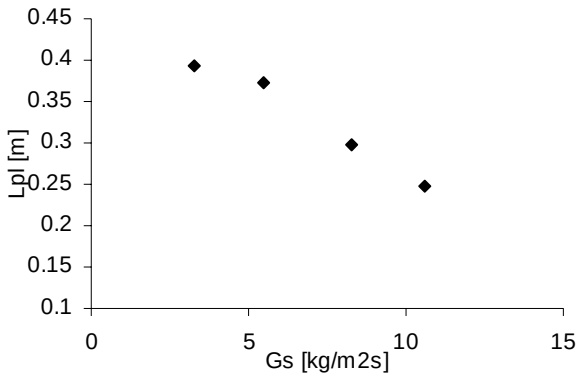

Figure 4: Plug length in middle zone of 44 mm diameter riser (129cm-191cm above distribution plate) as function of the solids flux. Average plug length calculated for different solids fluxes.

In the results for the 105 mm diameter riser a dependency on the solids flux was found. A specific middle zone was not measured. The lower and upper zones were large enough to occupy the whole riser zone.

When looking at the results of the plug lengths measured in the 105 mm diameter riser, it is clear that the larger diameter causes larger plugs to appear. The aspect ratio of the plugs in the lower part of the 105 mm diameter riser is roughly 5.2 whereas the aspect ratio for the plugs in the upper zone of the 44 mm diameter riser is 4.5. The plug lengths in the 105 mm riser are measured relatively lower than in the 44 mm riser, what means that the plugs were expected to be smaller: the trend in plug length versus height in the bed shows smaller plugs lower in the riser. When measurements higher in the 105 mm riser would have been possible, it is expected that even larger plugs would be found.

The gas velocity has a limited influence on the length of the plugs. The plug length is shorter at higher gas velocities, what is expressed most in the middle and upper zone of the 44 mm riser and in the 105 mm riser. The results for the middle zone of the 44 mm riser are scattered and a dependency is hard to determine. Still, for understanding a dependency is determined.

3.3 Solids raining rate

Raining rates were measured at different solids loadings of the standpipe, expressed as bed height. The larger the bed height is the larger the plugs will be that are pushed up. For accurate description of the plug length the height of the dense bottom zone of the bed is calculated. This height is only 5.5 cm in the 105 mm riser according to the calculations. This is however not the case in the raining experiments where the dense bed is much higher than that. It is assumed therefore that the plug length can be taken in the calculation for the raining rate since the packet of solids pushed up by the pulse will have approximately the same length as a normal plug.

In chapter 2 raining rates were measured for a combination of bed height, pulse gas velocity and pulse length. From the results of all experiments, no correlation between the raining rate and the gas velocity could be found. Also, no correlation between raining rate and pulse length was found, so the raining rate was concluded to be independent of the pulse length. However, a linear dependency of the raining rate on the bed height was found.

4 Discussion

4.1 Influence of the gas velocity

Gas velocity has a large influence on the plug velocity, as can be expected. However, the plug velocities are not the same as the gas velocities. Some of the gas ‘slips’ through the plugs.

When relations from literature are used to describe the measured plug velocity, it is clear that these relations do not apply. When equation 2 is fitted to the results for the middle zone in the 44 mm riser for all particle size ranges, it is clear that k_1 and k_2 do not have the same values as mentioned in literature (table 3).

Table 3: Fit of equation 2 to results of middle zone 44 mm riser and upper zone 105 mm riser.

Riser diameter [mm]	Zone in the riser	particle size range [μm]	k_1 [-]	k_2 [-]
44	lower	$70< d_p < 1600$	0.95	0.24
44	lower	$420< d_p < 800$	0.94	0.05
44	lower	$800< d_p < 1200$	0.90	0.03
44	lower	$d_p > 1200$	0.96	-0.10
44	middle	$70< d_p < 1600$	0.95	0.21
44	middle	$420< d_p < 800$	1.12	-0.3
44	middle	$800< d_p < 1200$	0.96	-0.25
44	middle	$d_p > 1200$	1.04	-0.38
44	upper	$70< d_p < 1600$	1.13	0.14
44	upper	$420< d_p < 800$	1.17	-0.04
44	upper	$800< d_p < 1200$	1.05	0.00
44	upper	$d_p > 1200$	1.07	0.12
105	lower	$70< d_p < 1600$	0.78	0.26
105	lower	$420< d_p < 800$	0.84	0.13
105	lower	$800< d_p < 1200$	0.72	0.12
105	lower	$d_p > 1200$	0.66	0.14
105	upper	$70< d_p < 1600$	0.85	0.22
105	upper	$420< d_p < 800$	0.89	0.08
105	upper	$800< d_p < 1200$	0.95	-0.02
105	upper	$d_p > 1200$	0.95	-0.05

Velocities of plugs are described in literature with the same expressions as are developed for the velocities of slugs. However, the basis for the development of these expressions is different from the nature of the plugs and can therefore not be expected to describe the velocity of the plugs. The basis for the description of the slug velocity was found by analysis

of streamlines around the noses of the slugs, but in the case of plugs in the square nosed slugging regime no streamlines are present in the fluidum. In fact in the square nosed slugging regime the fluidum does not flow around the slug, but particles fall through it so the relations for round nosed slugs will in principle not apply for square nosed slugs.

It seems that the value of k_1 is dependent on the position in the riser and on the riser diameter. The values for k_1 with the 105 mm riser diameter are lower than the values with the 44 mm riser. However, the trend in the values of k_1 and k_2 suggest a rotation: when the value of k_1 increases, the value of k_2 decreases. This suggests an influence of possibly one parameter in both constants. To be able to use the influence of different parameters in modeling, a new mathematical description for the plug velocity was derived.

A new relation was derived. The plug velocity is generally the same as the gas velocity, but with some adjustments. The basis for the plug velocity is given by equation 2, in that the first term accounts for the direct influence of the gas velocity on the plug, and that the second term is the result of a force balance around the plug in the fluidum.

In the force balance, the plug is described as a cylinder, its volume being calculated as $V = \frac{\pi D^2}{4} \cdot L_{pl}$. The derivation of the force balance around a plug is:

$$\Sigma F = -F_g + F_b + F_{fr,g} - F_{fr,w} \tag{9}$$

All forces from gravity, buoyancy and friction from the gas with the particles are taken into account. The friction with the wall is assumed to be negligible compared to the friction between the particles.

$$\Sigma F = -\rho_b g \frac{\pi}{4} D^2 L_{pl} + \rho_g g \frac{\pi}{4} D^2 L_{pl} + \frac{1}{2} \rho_b u_0^2 \frac{\pi}{4} D^2 c_f \tag{10}$$

with:

$$c_f \frac{1}{2} \rho_b u_0^2 = \rho_b g L_{pl} - \rho_g g L_{pl} \tag{11}$$

This results in the following relation for the plug velocity relative to the fluidum:

$$u_{pl,rel} = \sqrt{2\frac{\rho_b - \rho_g}{c_f \rho_b}} \cdot \sqrt{gL_{pl}} \tag{12}$$

As can be seen not the diameter of the column is of influence on the relative plug velocity, but the length of a plug. The term $\sqrt{2\frac{\rho_b - \rho_g}{c_f \rho_b}}$ in equation 12 is the same as the constant k_2 in equation 2. This means that a relation for the description of the plug length is needed.

With an expression for length of a plug the velocity of the plug relative to the fluidum can be calculated. The absolute plug velocity however is calculated with one more contribution: the apparent plug velocity due to raining of solids onto and from the plugs. Raining of solids takes place through the slugs and makes plugs grow and shrink, but raining of solids also increases the visual plug velocity. In fact, the absolute plug velocity is calculated as:

$$u_{pl} = k_1\left(u_0 - u_{mf}\right) + \sqrt{2\frac{\rho_b - \rho_g}{c_f \rho_b}} \cdot \sqrt{gL_{pl}} + u_{pl,r} \tag{13}$$

The structure is roughly the same as of equation 2, but the calculation of the various contributions to the plug velocity is different.

4.2 Influence of the plug length

When all influences are summarized and put together, a relation for the plug length is found that is dependent on the gas velocity, the riser diameter and the solids flux and is most valid for the middle zone. The solids flux is of influence only on the abscissas. When comparing this with the relation found by De Luca et al. (1992) there are a few differences. The dependency of the plug length with the riser diameter is quite different. Also the influence of solids flux is not taken into account. It is possible that these differences occur because De Luca et al described slug length whereas in this work the plug length is described. The relation of Kehoe and Davidson (1973) also deviates from the results found here.

Comparison with experimental data from the middle zone of the 44 mm diameter riser and the 105 mm diameter riser gives:

$$L_{pl} = -1.2 \cdot D^{0.68} \cdot u_0 - 0.019 \cdot G_s + 2.3 \cdot \sqrt{D} \tag{14}$$

A fit of this relation with experimental data is given in figure 5.

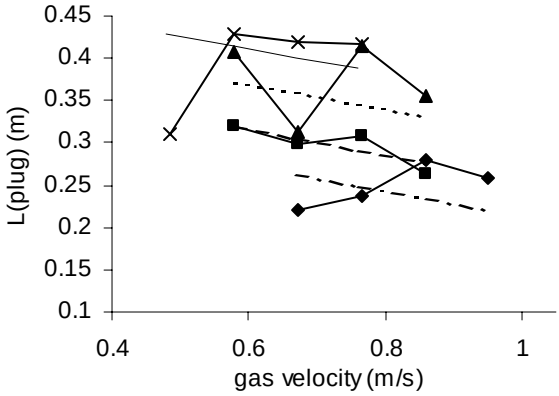

Figure 5a: plug velocity vs gas velocity, 44mm diameter riser, middle zone. Fit of eq. 14 to results. ♦: G_s= 10.52 kg/m^{2}s, __ _ __: fit; ■: G_s= 8.3 kg/m^{2}s, __ __: fit; ▲: G_s= 5.45 kg/m^{2}s, _ _: fit; ×: G_s= 3.27 kg/m^{2}s, ____: fit.

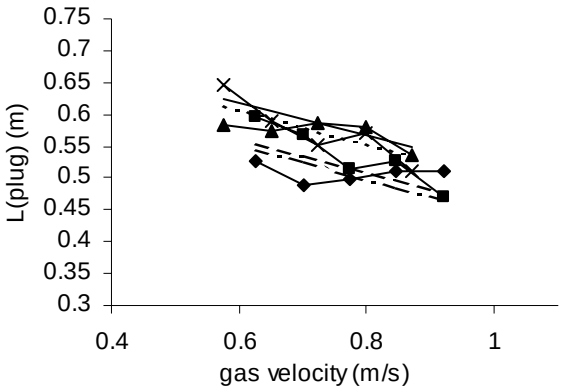

Figure 5b: plug velocity vs gas velocity, 105mm diameter riser, lower zone. Fit of eq. 14 to results. ♦: G_s= 6.45 kg/m^{2}s, __ _ __: fit; ■: G_s= 5.84 kg/m^{2}s, __ __: fit; ▲: G_s= 3.48 kg/m^{2}s, _ _: fit; ×: G_s= 2.9 kg/m^{2}s, ____: fit.

4.3 Solids raining rate

In chapter 2 an explanation was given for the increase in raining rate with an increase in bed height. In this work the results of the measurements are used. As an example the expression for the length of a plug (equation 14) is used. Although the actual length of the 'plug' in the raining rate measurements may be different, the trend of the plug velocity with the raining rate will be visualized. The contribution of the raining rate to the plug velocity will then be:

$$u_{pl,r} = 0.021 L_{pl} + 0.0234 \tag{15}$$

When this contribution to the plug velocity is compared to the other contributions in equation 13 it is clear that this contribution is only very small. Nonetheless, this influence from the raining of particles should be taken into account for the sake of completeness.

4.4 Influence of the particle size

In the derivation of the plug velocity the influence of the particle size was not taken into account. Measurements however have shown that the particle size has a profound influence on the plug velocity.

Table 4: results of fit of linear equation to experimental results for plug velocity

Riser diameter [mm]	Zone	Particle size range [μm]	a [-]	b [-]	$u(d_p)$ [-]
44	lower	$70< d_p < 1600$	0.9395	0.16	-0.053
44	lower	$420< d_p < 800$		0.03	0.077
44	lower	$800< d_p < 1200$		-0.01	0.117
44	lower	$d_p > 1200$		-0.05	0.157
44	middle	$70< d_p < 1600$	1.01	0.107	0
44	middle	$420< d_p < 800$		-0.13	0.237
44	middle	$800< d_p < 1200$		-0.19	0.297
44	middle	$d_p > 1200$		-0.25	0.357
44	upper	$70< d_p < 1600$	1.14	0.092	0.063
44	upper	$420< d_p < 800$		-0.01	0.165
44	upper	$800< d_p < 1200$		-0.06	0.215
44	upper	$d_p > 1200$		-0.12	0.275
105	lower	$70< d_p < 1600$	0.745	0.28	-0.173
105	lower	$420< d_p < 800$		0.185	-0.078
105	lower	$800< d_p < 1200$		0.11	-0.003
105	lower	$d_p > 1200$		0.075	0.032
105	upper	$70< d_p < 1600$	0.83	0.18	-0.073
105	upper	$420< d_p < 800$		0.055	0.052
105	upper	$800< d_p < 1200$		-0.01	0.117
105	upper	$d_p > 1200$		-0.025	0.132

When the plug velocities for the different particle size ranges are fitted with a simple linear $y = ax + b$ equation, with x the gas velocity and y the plug velocity, values for a are found that are not equal to 1 (table 4). The plug length L_{pl} however is a function of the gas velocity. When k_1 in equation 13 is set to 1, the deviation from 1 is caused by the term for the plug length L_{pl}. Values for b are found by addition of all contributions in equation 13 except the u_0-u_{mf} term.

Comparison of the results in figure 2 with the simplified equation shows that the influence in particle size is represented in the force balance term by the bulk density in the calculation for

k_2. But the plug velocity is also shifted to higher or lower values by the particle size ranges without a change in the trend in plug velocity with the gas velocity. This means that an additional term must be applied to describe the influence of particle size range.

The height at which the plug velocity measurements were done has influence on the values for *a* and *b*, but this influence is averaged for all measurements. When the system would be scaled up, the middle zone would become more important. However, the values for the 105 mm riser are more consistent with values for the lower and upper zone of the 44 mm riser. The influence of $u(d_p)$ will not change in character when other values are chosen, the structure stays the same. Therefore the values for the equation for $u(d_p)$ are chosen to fit most of the experimental data. Also the diameter of the riser has influence on the values of *a* and *b*. The riser diameter is used in the calculation of L_{pl} and that causes this influence.
It is clear that the particle size range almost has no influence on the slope of the line, but largely influences the abscissas. This means that the influence of particle size range contributes to the value of *b*. So *b* can be calculated with:

$$b = \sqrt{2\frac{\rho_b - \rho_g}{c_f \rho_b}} \cdot \sqrt{gL_{pl}} + u_{pl,r} + u_{d_p} \tag{16}$$

A possible explanation for the influence of the particle size range is the friction of the gas with the particles in a plug. When the particles are smaller, the friction may be larger, causing a larger velocity of the plug. However, the powder with the whole particle size range (the 'total' powder) has an even larger velocity. Therefore, another explanation is that not so much the particle size determines the plug velocity, but more the bulk density of the powder. The 'total' powder has the highest bulk density of all powders and also gives the highest value of *b*. The powder with particle size > 1200 μm has the lowest value of *b* and also the lowest bulk density. Then $u(d_p)$ becomes:

$$u_{d_p} = a \cdot \rho_b + c \tag{17}$$

The value of *c* is calculated and is the value for *b* minus all contributions other than that of $u(d_p)$. The average value is taken and corrected for the value for the 'total' powder; for *a* a slope of 0.0043 is taken. The result is:

$$u_{d_p} = 0.0043 \cdot \rho_b - 2.26 \tag{18}$$

4.5 Plug velocity

Summarizing the above-mentioned influences, the resulting expression for the plug velocity becomes:

$$u_{pl} = \left(u_0 - u_{mf}\right) + \sqrt{2\frac{\rho_b - \rho_g}{c_f \rho_b}} \cdot \sqrt{gL_{pl}} + 0.021L_{pl} + 0.0043\rho_b - 2.24 \qquad (19)$$

A fit of this equation through the experiments is shown in figure 6. For c_f a value of 85 was chosen. This value can be calculated when the Reynolds number of the powder is known but was used as a fit parameter in this study. The fit of the model through the experimental values is quite good, although a fairly large amount of scattering was shown in the experimental results. This could lead to large uncertainties in equation 19, and a fit would be worse. The relation for the plug velocity was found by mechanistic evaluation of the factors influencing the plug velocity. Although uncertainties in the experimental results remain, equation 19 should be valid in a broad range of applications. However, for different powders the constants in the equation need to be re-evaluated.

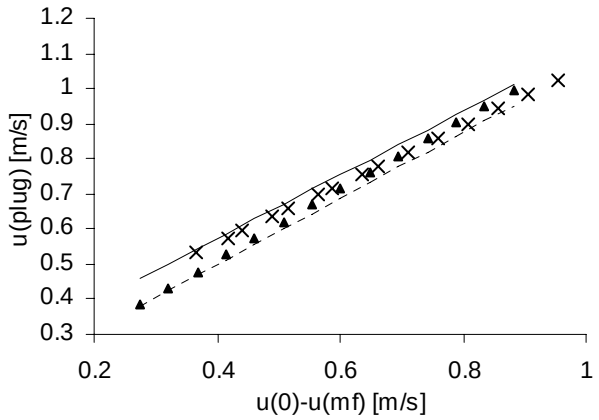

Figure 6: fit of equation 19 to results of plug velocity. ×: plug velocity 105 mm averaged for 'total' powder; ▲: plug velocity 44 mm middle zone for 'total' powder; ___ : model for 105 mm riser diameter; ----: model for 44 mm riser diameter

Equation 19 is valid for the square nosed slugging regime (gas velocities between 0.28 < ug < 0.95 m/s) and was found by analysis of measurements with a polymer powder (density ρ_{pol} = 900 kg/m^3 and 423 < ρ_b < 474 kg/m^3) with a broad particle size distribution (70 < d_p < 1600 μm).

5 Conclusions

A relation was derived for the plug velocity in a bed of polymer powder with a low density and a large particle size distribution. Influences of gas velocity, solids flux, riser diameter, particle size range and particle and powder properties were measured and quantified for their influence on the plug velocity.

Existing relation for the calculation of slug velocity were found not to apply to the powder used in the experiments. Also the derivation of the expression for the slug velocity was different in nature. A new relation for the description of the plug velocity relative to the fluidum was derived and all influences of system properties were added. The resulting equation for the plug velocity fits well with the experimental results and can be used to describe the plug velocity in a fluidized bed operated in the square nosed slugging regime in a broad range of applications.

6 Notation

a, b, c, d	constants	[-]
c_f	Friction coefficient	[-]
D	Riser diameter	[m]
d_p	Particle diameter	[m]
F_g	Gravity force	[N]
F_b	Buoyancy force	[N]
$F_{fr,g}$	Friction force due to gas	[N]
$F_{fr,w}$	Friction force due to wall	[N]
g	Acceleration of gravity	[m/s^2]
G_s	Solids flux	[kg/m^{2}s]
H_{mf}	Bed height at minimum fluidization	[m]
H_{bf}	Height of a freely bubbling zone in a fluidized bed	[m]
H_L	Limiting bed height where coalescence is complete and a stable plug length is achieved	[m]
k_1, k_2	constants	[-]
L_{max}	Maximum slug length	[m]
L_{pl}	plug length	[m]

L_{sl}	Slug length	[m]
r	Ratio between bubble and column diameter	[-]
T	Plug length/bed diameter	[-]
u_0	Gas velocity	[m/s]
u_{mf}	Minimum fluidization velocity	[m/s]
u_{pl}	Plug velocity	[m/s]
$u_{pl,r}$	Contribution to plug velocity due to raining of particles	[m/s]
u_{sl}	Slug velocity	[m/s]
u_{dp}	Contribution to plug velocity due to particle size	[m/s]
ρ_b	Bulk density of powder	[kg/m^3]
ρ_g	Gas density	[kg/m^3]
ρ_s	Solids density	[kg/m^3]
φ	Angle of internal friction	[-]

7 Literature

Baeyens, J. and D. Geldart (1974). "An investigation into slugging fluidized beds." Chemical Engineering Science **29**: 255-265

Davidson, J.F. and Harrison, D. (1963). From: “Fluidised particles”, Cambridge University Press, p. 29 (2.09)

Davies, R.M., Taylor, Sir G. (1950). “The mechanics of large bubbles rising through extended liquids and through liquids in tubes.” Proc. Roy. Soc., **A200**: 375-390

Fan, L.T., T.C. Ho, W.P. Walawender (1983). "Measurements of the rise velocities of bubbles, slugs and pressure waves in a gas-solids fluidized bed using pressure fluctuation signals." AIChE J, **29**: 33

Kehoe, P.W.K. and J. F. Davidson (1970). Chemeca '70, Australia, Butterworth, p. 97

Kehoe, P.W.K., J.F. Davidson (1973). "The fluctuation of surface height in freely slugging fluidized beds." AIChE Symposium series, **69**(128): 41-48

Layzer, D. (1955). Astrophys. J., **122**: 1 (2.09)

Lee, S.H., D.H. Lee, S.D. Kim (2002). "Slug characteristics of polymer particles in a gas-solid fluidized bed." Korean Journal of Chemical Engineering **19**(2): 351-355

De Luca, L., R. Di Felice, P.U. Foscolo, P.P. Boattini (1992). "Slugging behaviour of fluidized beds of large particles." Powder Technology **69**: 171-175

Noordergraaf, I.W., A. Van Dijk, Van den Bleek, C.M. (1987). "Fluidization and slugging in Large-particle systems." Powder Technology **52**: 59-68

Ormiston, R.M., F.R.G. Mitchell, Davidson, J.F. (1965). "The velocities of slugs in fluidised beds." Trans. Instn. Chem. Engnrs **43**: T209-T216

Stewart, P.S.B. and J.F. Davidson (1967). "Slug flow in fluidised beds." Powder Technology **1**: 61-80

Weickert, G. (2000). Deutsches Patent- und Markenamt, DE 199 07 021 A1

Chapter 4

Two-stage polymerization of propylene: the influence of degassing between liquid phase and gas phase

Abstract

A two-stage polymerization comprising liquid phase prepolymerization and gas phase main polymerization was investigated. Two methods were used for the shift to gas phase main polymerization. The first method was a warm up after prepolymerization, ending up in gas phase at higher temperature and pressure. The second method implied a purging of the liquid phase propylene, followed by flushing the reactor with gaseous propylene at low pressure and pressurizing the reactor with gaseous propylene up to a pressure of 25 bar. Without depressurizing between prepolymerization and main polymerization the total catalyst activity was found to be 45 % higher compared to the flushing method. Two hypotheses were proposed to explain this phenomenon.

1 Introduction

In industry often a prepolymerization in liquid phase is done to have better control of the morphology of the polymer and to overcome overheating of particles. This includes a step from the prepolymerization to the main polymerization and this step can be performed in different ways. On smaller scale the same step can be made, to study the effect of the step and to overcome problems like “wall sheeting”.

When fresh catalyst particles are injected into an empty autoclave filled with gaseous propylene, the particles are likely to stick to the wall of the autoclave and the surface of the stirrer, causing “wall sheeting”: a sheet of polypropylene growing on the wall of the autoclave. This gives massive operational problems, and the product needs to be scraped off the wall.

To overcome this problem a bed of inert solids can be used in the reactor, for instance polymer powders or salt. A major problem related to the introduction of such a bed of solids is that it is very likely to introduce contaminations with the inert bed.

A new method was designed to overcome these problems. The method is based on the idea that a bed could be created in the reactor itself. By performing a well-defined polymerization with the catalyst of research in liquid phase before the actual gas phase polymerization, the bed that is necessary is created. The very small catalyst particles also do not exist anymore because a moderate layer of polymer has grown around it. This first step is called the prepolymerization step or the reactive bed preparation.

With the first investigations using the reactive bed preparation method a few results came out that were not expected. Different procedures were used to make the step from liquid phase prepolymerization to gas phase main polymerization. The current work focuses on the differences in activity in the gas phase that result from the different procedures and what influences these differences.

The “warm up” method or method A resembles the handling of catalyst in industry without a depressurization: after reaction in a prepolymerization reactor the catalyst is transported to the main reactor where the main polymerization takes place. During the transport the catalyst stays in a pressurized propylene environment. This situation is simulated with an experiment performed with the warm-up method.

The “flushing” method or method B resembles circumstances in industry where a depressurization is necessary to transport the particles from the prepolymerization reactor to

the main polymerization reactor or when the powder is transported from a reactor with for instance a high hydrogen concentration to a low hydrogen concentration. The depressurization is then used to get the hydrogen out of the powder.

The objective of this paper is to quantify the difference in activity in the gas phase part of the experiment between method A and method B and to interpret and correct reaction kinetics in the gas phase reactor using these quantified differences.

2 Experimental

In the experiments, influences of the flushing time, the application of several flushing procedures and the concentrations of cocatalyst and external donor on the reaction rate in the gas phase main polymerization were studied.

2.1 Reactor system

Experiments were performed in a 5 l jacketed stainless steel tank reactor (figure 1) with a helical stirrer inside. The cooling/heating system of the reactor consists of two water baths, a cold-water tap and an oil circuit for heating the cover plate. The cover plate is heated slightly above the reaction temperature to prevent condensation of propylene on the cover plate during the reaction.

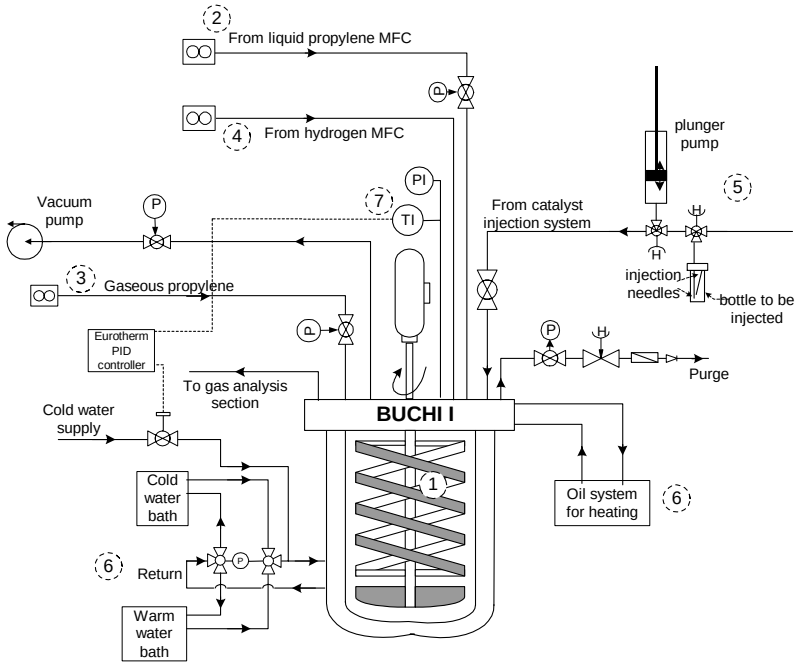

Figure 1: Schematic of experimental set up. Numbers in dotted circles refer to: 1: autoclave with helical stirrer; 2: liquid propylene feed; 3: gaseous propylene feed; 4: hydrogen feed; 5: catalyst injection system; 6: temperature control system for

autoclave; 7: temperature control of reactor.

The temperature of the cooling water in the jacket is also measured; via a heat balance over the reactor and assuming steady state operation, it is possible to calculate the heat produced from the polymerization reaction, see Samson et al (1998). For liquid phase experiments this method is used to calculate the reaction rate.

When the reactor system runs isoperibolically, meaning constant jacket temperature, the rise in the reactor temperature is caused by the highly exothermic polymerization reaction (at constant pressure). The small temperature rise stands for the polymerization rate as long as the heat transfer conditions are constant (Weickert, 2004). The isoperibolic mode is mainly applied in the gas phase reaction.

2.2 Catalyst

A Ziegler-Natta system was used, which is a $TiCl_4$ supported on MgCl with a phthalate as internal donor and an external silane donor. Tri Ethyl Aluminum (TEA) was used as cocatalyst. The catalyst system was prepared for reaction in a glove box under a nitrogen atmosphere. For most experiments, 3.75 mg of bare catalyst was mixed with 6.94 mg of silane donor and 2 g of hexane. As cocatalyst in total 160 mg of TEA were used. 28 mg of TEA was used both as cocatalyst and as scavenger and prepared in a separate vial. The mixture was injected 5 minutes prior to catalyst injection in the reactor filled with propylene. 132 mg of TEA was mixed with the catalyst, silane donor and hexane mixture 30 minutes before injection. For some experiments the amounts of all components were increased with a factor of 1.25 to get sufficient activity.

2.3 Prepolymerization

For the prepolymerization step in the experiments, the “reactive bed preparation” method was applied by carrying out the following steps:

1) Purification of the reactor
2) Purging of the reactor with monomer gas at room temperature
3) Addition of 420 grams of propylene
4) Injection of 350 mg of hydrogen

5) Heating the reactor to 40 °C, resulting in 503 ml of liquid propylene and 4.502 ml of gaseous propylene
6) About 20 min stirring of the reactor with a helical stirrer at 600 rpm until readings of the temperature were stable, indicating thermal equilibrium
7) Injection of scavenger (28 mg), followed by 5 minutes stirring time
8) Injection of the catalyst mixture.
9) 30 minutes of isoperibolic polymerization at 40 °C cooling water temperature; the isoperibolic temperature rise was approximately 0.6 K.

2.4 Main polymerization

After a reaction time of 30 minutes in the prepolymerization step, the preparations for the main polymerization could be done. Two methods were used to arrange the transition from prepolymerization to main polymerization.

In method A the reactor is heated up to 70 °C after the prepolymerization. Since the amount of propylene in the reactor is limited, all propylene present in the reactor will evaporate during the warm-up. With this procedure propylene will remain sorbed in the polymer since the overall pressure is still high. The hydrogen added before the start of the liquid phase part of the experiment is still present in the reactor.

In method B the propylene is purged after the prepolymerization and the reactor is heated up to 70 °C. The reactor is then rinsed. With this procedure propylene will be desorbed from the polymer because of the pressure release. After rinsing the reactor is filled with gaseous propylene and hydrogen resulting in a total pressure of 25 bars.

Method A: warm up of the reactor contents without intensive monomer desorption from the polymer phase. The following steps were done after the prepolymerization:

10A) Heating up the reactor to 70 °C by switching from the ‘cold’ water bath to the ‘hot’ water bath.
11A) After about 3 minutes pressures between 28 and 29.4 bar are reached, which is more than 2 bars below the saturation pressure for propylene at 70 °C. The pressure in the reactor has to become stable; temperature and sorption effects cause fluctuations in the pressure.

12A) Typically, after another 3 minutes a maximum stable pressure is reached and the pressure starts to drop because of monomer consumption. The mass flow controller is started to keep the pressure in the reactor constant.

13A) 60 minutes of reaction time.

14A) Purging of the reactor and flushing with N_2.

In method B the reactor is purged and flushed with propylene after the prepolymerization step, involving intensive monomer removal from the polymer phase:

10B) Depressurization, purging of propylene from the reactor.

11B) Heating the reactor to 70 °C by switching from the 'cold' water bath to the 'hot' water bath.

12B) Rinsing 5 times with gaseous propylene by pressurizing to 5 bars followed by pressure release to 1 bar.

13B) Feed of gaseous propylene to the reactor to 25 bar. The temperature and pressure in the reactor have to stabilize and the monomer will be sorbed in the polymer. The pressure will fluctuate and drop a few bars.

14B) Addition of 350 mg of hydrogen.

15B) Feed of gaseous propylene to 25 bar. Waiting till the system reaches a maximum stable pressure of 25 bar. Then the pressure starts to drop because of monomer consumption.

16B) Start of the mass flow controller to keep the pressure constant at 25 bars.

17B) 60 minutes of reaction time.

18B) Purging of the reactor and flushing with N_2.

In both methods, the readings from the MFC are used to calculate the reaction rate in the gas phase. At opening of the reactor the catalyst is killed in the contact with air. The powder is dried four hours at 50 °C in a vacuum oven.

3 Results

The experimental program is given in table 1. First an experiment (experiment 1) with method A was done, see figure 2. On the left axis the temperature and the reaction rate are given, on the right axis the pressure is given. As can be seen, first 30 minutes of liquid phase reaction is done. The reaction rate drops from about 12 kg/g_{cat}hr to 9 kg/g_{cat}hr, the pressure is about 16

Table 1: overview experiments. Method A and method B are explained in the 'experimental' section

Exp.nr.	Switch method	Total yield [g]	Catalyst [mg]	Cocatalyst [mg]	Donor [mg]	Hydrogen [mg]	gas phase pressure [bar]
1	A	304.5	3.75	159.9	6.94	350	29.4
2	B	139.0	4.73	202.7	8.69	350	25
3	A + repeated B	266.1	3.74	161.1	6.94	350	25
4	A + B	226.3	3.75	160.5	6.94	350	25
5	A + B + 2 days storage	261.7	3.72	160.1	6.94	350	25

bar and the reactor temperature is around 42 °C. After 30 minutes the reactor is heated up and the reactor temperature as well as the pressure increase. After a stabilization of the pressure the mass flow controller is started at 47 minutes and the pressure stays constant from that moment on. The reaction rate at this higher temperature is much higher and drops faster. Comparing temperature and pressure in the period after 47 minutes shows the reaction takes place in the gas phase (71 °C, 28.5 bar).

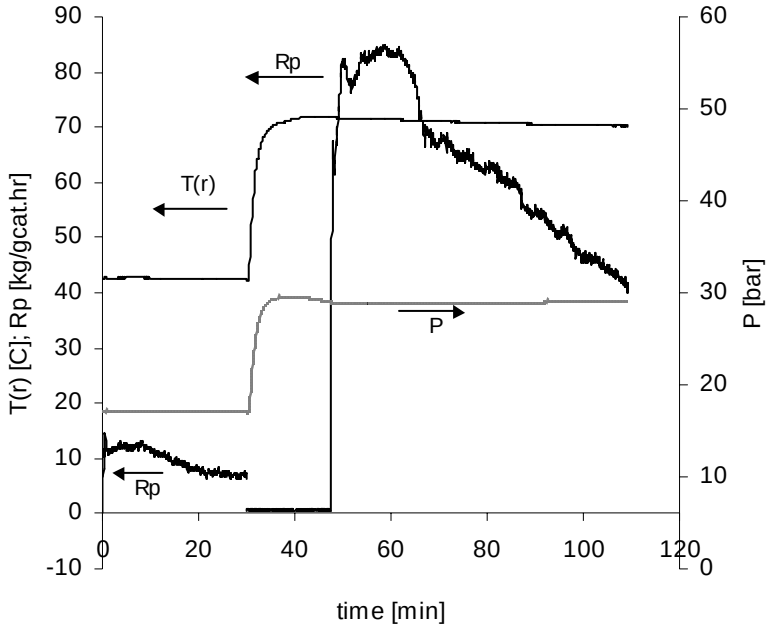

Figure 2: Reaction rate and total pressure of experiment nr. 1 with method A: after prepolymerization warm up of the liquid phase. Liquid phase reaction: 30 min, 40°C, 420 g propylene, 350 mg hydrogen. Gas phase: 60 min, 70°C, remainder of liquid phase on propylene and hydrogen.

This experiment was compared with an experiment done with method B (experiment 2, figure 3) to compare the effect of both methods with each other. Figure 3 can be read in the same way as was shown for figure 2.

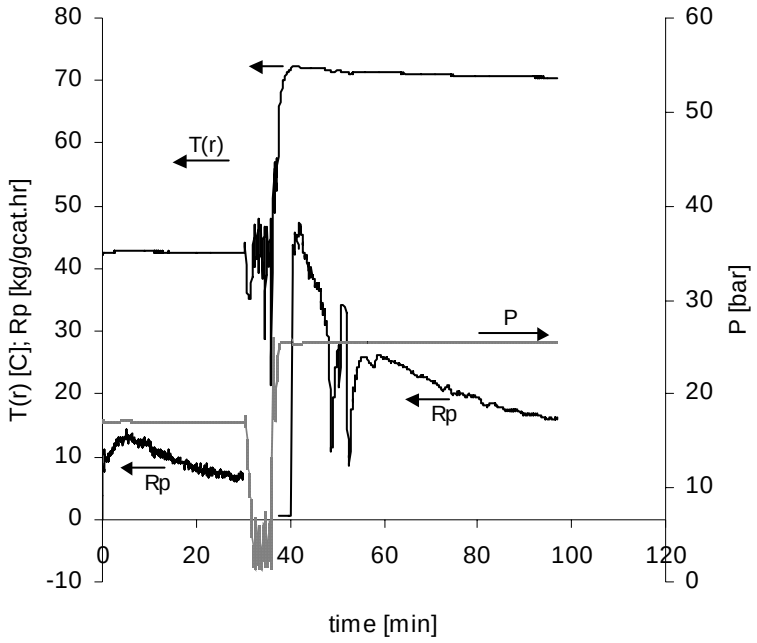

Figure 3: Reaction rate, total pressure and temperatures of reactor and jacket of experiment nr. 2 with method B: after prepolymerization purging of the liquid phase and flushing. Liquid phase reaction: 30 min, 40°C, 420 g propylene, 350 mg hydrogen. Gas phase: 60 min, 70°C, 350 mg of hydrogen, propylene added to 25 bar total pressure

The concentrations of hydrogen and monomer in experiment 1 are not equal to those in experiment 2, because the total pressure in the reactor becomes 29 bar in experiment 1, instead of 25 bar in experiment 2. This means that a correction needs to be made to be able to compare the results of these experiments with each other. The concentration of monomer was corrected with a factor of 25/29, the pressures of experiment 1 and 2.

The correction for the concentration of hydrogen was done on basis of its influence on the reaction rate. A model for this dependency is given in chapter 5 of this work. The experiments were initially done for a different reason, but the interpretation in terms of the step between the two polymerizations was done later. That is the reason for the slight difference in hydrogen concentration.

The results of both methods are depicted in figure 4. The average activity of experiment 1 (with method A) in the gas phase is approximately 30 kg/g_{cat}hr higher than the average

activity of experiment 2 (with method B) (figure 5), whereas the average activity of experiment 1 in the gas phase starts at 65 kg/g_{cat}hr. This means a drop in activity of almost 45 %, assuming that no deactivation of the catalyst took place during the flushing procedure.

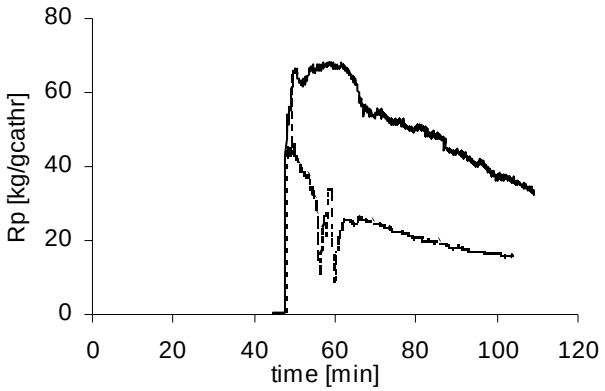

Figure 4: comparison of gas phase main polymerization. ___:experiment 1 with method A resulting in gas phase 29 bars total pressure at 70 °C. - - - -: experiment 2 with method B. Both experiments with hydrogen amount of 350 mg added in 5 L reactor. Both experiments compensated for hydrogen concentration.

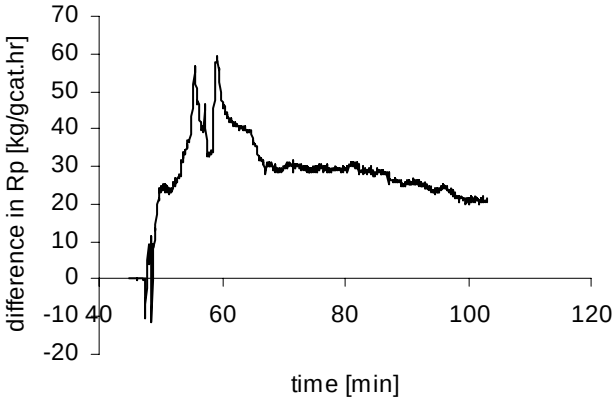

Figure 5: Difference in activity between experiment 1 and 2. Gas phase reactions synchronized with each other at start of MFC pressure control.

The experiments 1 and 2 are compared with experiment 3. Experiment 3 was done with method B for the change to main polymerization, but with a “warm up” of the prepolymerization mix to the gas phase like in method A and 10 minutes of reaction in the gas phase prior to the change to the main polymerization (exp.nr. 3, figure 6). So, both methods are combined in this experiment.

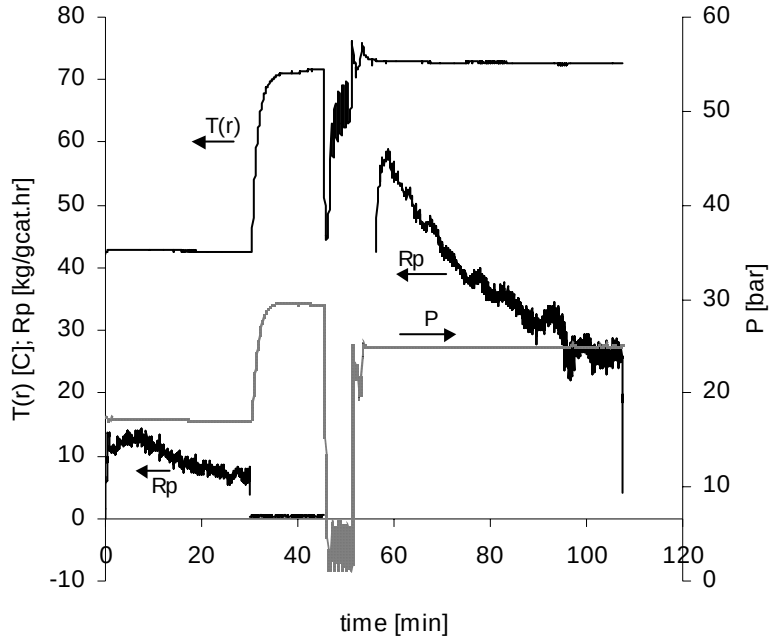

Figure 6: Reaction rate and total pressure of experiment nr. 3: after prepolymerization warm up of the liquid phase(method A), after 10 min of gas phase reaction flushing (method B). Liquid phase reaction: 30 min, 40°C, 420 g propylene, 350 mg hydrogen. Gas phase: 60 min, 70°C, 350 mg hydrogen, propylene added to 25 bar total pressure

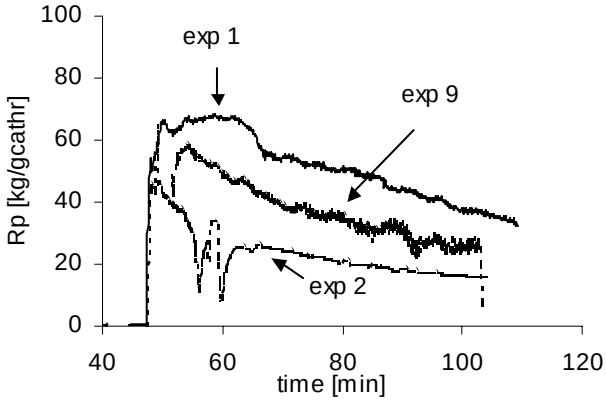

Figure 7: Comparison of experiments 1 (method A), 2 (method B) and 3 (method A and B).

When looking at experiment 3, with a part warm up of the liquid phase, followed by the flushing procedure of method B, the activity lies in between the two extremes (figure 7). See also table 1. The yield in experiment 3 is much larger than in experiment 2, but this difference can be explained from the 10 minutes reaction at 70 °C before the flushing procedure of method B. From a number of experiments it is calculated that an average of 92 grams is

produced in 18 minutes. It takes time before the temperature in the reactor is at 70 °C and during that warm up time the reaction continues. This means an average production of 5.1 g/min. The difference in activity in the gas phase part of the experiment between experiments 1 and 3 is 23 %.

This experiment is repeated a number of times, since this experiment was used as a check for the general performance of the set up. The reproducibility of these experiments was high: activities in the gas phase differed no more than 11 % (figure 8).

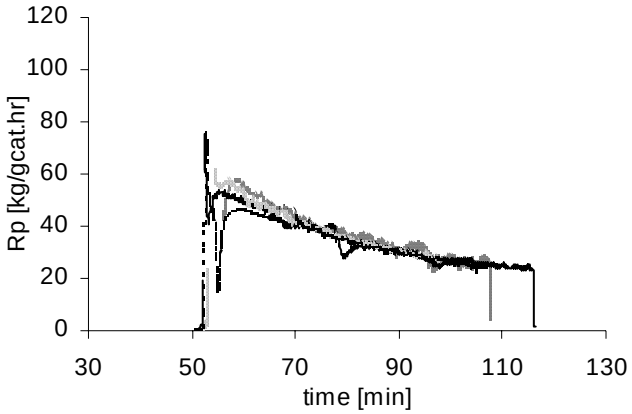

Figure 8: Comparison of different experiments with recipe and procedure of experiment nr 3. Experiments were done to check system for reproducibility.

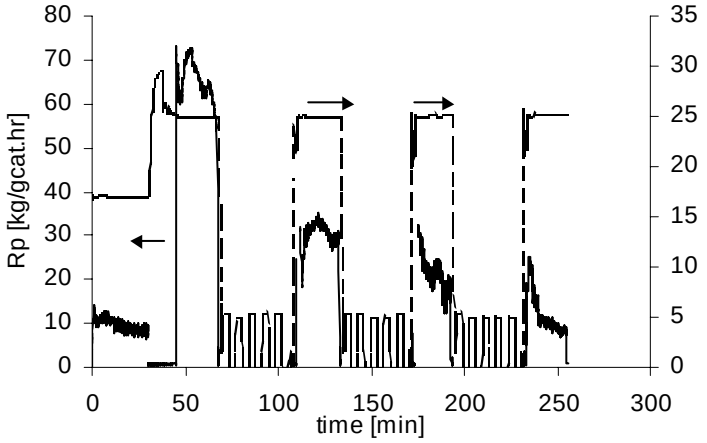

Figure 9: Reaction rate and total pressure of experiment nr 4: method A followed by three times method B. Liquid phase reaction: 30 min, 40°C, 420 g propylene, 350 mg hydrogen. Gas phase: 60 min, 70°C, 350 mg hydrogen, propylene added to 25 bar total pressure.

To check the assumption of no deactivation, an experiment (experiment 4) was done with repeated application of method B: flushing and gas phase reaction. In experiment 4 first method A is applied, with a lowering of the pressure to 25 bar by purging (figure 9). This made it comparable to experiment 3. After 30 minutes gas phase reaction method B is performed, after which another 30 minutes of gas phase reaction is done. This sequence of flushing (method B) and 30 minutes of gas phase reaction is repeated two more times.
In this experiment it is clear that after the first flushing sequence the activity drops significantly (40 %). After the following flushing sequences the activity does not drop more than expected, as can be seen in figure 10. The activity during the reaction follows the normal deactivation of the catalyst as a result of reaction.

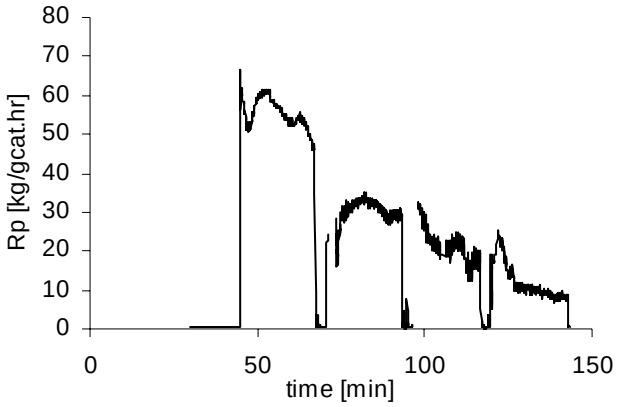

Figure 10: experiment nr 4 compressed in time. Flushing time is left out (see figure 9)

The deactivation of the catalyst could be due to the longer time that the experiment takes. The total running time of the experiment was 255 minutes. To illustrate that this decay in activity is not time dependent, an experiment with much longer time between the prepolymerization and the main polymerization step was done (experiment 5). In this experiment the product from the prepolymerization step was stored at 1 bar of propylene for 2 days. The switch procedure between prepolymerization and main polymerization was the same as in experiment 3, so first applying method A, 30 minutes of reaction in the gas phase, then performing method B. After starting method B the set up was kept at 1 bar of propylene (after step 12B). After 2 days the sequence of method B was continued with step 13B and further: the set up was heated up to 70 °C and 25 bar of propylene and 350 mg of hydrogen were added. Then the mass flow controller was started to keep the pressure constant.

As can be seen in figure 11, experiment 5 has an activity in the main polymerization that is comparable with experiment 3 and with experiment 4. The lowering of the activity in experiment 5 between prepolymerization and main polymerization is in the same order of magnitude. This means that no time dependent decay in activity will occur.

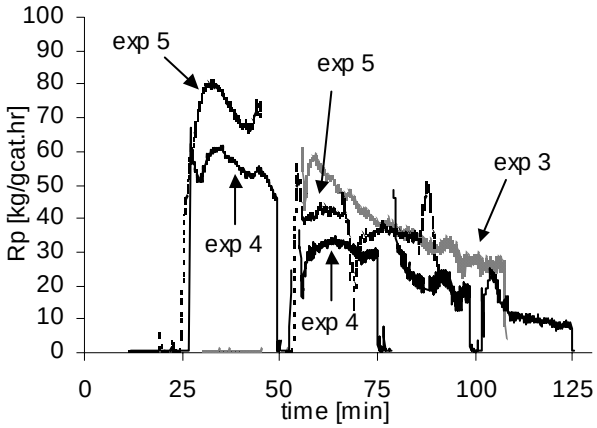

Figure 11: Comparison of experiments 3 (methods A and B), 4 (method A and repeated method B) and 5 (method A and B, with 2 days storage at 1 bar propylene after flushing of method B). Experimental results for the gas phase main polymerization are shifted in time to make comparison of the main polymerization reaction rates possible. For experiments 4 and 5 the reaction rate after warm up are added to illustrate the decay in activity due to lowering of the pressure but the time scale of these parts are also shifted.

It could be possible that with the flushing TEA or donor is removed. To check this idea, experiments were done with different cocatalyst concentrations (experiments 6, 7 and 8, table 2, figure 12) and with different external donor concentrations (experiments 7, 9 and 10, table 2, figure 13). All experiments were done with the standard prepolymerization recipe and method A for the switch to gas phase main polymerization. With this method the TEA and external donor concentrations did not change because of flushing and therefore the effect of these different concentrations in the main polymerization could be determined.

Table 2: overview of experiments with different cocatalyst and donor concentration. All experiments were performed with method A for the switch to main polymerization.

Exp. nr.	Catalyst [mg]	Cocatalyst [mg]	Donor [mg]	Hydrogen [mg]	Pressure [bar]	Yield [g]
6	3.74	159	6.94	350	27.3	300
7	4.1	39.1	6.94	350	26.7	320
8	3.96	20.1	6.94	350	24.9	99.6
9	3.75	41.1	1.71	350	25.9	295.9
10	3.88	41	0	350	28.5	217.8

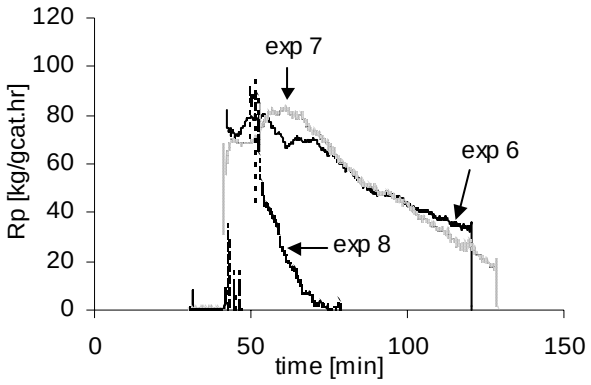

Figure 12: Comparison of gas phase reactions with different cocatalyst (TEA) concentrations. Exp. 6: 160 mg TEA; exp. 7: 40 mg TEA; exp. 8: 20 mg TEA.

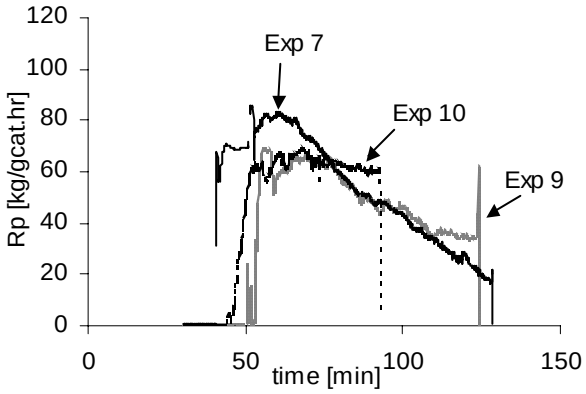

Figure 13: Comparison of gas phase reactions with different external donor concentrations. Exp. 7: 6.94 mg donor; Exp. 9: 1.71 mg donor; Exp. 10: 0 mg donor.

A lower concentration of cocatalyst causes a rapid decay of activity in the gas phase. After approximately 20 minutes the activity becomes zero in the specific experiment. The

cocatalyst also acts as a scavenger and neutralizes contaminations in the gas, but when the concentration of cocatalyst is very low, all cocatalyst will react with contaminations present in the gas, even if the concentration of contaminations is very low. Also a minimum amount of cocatalyst is necessary for activation of the catalyst.
A lower donor concentration leads to a slightly lower deactivation caused by normal reaction. When no donor is present anymore the deactivation becomes almost zero. The isotacticity of the product will be lower.
The two effects do not counterbalance each other, since the effect of lower cocatalyst concentration is much larger than the effect of lower donor concentration. Both descriptions of the behavior of the activity in the gas phase cannot be found in the present results, so it is concluded that the lower activity is not caused by removal of cocatalyst or external donor.

4 Discussion

Two hypotheses are proposed. The first hypothesis lies in the nature of crystallization behavior. It is expected that the polymer is able to crystallize when monomer is desorbed from the polymer in the flushing procedure. Monomer molecules do not hinder the polymer chains anymore and they can come closer together to form crystals. When the reactor is only warmed up the monomer stays in the polymer and prevents crystallization.
The flushing procedure in experiment 2 requires approximately 11 minutes. When the crystallization is assumed to be complete, it means that the speed of crystallization is faster than those 11 minutes. Many people have found however that catalyst particles are not enclosed in polypropylene crystals in the range of a crystallization degree of 50-60 %. This would mean that the crystallization does not have an influence on the activity in the gas phase. Since the degree of in situ crystallization cannot be measured, it is very hard to draw conclusions on it.

A second hypothesis lies in the nature of the reaction mechanism based on the trigger mechanism by Ystenes (1991). In the trigger mechanism a monomer molecule forms a complex with the active site and the insertion takes place after incoming of a second monomer molecule. Shimizu (2001) proposed that in the trigger mechanism not the complexed monomer is inserted in the polymer chain but the incoming monomer. This was based on a largely increased activity for propylene polymerizations, only due to adding a small amount of ethylene in the presence of hydrogen, a small amount of insertions of

ethylene and due to NMR data, which did not show a peak due to reactivating dormant sites by ethylene.

The complex mechanism can be represented as following (Bergstra and Weickert, 2004):

Complex forming: $C^0 + M \underset{k_2}{\overset{k_1}{\rightleftarrows}} C^M$

Propagation reaction: $C_j^M + M \xrightarrow{k_3} C_{j+1}^M$

with: $C^M = \sum_j C_j^M$

The lowering of the pressure and afterwards continuation of the reaction may have an influence on the equilibrium between the complex and the catalyst site. The relief of pressure may cause the equilibrium to shift to the left, thereby lowering the resulting activity since only the complex reacts. The less polymer is formed, the more the equilibrium shifts to the left.

5 Conclusions

When performing experiments that contain a release of pressure without exposing the catalyst to contaminations, the apparent activity of the catalyst mixture is approximately 55% lower after the pressure release than when the pressure is not lowered. Influences of phenomena such as time between prepolymerization and main polymerization, possible contaminations due to flushing, changing cocatalyst and external donor concentrations could not explain the lower activity after a pressure release. Also the quality of monomer and catalyst was reproducible, no problems were encountered.

Two hypotheses are proposed to explain this phenomenon. One hypothesis is based on the in situ crystallization behavior of the polymer when the pressure is lowered and thus desorption of monomer from the polymer takes place. The monomer molecules are believed to block the polymer chains from coming close to each other to form crystals. When the monomer molecules are removed from the polymer the crystals are formed. Catalyst particles enclosed in the crystalline part of the polymer are blocked from the monomer by the crystals. The catalyst particles do not contribute to the formation of polymer anymore, resulting in a lower apparent activity.

The second hypothesis is based on the reaction mechanism of the catalyst system. With the trigger mechanism it is believed that a complex is formed that is in equilibrium with the catalyst site and the free monomer. The lowering of the pressure may influence the equilibrium and thus may result in a lower activity after the pressure relief.
Both hypotheses however where not checked, but just proposed. Experimental evidence has so far not been found. New research needs to be done. The authors want to draw attention to the phenomenon, in order to find an explanation.

6 Literature

Bergstra, M.F., Weickert, G. (2004). JAIST conference proceedings, *to be published*

Samson, J. J. C., Weickert, G., Heerze, A. E., Westerterp, K. R.(1998); "Liquid-phase polymerization of propylene with a highly active catalyst." AIChE Journal **44(6)**, 1424-1437

Shimizu, F. (2001), “Liquid Pool Polymerization of Propylene and Ethylene Using a Highly Active Ziegler-Natta Catalyst”, Chapter 5, PhD-thesis, University of Twente, Enschede, The Netherlands; Sagamihara, 2001, ISBN 90-365-1668-4

Ystenes, M.(1991). "The trigger mechanism for polymerization of alpha-olefins with Ziegler-Natta catalysts: a new model based on interaction of two monomers at the transition state and monomer activation of the catalytic centers." J. Catal., **129**, p. 383

Chapter 5

Hydrogen response of reaction rate and molecular weight in gas phase propylene polymerization with a Ziegler-Natta catalyst: experiments and modeling

---

Abstract

The influence of hydrogen concentration on initial reaction rate in the gas phase and the average molecular weight in the gas phase polymerization of propylene with a Ziegler-Natta catalyst was investigated. The initial reaction rate increases with increasing hydrogen concentration to a maximum of 45 kg/g_{cat}hr and drops at further increase of the hydrogen concentration. The molecular weight first drops quickly at an increase in the hydrogen concentration followed by a slower decrease at higher hydrogen concentrations, in agreement with theory. Simple hydrogen transfer does not describe the sharp drop of the molecular weight when small amounts of hydrogen are added.

A single site model was adapted to describe simultaneously the propylene polymerization kinetics and the produced average molecular weight based on the dormant site theory assuming a lower propagation rate of Ti-H active sites and assuming single site behavior. The model can accurately describe both influences of hydrogen and is a good tool for predicting polymerization performance.

1 Introduction

One of the most important tools for generating different polymer grades is the use of hydrogen as a chain transfer agent. Hydrogen not only influences the molecular weight of the polymer, but also the activity of the catalyst system, as was already noticed by Natta in 1959. Furthermore, the morphogenesis of polypropylene is strongly determined by the local reaction rate (Pater et al. 2001). Therefore, it is necessary to have detailed knowledge of the sensitivity of a catalyst to hydrogen and its response to different hydrogen concentrations. The focus of this work is on Ti based catalysts.

1.1 Increased polymerization rate

1.1.1 Increased chain mobility

The most remarkable effect of the hydrogen concentration on the reaction rate is an increase in reaction rate when hydrogen is added to the system. In the last decennia, several explanations were given. Guastalla and Giannini (1983) used a $MgCl_2$ supported $TiCl_4$ catalyst without internal or external donors and explained the increase in reaction rate by the ability of migration of polymer chains.

1.1.2 Increased number of active sites

A different explanation is given by the state of the titanium complex. When the complex is activated, the valence of the titanium species changes from Ti^{4+} to Ti^{3+} and these Ti^{3+} sites are the active sites in the catalyst. The Ti^{3+} can be further reduced to Ti^{2+}, thereby reducing the number of active catalyst sites, since Ti^{2+} is believed to be inactive or less active. Introduction of hydrogen leads to increased activity, caused by the reactivation of the Ti^{2+} sites to Ti^{3+} sites by hydrogen. The number of active sites is thus increased, leading to a higher activity.

This theory is supported by Chien and Kuo (1986), who worked with a $MgCl_2$\$TiCl_4$-3TEA\TEA*p*-cresol\methyl-*p*-toluate catalyst (CW-catalyst) and found that hydrogen increases the reaction rate but also causes a more rapid deactivation, leading to almost the same overall yield. Their explanation for these effects was found in an increase of the number of active Ti* sites by hydrogen as explained. No change in the propagation constant k_p was assumed. The theory of Chien on the oxidative adsorption of hydrogen to re-oxidize lower

titanium valences is supported by Keii (1986). Han-Adebukan et al. (1997) also agreed with Chien about the hydrogen effect. They state that the number of Ti^{3+} sites increases with increasing hydrogen concentration.

Spitz et al. (1988) ($MgCl_2$\$TiCl_4$\TEA or IPRA\EB\ethyl-*p*-toluate or ethyl anisate) saw that after an initial increase the activity drops again within a few minutes after addition of hydrogen and comes back at the level of activity it had without the addition of hydrogen. Adding more hydrogen again leads to an increase in activity, followed by a drop. The increase however is not as large as after the first addition of hydrogen. They explain this drop in activity by the change in Ti sites as proposed by Chien (1986).

Chien and Nozaki (1991) continued the work on the hydrogen effect and investigated the occurrence of Ti^{3+} sites and Ti^{2+} sites while using the same CW catalyst; see above. The concentration of Ti^{3+} sites increased after the addition of hydrogen, but the increase in Ti^{3+} concentration cannot fully explain the increase in activity. Rishina (1994) ($MgCl_2$\$TiCl_4$\TEA\ dibutylphtalate\ triethoxyphenylsilane) also found a large increase in activity after addition of hydrogen. They presume that the activation effect is the result of an increase in the number of active centres.

1.1.3 Dormant site theory

In the so-called ‘dormant site’ theory it is said that the methyl group of the propylene monomer can block the activated Ti sites on the catalyst when it is inserted with the methyl group facing the active site, the so-called 2,1-insertion of propylene; see figure 1. The active sites are not deactivated but sterically blocked and therefore temporarily not reacting, or sleeping. When hydrogen is added, it is suggested that hydrogen is small enough to pass the methyl group and decouple the polymer chain by reacting with the Ti-polymer complex. The active site is then freed again and can react further. This leads to an increase in the apparent reaction rate.

This dormant site theory is in conflict with the theory of an increase in the number of active sites by hydrogen in that it explains the increased reaction rate by a freeing of blocked active sites rather than the creation of active sites. This theory is supported by Kioka and Kashiwa (1991), who investigated the hydrogen effect by doing experiments with a short reaction time with a $MgCl_2$\$TiCl_4$\TEA\Diethylphtalate\phenyltriethoxysilane catalyst and polymerizing either propylene or 1-butene. They found that the number of active sites stays the same within one experiment because the polymer yield increases linearly with time (10-60 sec), and in

experiments at different hydrogen concentration the same trend is found, although the yield was different. Calculations on the produced number of polymer chains per mole of Ti atoms show that the number of polymer chains increases linearly with the polymer yield. They state that the hydrogen effect can be described by an increase in the propagation constant k_p rather than an increase in the number of active sites. However, we think that the time of reaction is too long to draw such conclusions on the rate enhancement behavior. Within 1 second dormant sites have been formed and no distinction can be made between the formation of new active sites and the freeing of dormant sites, expressed in k_p.

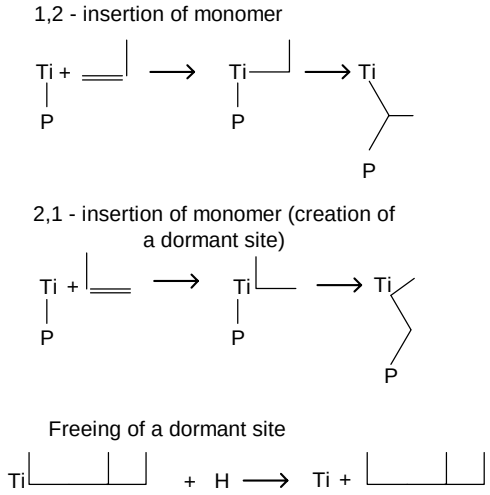

Figure 1: Generation and reactivation of dormant sites

Mori et al. (1999, p 153) ($MgCl_2$\$TiCl_4$\TEA\no donors) used the stopped flow method to investigate the hydrogen effect. Based on their results they agreed with the validity of the dormant site theory by proving that the number of active sites does not increase. Because of the short reaction times (0.05 – 0.20 s) only the formation of the first polymer chains is visible and dormant sites are not yet created. Experiments with catalyst prepared with TEA showed that hydrogen does not reactivate Ti^{2+} sites, because larger activity was not found.

In a different publication Mori et al. (1999, p211) ($MgCl_2$\$TiCl_4$\TEA\EB catalyst and a $Mg(OEt)_2$\$TiCl_4$\DEAC\dibutylphtalate catalyst, both without external donor) state that the number of dormant sites is about the same for different catalyst systems, but that the catalysts give a different molecular weight.

Shimizu (2001, PhD) used a $MgCl_2$\$TiCl_4$\TEA\diethylphtalate\t-$BuEtSi(OMe)_2$ catalyst and concludes from TREF data that the increase in activity caused by hydrogen is due to the freeing of dormant sites by hydrogen. Liu et al. (2001) ($MgCl_2$\$TiCl_4$\EB or CMDMS)

however showed that hydrogen only has a chain transfer effect at catalyst treated with TEA as opposed to catalyst not treated with TEA, in contrast to the findings of Mori (1999(5.36)).

1.1.4 How to explain dormant site formation?

Explanations as to how dormant sites are formed and at what kind of sites they are formed lead to the notion of stereospecific sites and the ability for an active site to become dormant. Chadwick et al. (1994), using a $MgCl_2$\$TiCl_4$\TEA\phtalate ester with different silanes, saw that hydrogen influences the stereospecificity. The presence of *n*-butyl chain end groups in polymers produced in the presence of hydrogen supports the theory of reactivation of dormant, 2,1 inserted sites.

Bukatov et al. (1994) concluded that the reactivation of active sites is confined to propylene polymerizations. They used a $MgCl_2$\$TiCl_4$\TEA\diisobutylphtalate\phenyltriethoxysilane catalyst. They suggest the reactivation of the sites may be resulting from the presence of two different kinds of active centers. The first is highly stereospecific, and forms a dormant site after 2,1 insertion, the second kind is less stereospecific.

Chadwick et al. (1995) ($Mg(OEt)_2$\$TiCl_4$\TEA\ diisobutylphtalate\different silanes) have the same assumption as Bukatov et al. Addition of hydrogen leads to an increase in isotacticity index. It is said that hydrogen frees mostly isospecific dormant sites, which mainly contribute to the dormant site formation. At higher hydrogen concentrations the xylene soluble fraction increases because of the solubility of low molecular polymer chains in xylene that are not necessarily non-isotactic.

Soares and Hamielec (1996, p. 4607) proved in 1996 the dormant site theory by using the analysis of the polymer produced with a second generation $MgCl_2$\$TiCl_4$\DEAC catalyst (LYNX 900). They also show that the hydrogen apparently activates different kinds of active sites, resulting in different polymer. Without hydrogen the polymer has a narrow molecular weight distribution, and with hydrogen a broader molecular weight distribution because of the activation of sites with a different behavior by hydrogen.

Chadwick et al. (2000) ($MgCl_2$\$TiCl_4$\TEA\diisobutylphtalate or diether\different silanes or no donor) found that hydrogen increases the stereoregularity. They measured the concentration of propane and conclude that propane is formed at higher hydrogen concentrations. Because of the higher hydrogen concentration more chain transfer takes place with hydrogen, and state that 2,1 insertion of monomer takes place more on Ti-H sites, which leads to the formation of propane, as opposed to β-H abstraction.

1.2 Decreased polymerization rate

Hydrogen apparently not only increases the reaction rate in propylene polymerization, but can also decrease the activity at higher hydrogen concentrations. It is thought that the occurrence of Ti-H sites is responsible for the decrease. Already in 1959 Natta (1959) stated that the decrease in reaction rate caused by hydrogen could be ascribed to a slow addition of monomer to the catalyst-hydrogen bond formed in the step of chain transfer to hydrogen. Schindler (1965) agrees with this theory as well as Soga and Sino (1982).

Spitz et al. (1988) see an increase in reaction rate upon addition of hydrogen, but at high concentrations of hydrogen the activity drops again, even to lower values than in the case of no hydrogen. Kioka and Kashiwa (1991) find the same behavior: they see a more profound decrease in activity after the initial increase after hydrogen is added. Ystenes (1991) states in his theory on the trigger mechanism, that the activation of a Ti-H complex would be more difficult for a monomer than activation of a Ti-C complex.

For comparison: it is well known that hydrogen lowers the reaction rate in ethylene polymerizations: Guastalla and Giannini (1983), Spitz et al. (1988), Han-Adebukan et al. (1997), Soares and Hamielec (1996, p. 4599).

1.2.1 Faster deactivation

Not only the reaction rate is lower at higher hydrogen concentrations, it might be also a faster deactivation of the catalyst that causes a lower productivity. However, this faster deactivation rate is measured but hardly explained and the explanations that are given are different in nature. Chien and Kuo (1986) find a more rapid deactivation when hydrogen is present. It is explained by the change in the valence of Ti sites. Also Spitz et al. (1988) finds a more rapid deactivation under the influence of hydrogen. In the experiments of Rishina et al. (1994) the more profound deactivation is also visible and is explained by the bimolecular deactivation law.

1.3 Reaction rate modeling

Having knowledge on the mechanism behind the hydrogen effect is one thing, being able to describe it mathematically is something else. A few authors however did model the hydrogen effect to some extent. Samson et al. (1999) describe the initial reaction rate as a function of

hydrogen concentration in a steady state model. They mentioned the dormant site theory, but not used it to describe the increase in initial reaction rate as a function of hydrogen concentration. They define an empirical function F_{H2} to multiply the $R_{p,0}$ at standard conditions with other hydrogen concentrations, but they do not describe the decrease in initial reaction rate at high hydrogen concentrations.
Meier et al. (2001) used a metallocene catalyst and modeled both reaction kinetics and molecular weight as a function of hydrogen concentration, but modeled reaction rate as a function of time based on the two site model.

1.4 Molecular weight modeling

Hydrogen acts as a chain transfer agent, but not only lowers the molecular weight; it is also well known that hydrogen broadens the molecular weight. However, this is nearly only qualitative knowledge and quantification of the effect hardly exists. In industry mostly empirical relations are used to predict the broadening. Gaining insight in the mechanism of the broadening is an ongoing process challenged by the constant introduction of new catalysts. Every catalyst gives a different molecular weight (Mori et al. 1999, p. 211) and broadening effect.
The mechanism is also not clarified. It is believed that Ziegler-Natta catalysts do not have a single kind of sites that all produce the same polymer. As Chadwick et al. (1995) said that hydrogen frees mostly isospecific dormant sites, and Soares and Hamielec (1996) stated that addition of hydrogen leads to broadening of the molecular weight because of activation of sites by hydrogen with a different behavior.
Poylpropylene with an isotactic and atactic part leads to the idea of sites that either produce isotactic or atactic polymer. Within the isotactic part a distinction can be made between highly isotactic material and less isotactic material, giving rise to the idea of even more types of sites. Shimizu et al. (2001) gave an overview of ideas on a three-site mechanism; Fait et al. (1999) propose a single site, two state catalyst as model for a metallocene catalyst.

1.4.1 Modeling of molecular weight distribution

Since the mechanism is not yet clear, i.e. the nature and number of active sites is unknown and their concentration is not clear, it is also difficult to model the broadening of the

molecular weight by hydrogen. For modeling of this broadening based on a complete set of reactions for each site many constants would be required that are unknown and that makes parameter estimation extremely difficult. Meier et al. (2001) derived an equation for the chain termination probability leading to an expression that corresponds to the well-known Mayo equation. He used a metallocene catalyst in his work and described the molecular weight by a single site model. Experiments show however that the Mayo equation cannot fully describe the rapid, non-linear decrease in molecular weight at low hydrogen concentrations.

Weickert et al. (2002) modeled both the reaction rate and molecular weight based on the dormant site theory and in a single site model. He took into account the deviation from the Mayo equation for low hydrogen concentrations. However the decreasing reaction rate at higher hydrogen concentration was not described in the model.

In this work the molecular weight of the polymer and changes in the molecular weight caused by hydrogen will be modeled according to a single site model, though Ziegler-Natta catalysts are not single site catalysts. It is however not yet clear how many sites should be chosen to describe Ziegler-Natta catalysts. Also no quantitative data is available on the propagation rates of these alleged different sites; even Fait et al. (1999) who used a metallocene catalyst, proposed a single site, two-state model for the catalyst. The two states they propose are a fast and slow state and hydrogen influences the state of the catalyst. The single site model is expected to predict the average molecular weight of the polymer.

1.5 Theoretical considerations

Mainly two theories on the mechanism of rate enhancement by hydrogen have been discussed above. From mechanistic point of view, the dormant site theory gains more support. The end-group analysis and detection of propane as Chadwick et al. (2000) did are examples.

However, the reaction rate can qualitatively be described by both theories. They promote to describe the enhancement effect with an increase in C*, the number of active sites or with an increase in k_p, the propagation rate constant. From the results of most experiments it is impossible to determine which factor is responsible for the increase in the reaction rate. Most experiments with hydrogen in the literature are over a too long time period and that means the enhancement effect can be described both by an increase in C* and an increase in k_p. A distinction cannot be made.

To determine the true responsible factor in the rate enhancement effect of hydrogen very short residence time experiments should be done. If the reaction time could be shortened to much less than the formation time of one polymer chain a clear distinction could be made between the two main factors (C* and k_p) mentioned above. Three possibilities exist: first, the increase is caused by an increase in the propagation rate constant k_p. Then the production is increased and the length of the chain produced in the experiment is longer. Secondly, the increase is caused by an increase in the number of active sites ($Ti^{2+} \rightarrow Ti^{3+}$) C*. Then the production is increased, but the length of the produced chains is not increased. Thirdly, freeing of dormant sites causes the increase in reaction rate. Because dormant sites or not yet created (the first chains are being created) neither the production nor the chain length will have increased.
When experiments over much longer time are done this distinction cannot be made. Chain lengths will be the same, as will be the production. Dormant sites are freed in this longer time and that could have caused the higher production. However, when assuming one of the mechanisms, in this case the dormant site theory, it is possible to describe the enhancement effect satisfactorily. When both reaction rate and molecular weight are modeled simultaneously which is the intention of the present paper, the deviation from the Mayo-equation at lower hydrogen concentrations can only be described when assuming the dormant site theory. This supports the notion that the dormant site theory is the true mechanism. Further conclusions can only be drawn on the results of the suggested experiments, see above.

1.6 Current work

In the current work hydrogen response is investigated in gas phase propylene polymerization. Both the initial reaction rate and the average molecular weight are measured and modeled simultaneously. A model is constructed that predicts the changes in reaction rate of propylene polymerization as a function of hydrogen concentration due to both dormant sites and slower insertion of monomer at a Ti-H active site simultaneously with modeling of the average molecular weight with the description of the chain termination probability constant as was proposed by Weickert et al. Such a combined model is unprecedented.
Also a possible explanation will be given for the faster deactivation of the catalyst at high hydrogen concentrations, as is observed in the experiments.

2 Experimental

Experiments were performed in a 5 l jacketed stainless steel tank reactor (figure 2) with a helical stirrer inside. This stirrer guarantees good mixing and heat transfer in both the liquid and the gas phase polymerizations. Liquid and gaseous propylene can be added to the reactor with a mass flow controller (MFC), as well as hydrogen. The suspended catalyst system prepared in glass vials is injected with purified hexane by means of a pneumatic injection system. Glass vials can be connected to a syringe of the injection system to add extra hexane to the vial and suck up the catalyst mixture. The vial is rinsed with hexane, which is also injected into the reactor to ensure that all catalyst is injected into the reactor.

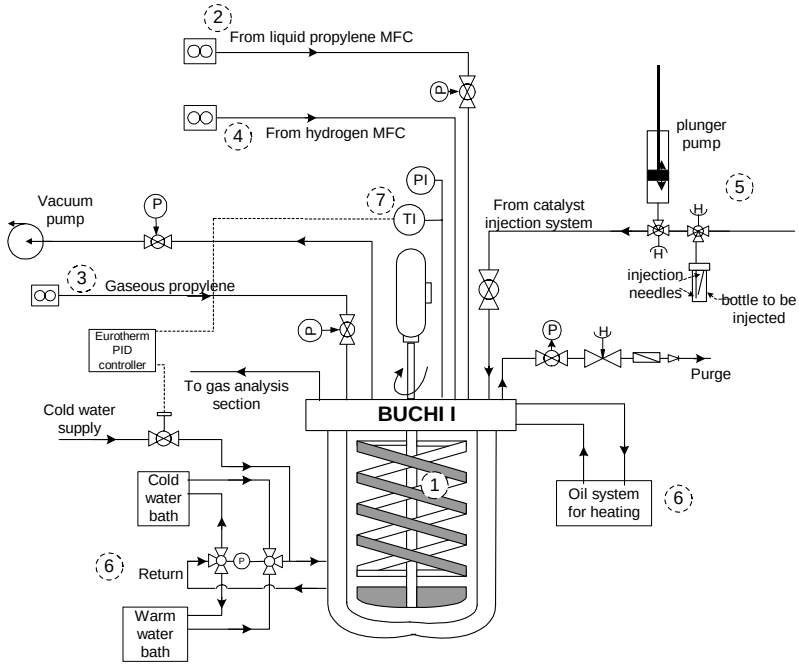

Figure 2: Schematic of experimental set up. Numbers in dotted circles refer to: 1: autoclave with helical stirrer; 2: liquid propylene feed; 3: gaseous propylene feed; 4: hydrogen feed; 5: catalyst injection system; 6: temperature control system for autoclave; 7: temperature control of reactor.

The cooling/heating system consists of a warm and cold-water bath, a cold-water tap and an oil circuit for heating the cover plate. The cover plate is heated slightly above the reaction temperature to prevent condensation of propylene on the cover plate during the reaction. Precise temperature control is very important in this system, since a calorimetric method is

used to determine the reaction rate in the liquid phase. The temperature of the cooling water in the jacket is also measured; via a heat balance over the reactor and assuming steady state operation, it is possible to calculate the heat produced from the polymerization reaction, see Samson et al (1998).

When the reactor system runs isoperibolically, meaning constant jacket temperature, the rise in the reactor temperature is caused by the highly exothermic polymerization reaction (at constant pressure). The isoperibolic mode is mainly applied in the gas phase reaction. The heat balance over the reactor should effectively not change because otherwise the reaction rate is influenced by the temperature differences. So the temperature rise at the start of the gas phase reaction should be kept low and the following temperature decrease caused by deactivation of the catalyst should also be low and gradual.

2.1 Catalyst

It was decided to work with a 4^{th} generation Ziegler-Natta system, which is a $TiCl_4$ supported on MgCl with a phthalate as internal donor and an external silane donor. Tri Ethyl Aluminum (TEA) was used as cocatalyst. The catalyst system was prepared for reaction in a glove box under a nitrogen atmosphere. For every experiment, 3.75 mg of bare catalyst was mixed with 6.94 mg of silane donor and 2 g of hexane. As cocatalyst in total 160 mg of TEA were used. 28 mg of TEA was used both as cocatalyst and as scavenger and prepared in a separate vial. It was injected 5 minutes prior to catalyst injection in the reactor filled with propylene. 132 mg of TEA was mixed with the catalyst, silane donor and hexane mixture 30 minutes before injection.

2.2 Reactor preparation

The reactor had to be devoid of contaminations. Therefore the reactor was heated to 95 °C after closing to bake contaminations off the wall and the coverplate. The reactor was evacuated and brought to vacuum with a vacuum pump, then pressurized with nitrogen to 5 bars for 180 seconds and evacuated afterwards. This sequence was repeated 6 times. After completion of the flushing procedure, the reactor was left at vacuum. Gaseous propylene was added up to 5 bars and evacuated again. The reactor was flushed with propylene two times, without evacuating the reactor.

2.3 Prepolymerization

Normally an inert bed is used in gas phase reactions to obtain proper mixing and heat removal of the polymerizing particles. Contaminations are very likely to be introduced into the system and reproducibility can be lowered considerably. To avoid this a new so-called reactive bed preparation method was designed. In this method a prepolymerization step at mild conditions is applied. The polymerization is performed in liquid phase propylene at low temperature. Reaction rate is relatively low thus heat production is low in the initial phase of the reaction. No overheating of particles will take place and morphology of the initial polymer particles can be controlled better. After producing enough polymer powder in the liquid phase, propylene is evaporated by opening the purge and after rinsing the reaction continues in the gas phase. Since the prepolymerization resulted in a polymer bed, i.e. the just produced prepolymer, no inert bed is necessary for gas phase reaction.

For the prepolymerization step the reactor was cooled to 20 °C and 420 grams of liquid propylene were added. Then 350 mg of hydrogen were added and the system was heated up to the required reaction temperature for the liquid phase reaction, in all experiments 40 °C. At 40 °C at saturation pressure this resulted in 503 ml of liquid propylene. When the system was at constant temperature, the scavenger was injected and 5 minutes later the catalyst mixture was added to start the polymerization reaction.

2.4 Polymerization

After having produced enough polymer in the prepolymerization step, the propylene is flushed and the reactor is heated up to 70 °C. The reactor is then rinsed five times with gaseous propylene up to 5 bars to remove hexane from the reactor. After rinsing the reactor is filled with gaseous propylene and hydrogen resulting in a total pressure of 25 bars. The pressure is then kept constant by adding gaseous propylene through a MFC. It is assumed that hydrogen is not consumed. The readings from the MFC are used to calculate the reaction rate in the gas phase. The temperature in the reactor is controlled isoperibolically.

In the procedure for addition of the gasses before the start of the gas phase experiment not all the consumed monomer is registered, because the MFC is not working at the time the hydrogen is added. Also polymer with a different average molecular weight is produced in the period of hydrogen addition since the hydrogen concentration changes. However, the amount

of produced polymer during this period is approximately at maximum 5.6 g (with an average catalyst activity of 30 kg/gcat.hr at 25 bars, a catalyst amount of 3.75 mg and a time of 3 minutes at maximum, although the average pressure in this period is lower). In the experiments with low activity 5.6 g would be about 10% of the produced polymer with a full activity during the 3 minutes, which is unlikely. That means the amount of this polymer with a different average molecular weight is low compared to the total amount of product and will not influence the properties of the final product.

Flushing the reactor after gas phase reaction terminates the experiment. The pressure and temperature drop lower the reaction rate after a few seconds. Flushing the reactor with nitrogen and applying vacuum removes the remaining propylene. At opening of the reactor the catalyst is killed in the contact with air. The powder is dried four hours at 50 °C in a vacuum oven.

3 Results

3.1 Prepolymerization

A number of experiments were done to define an optimized recipe for the prepolymerization step. Since the focus of the research is on the main polymerization in the gas phase, the total experiment should be optimized for the gas phase part of the experiment. That puts a few constraints on the prepolymerization recipe in the liquid phase:

- The reaction time of the prepolymerization step should be kept short, considering the deactivation of the catalyst over time in this ‘preparation’ step. Enough activity must be left when the experiment enters the gas phase step.
- The prepolymer step should produce enough polymer to obtain circulation of powder through the reactor caused by the stirrer in the gas phase part of the experiment. A survey of different amounts of polymer used showed that 18 grams of polymer ensure this circulation.
- The temperature rise at the start of the gas phase step and the following expected temperature decrease because of deactivation should be kept low when running in isoperibolic mode, as explained above. That means the activity of the catalyst in the gas phase should not be too high, but as also explained above the reaction in the liquid phase step of the experiment should be large enough to produce 18 grams of polymer

in a as short as possible period of time. This way the amount of catalyst used is to be optimized for a given reaction temperature.

- The activity of the catalyst system is influenced by the concentration of hydrogen. To obtain a sufficient activity in the liquid phase step of an experiment, the concentration hydrogen should not be too low or too high.
- Hydrogen also influences the molecular weight of the prepolymer significantly and this prepolymer is also present in the final product that is produced in the gas phase step. To be able to distinguish between the polymer produced in the liquid phase (the prepolymer) and polymer produced in the gas phase step (main polymer) the prepolymer should have an either very high or very low molecular weight or should be exactly the same as the main polymer in every experiment. However, the reproducibility of the prepolymerization step is violated when trying to produce the same polymer in the liquid phase as in the gas phase step. The prepolymerization step can influence the performance of the catalyst in the gas phase step. Producing prepolymer with a very high molecular weight would require more reaction time in the prepolymerization step or a larger catalyst amount. A low molecular weight prepolymer can become sticky and cause mechanical problems in the gas phase part of the experiment. The hydrogen concentration in the liquid phase should be chosen within these boundaries, and the molecular weight of the resulting prepolymer should be analyzed.
- The deactivation of the catalyst in the gas phase should not be too high. Deactivation can be caused by contaminations in the gas phase propylene feed. The catalyst is likely to be poisoned except when enough scavenger is present. The cocatalyst TEA can act as a scavenger. The cocatalyst also influences the performance of the catalyst, but it is our belief that in these experiments the scavenger function should be optimized. The lowest amount of 'extra' TEA for this scavenger function should be used.

Considering the above-mentioned constraints, a recipe for the prepolymerization step was constructed. The recipe of the prepolymerizaton was set at 30 min reaction in liquid phase propylene at 40 °C with addition of 350 mg of hydrogen in the gas phase (1.15 mol% H_2 in liquid phase) with 3.75 mg of bare catalyst, 6.94 mg of external donor and 160 mg of TEA. This recipe, called 'standard', was used in all subsequent experiments.

3.2 Polymerization

Determination of the dependency of the pseudo initial reaction rate and the molecular weight on the hydrogen concentration in the gas phase was done in a series of experiments (Table 1). The hydrogen concentration in the main polymerization in the gas phase was varied systematically from zero hydrogen to 11 mole% hydrogen while the total pressure was kept at 25 bars.

To compare the experimental results of the different hydrogen experiments, a method was developed based on a first order kinetic model:

$$R_p = R_{p,0}^{"} e^{-k_d^{"} t} \qquad (1)$$

Table 1: Experiments after 'standard' prepolymerization in hydrogen series at 25 bar and 70 ^{0}C.

Experiment code	Hydrogen conc. [mol%]
UT00847	0.00
UT00904	0.18
UT00902	0.37
UT00905	0.73
UT00901	1.09
UT00907	1.80
UT00971	2.50
UT00974	3.54
UT00910	4.89
UT00975	7.47
UT00848	9.92

Using the first order model, a pseudo initial reaction rate $R_{p,0}$" and deactivation constant k_d" for the gas phase could be obtained. The reaction rate fluctuates in the first few minutes of the gas phase reaction. This is caused by the pressure control that has to find its set point of 25 bars. The first order deactivation model is fitted to the experimental results and extrapolated towards t = 0 (figure 3). The reaction rate at the start of the gas phase polymerization is taken at the moment in time when all the hydrogen is added (figure 3).

Assuming steady state operation in the model, the pseudo initial reaction rate in the gas phase is a measure for the steady state activity since deactivation does not play a role. These measurements can therefore be used in the kinetic model.

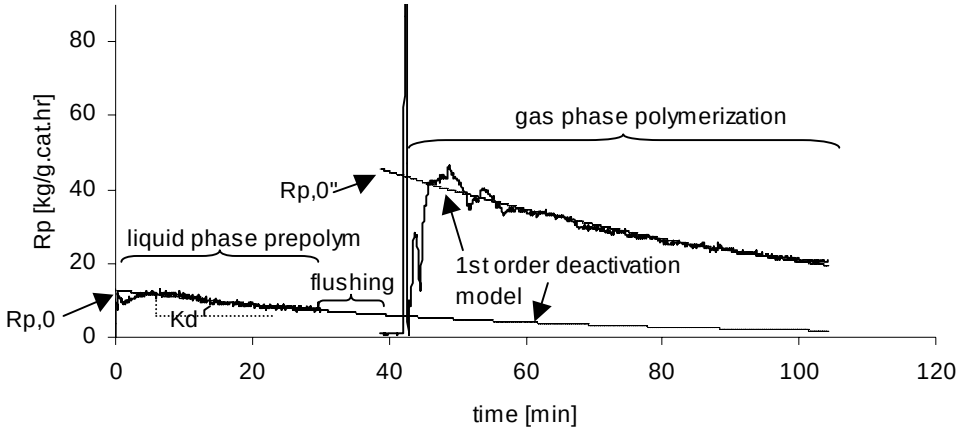

Figure 3: Determination of reaction rate and $R_{p,0}$ from experimental results

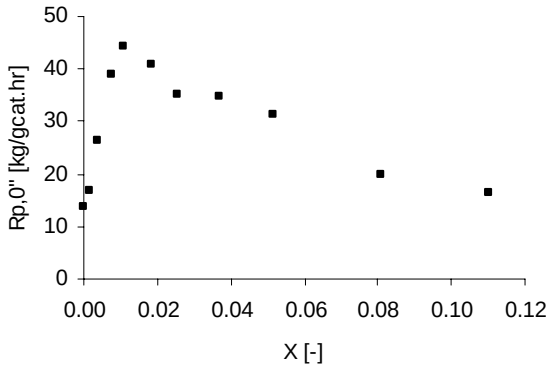

Figure 4: Pseudo initial reaction rate in the gas phase as a function of the hydrogen concentration. Experiments done at 70 °C and 25 bars total pressure.

The $R_{p,0}$" increases with increasing hydrogen concentration to a maximum of 45 kg/gcat.hr at a concentration of 1.1 mole% hydrogen; that is three times higher than the initial activity without hydrogen (figure 4). This is in agreement with the dormant site theory. When the hydrogen concentration is further increased the initial activity drops again. We interprete this phenomenon as follows:

because of the large number of dormant sites being reactivated with hydrogen or by chain transfer reaction with hydrogen, the concentration of Ti-H sites, becomes larger. They are

thought to have a significantly lower propagation rate constant for insertion of the first monomer than polymerizing active sites with one or more monomer units in the growing chain.

Chadwick et al. (2000) gave a different explanation. They stated that the Ti-H active sites would also produce propane in the presence of a large concentration of hydrogen. Insertion of the first monomer can take place via a 1,2 insertion or via a 2,1 insertion.

$$T_0 + M \xrightarrow{k_{ts}} S_1 \qquad (2)$$

In the case of 2,1 insertion a dormant site is created that will be reactivated almost immediately by hydrogen with the production of a propane molecule. Dormant site S_1 will react immediately with hydrogen to form T_0 again. If this cycle is done repeatedly one should be able to measure propane in the reactor. This may be done in the future experiments; it is however expected that the propane formation does not explain the slower reaction rate. The formation of dormant sites and the freeing of these dormant sites is expected to be very fast, there is no rate limiting step. Thus, reaction (2) is neglected.

The deactivation rate in the gas phase k_d" seems to be dependent on the amount of hydrogen as well (figure 5). This increase in k_d" could be explained by a faster deactivation of T_0 sites, since they become more abundant at higher hydrogen concentrations. It is also possible that the Ti-H sites are more vulnerable to contaminations.

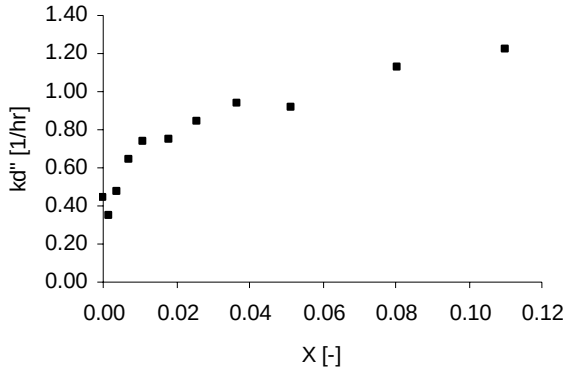

Figure 5: Deactivation constant in the gas phase versus hydrogen concentration.
Experiments done at 70 °C and 25 bars total pressure.

The powders produced in the series for hydrogen response were analyzed by GPC measurements. The weight average molecular weight (M_w) and the number average molecular weight (M_n) were determined, as well as the polydispersity PD. As can be seen in figure 6 the average molecular weight decreases rapidly with increasing hydrogen concentration followed by a slower decrease of the molecular weight at higher hydrogen concentration, as was

expected. The molecular weight is very high without the addition of hydrogen (X=0). This indicates that the rate constant of the chain transfer reaction with monomer, k_m in equation (9), is very small.

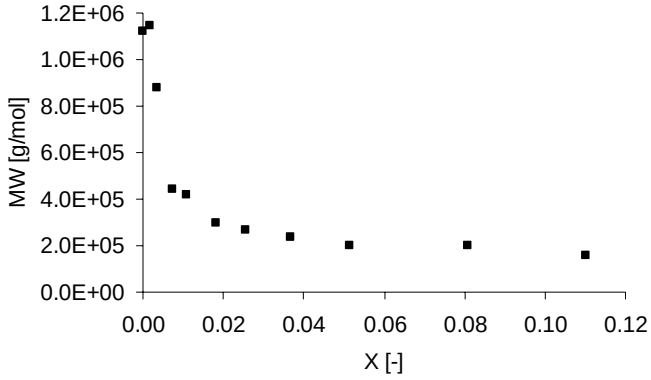

Figure 6: Weight average molecular weight as a function of mole fraction hydrogen in gas phase. Experiments performed at 70 °C and 25 bars total pressure.

3.3 Modeling

Goal of the research is to construct a kinetic model for the catalyst that can simultaneously describe the influence of hydrogen on initial reaction rate and molecular weight. The model is described with a single site model, whereas the Ziegler-Natta catalyst is not a single site catalyst. As explained earlier in this work, the single site model is expected to predict the average behavior of the catalyst.

The modeling of the reaction rate and molecular weight is based on the following reaction scheme:

Insertion of the first monomer:

$$T_0 + M \xrightarrow{k_{st}} C_1 \qquad k_{st}T_0M \qquad (3)$$

2,1 insertion of monomer is not included in the system as explained. Next to that, the amount of propane formed is small compared to the amount of monomer consumed.

Propagation of the polymer chain:

$$C_j + M \xrightarrow{k_p} C_{j+1} \qquad k_pCM \qquad (4)$$

Formation of dormant sites:

$$C_j + M \xrightarrow{k_s} S_{j+1} \qquad k_sCM \qquad (5)$$

Reactivation of dormant sites by hydrogen:

$$S_j + H_2 \xrightarrow{k_{reh}} T_0 + D_j \qquad k_{reh}SH_2 \qquad (6)$$

Reactivation of dormant sites without hydrogen:

$$S_j \xrightarrow{k_{rem}} C_j \qquad k_{rem}SM \qquad (7)$$

Chain transfer to hydrogen:

$$C_j + H_2 \xrightarrow{k_h} T_0 + D_j \qquad k_hCH_2 \qquad (8)$$

Chain transfer to monomer:

$$C_j + M \xrightarrow{k_m} C_1 + D_j \qquad k_mCM \qquad (9)$$

Chain transfer to co-catalyst is not taken into account because its concentration was not varied. The deactivation reaction is neglected for instantaneous modeling because of its larger time constant.

3.3.1 Reaction rate model derivation

Basis for the kinetic model is the reaction rate definition:

$$R_p = k_pCM + k_{st}T_0M + k_sCM \qquad (10)$$

This is a model for long chain polymerization; the chains normally have a length of >> 1000 monomers, thus reaction (3) and (5) occur only once per >> 1000 times of reaction (4) (long chain hypothesis). The expression for the reaction rate is therefore simplified to:

$$R_p = k_pCM \qquad (11)$$

With the activated catalyst concentration per gram supported catalyst C:

$$C = C_{\max} - S - T_0 \qquad (12)$$

S represents the amount of sites that are temporary dormant. A distinction is made between regular active sites and Ti-H active sites formed by reaction with hydrogen T_0.

The quasi steady state assumption is applied twice to obtain an expression for the concentration of S and the concentration of T_0:

$$R_s = 0 = k_s CM - k_{reh} SH_2 - k_{rem} SM \qquad (13)$$

$$R_{T_0} = 0 = -k_{st} T_0 M + k_{reh} SH_2 + k_h CH_2 \qquad (14)$$

Resulting in:

$$S = \frac{k_s C}{k_{reh} X + k_{rem}} = \frac{k_0 C}{1 + k_1 X} \qquad (15)$$

and

$$T_0 = \frac{k_{reh} SX + k_h CX}{k_{st}} = k_2 SX + k_3 CX \qquad (16)$$

respectively. With $X = H_2/M$ and

$$k_0 = \frac{k_s}{k_{rem}} \;; k_1 = \frac{k_{reh}}{k_{rem}} \;; k_2 = \frac{k_{reh}}{k_{st}} \;; k_3 = \frac{k_h}{k_{st}} \qquad (17)$$

Note that if reaction (2) would have been included in this model only k_2 and k_3 would be defined in a different way, but the mathematical structure would remain the same.

Combination of equation (12), (15) and (16) leads to:

$$C = \frac{C_{\max}}{1 + \frac{k_0}{1 + k_1 X}\left(1 + k_2 X\right) + k_3 X} \qquad (18)$$

Thus, equation (11) becomes

$$R_p = \frac{k_p MC_{\max}}{1 + \frac{k_0}{1 + k_1 X}(1 + k_2 X) + k_3 X} = \frac{k_p MC_{\max}(1 + k_1 X)}{1 + k_0 + X(k_1 + k_0 k_2 + k_3) + k_1 k_3 X^2} \quad (19)$$

This reaction rate model contains five unknown kinetic constants that should be fitted to figure 4. Moreover, C_{max} should be lumped with k_p to $k_p C_{max}$ for it is not known and cannot be derived from these measurements. Fixing the data point with no hydrogen (X = 0) leads to an expression for $k_p MC_{max}$:

$$R_p = \frac{k_p MC_{\max}}{1 + k_0} \quad (20)$$

$$k_p MC_{\max} = R_{p,0}''(1 + k_0) = 13.9 \cdot (1 + k_0)$$

Equation (20) can be inserted in the reaction rate model (19), resulting in a four-parameter reaction rate model:

$$R_p = \frac{13.9(1 + k_0)(1 + k_1 X)}{1 + k_0 + X(k_1 + k_0 k_2 + k_3) + k_1 k_3 X^2} \quad (21)$$

We receive:

$$R_p = \frac{13.9(1 + k_1 X)}{1 + \mathrm{K}_1 X + \mathrm{K}_2 X^2} \quad (22)$$

with

$$\mathrm{K}_1 = \frac{k_1 + k_0 k_2 + k_3}{1 + k_0} \; ; \mathrm{K}_2 = \frac{k_1 k_3}{1 + k_0} ; R_{p,0}'' = 13.9 \quad (23)$$

The reaction rate model in equation (22) is fitted to the experimental data from the hydrogen response in figure 4. Note that the initial reaction rate from these experiments can be used in the reaction rate model because deactivation is zero in this steady state model; $R_p = R_{p,0}$".

3.3.2 Molecular weight model derivation

The second part of the kinetic model for the catalyst is the modeling of the molecular weight of the product. In modeling the product molecular weight, the experimental molecular weights are described by the termination probability q. Note again that a multi site M_w is used to determine a single site q.

$$q = \frac{2M_M}{M_w^d} \tag{24}$$

The goal is to integrate the molecular weight model with the kinetic model by describing termination probability q with the same kinetic constants as used in the reaction rate model. The molecular weights from GPC analysis are used to determine the experimental termination probability (figure 7).

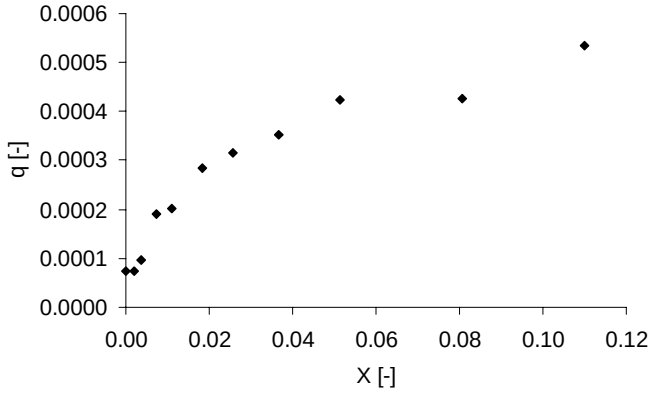

Figure 7: Experimentally determined termination probability q vs. hydrogen concentration

Balance of dormant sites of chain length j S_j:

$$R_{S_j} = 0 = k_s C_{j-1} M - k_{reh} S_j H_2 - k_{rem} S_j M \tag{25}$$

leading to

$$S_j = \frac{k_s C_{j-1}}{k_{reh} X + k_{rem}} = \frac{k_0 C_{j-1}}{k_1 X + 1} \tag{26}$$

Balance of active sites of chain length j C_j:

$$R_{C_j} = 0 = -k_p M C_j + k_p M C_{j-1} - k_s C_j M + k_{rem} M S_j - k_h C_j H_2 - k_m M C_j \tag{27}$$

leading to

$$C_{j-1}\left(k_p M + \frac{k_{rem} M \cdot k_s}{k_{reh} X + k_{rem}}\right) = C_j\left(k_p M + k_s M + k_h H_2 + k_m M\right) \quad (28)$$

The assumption

$$C_j = pC_{j-1} \quad (29)$$

is applied to obtain the propagation probability p:

$$p = \frac{1 + \frac{k_s}{k_p}}{1 + X\frac{k_{reh}}{k_{rem}}} \Bigg/ \left(1 + \frac{k_s}{k_p} + X\frac{k_h}{k_p} + \frac{k_m}{k_p}\right) \quad (30)$$

Termination probability can now be determined by:

$$q = 1 - p \quad (31)$$

Assuming long chain polymerization process ($1 >> k_s/k_p + q_{,min}$) again this leads to:

$$q = \frac{k_m}{k_p} + X\frac{k_h}{k_p} + \frac{k_s}{k_p}\left(\frac{k_1 X}{1 + k_1 X}\right) \quad (32)$$

This expression for q can be divided into q_{min} and Δq, where q_{min} is the termination probability without dormant site formation as described by Mayo. Thus, Δq is the deviation from Mayo's equation caused by the 2,1 insertions that form dormant sites.

$$q_{\min} = \frac{k_m}{k_p} + X\frac{k_h}{k_p}$$
$$\Delta q = \frac{k_s}{k_p}\left(\frac{k_1 X}{1 + k_1 X}\right) \quad (33)$$

Note that k_1 is present in both the reaction rate model and the model for the molecular weight. Thus k_1 is an important fitting parameter that links the two models.

The kinetic ratios in Mayo's equation can be determined from the two extremes:

1. The point at which the hydrogen concentration is zero (X=0), leading to:

$$q = \frac{2M_M}{M_w^d}$$
$$\rightarrow \frac{k_m}{k_p} = 7.5 \cdot 10^{-5} \quad (34)$$

2. The point at which the dormant site concentration is assumed to be zero (S=0), leading to:

$$q = q_{\min} + \Delta q = q_{\min}$$
$$\frac{k_h}{k_p} = 4.18 \cdot 10^{-3} \quad (35)$$

The highest hydrogen concentration in the experiments was about 10 mol%. This data point was used to calculate k_h/k_p, assuming that S = 0. The above model for the termination probability should be fitted to the experimental data from molecular weight measurements, using equation (24).

3.3.3 Parameter estimation

A simultaneous fit of the reaction rate model and the molecular weight model was done in Matlab with a Marquardt procedure; see figure 8 and figure 9 and table 2. The results agree well with the experimental data. The final kinetic model is, with $X=H_2/M$:

$$R_p = \frac{13.9 \cdot (1 + 378.53 \cdot X)}{1 + 40.49 \cdot X + 2641 \cdot X^2} \quad (36)$$

and

$$q = 7.5 \cdot 10^{-5} + 4.18 \cdot 10^{-3} X + 0.000090 \cdot \left(\frac{378.53 \cdot X}{1 + 378.53 \cdot X} \right) \quad (37)$$

Table 2: Matlab simultaneous fit through experimental data

Parameter	Value [-]	Standard deviation	Lower 95% confidence interval	Upper 95% confidence interval
k_1	378.53	98.0	172.7	584.4
K_1	40.49	30.4	-23.4	104.3
K_2	2641.00	469.1	1655.5	3626.5
k_s/k_p	0.000090	0.000021	0.000045	0.000135

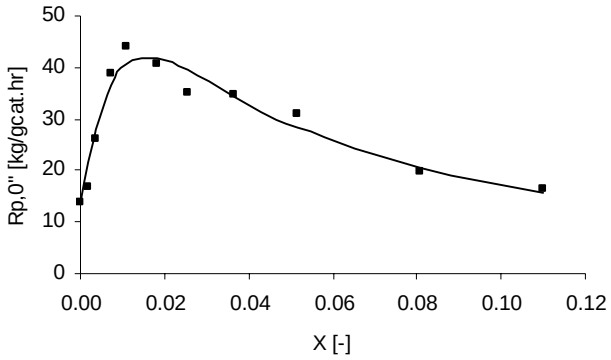

Figure 8: Model fit through experimental data for pseudo initial reaction rate in gas phase vs fraction hydrogen in gas phase. Experiments done at 70 °C and 25 bars total pressure.

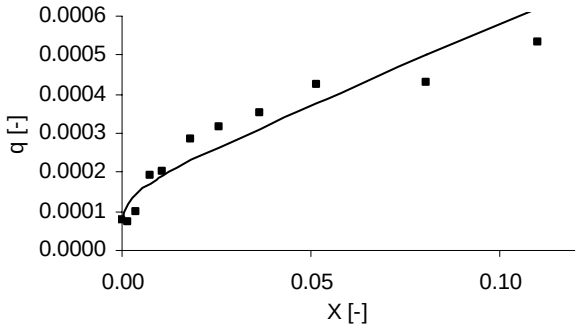

Figure 9: Model fit through the experimentally determined termination probability vs hydrogen fraction in gas phase. Experiments done at 70 °C and 25 bars total pressure.

4 Conclusions

The influence of hydrogen concentration in gas phase propylene polymerization on the pseudo initial reaction rate in the gas phase and the average molecular weight was investigated. The initial reaction rate increases with increasing hydrogen concentration to a maximum of 45 kg/gcat.hr at a concentration of 1.1 mole% hydrogen; this is in agreement with the dormant site theory. When the hydrogen concentration is further increased the initial activity drops again, in agreement with findings of other authors. The proposed occurrence of Ti-H active sites as a result of the increased occurrence of chain transfer reactions and freeing of dormant sites with hydrogen was assumed to be responsible for the behavior. The Ti-H sites are supposed to have a different propagation rate for insertion of the first monomer than Ti-C_3H_6 sites.

The trend in molecular weight as a function of the hydrogen concentration follows the theory; molecular weight decreases with increasing hydrogen concentration.

A simultaneous model of initial reaction rate an molecular weight as function of hydrogen concentration was constructed. To describe the reaction rate behavior the dormant site theory was used, assuming a slow insertion of the first monomer at a Ti-H active site that is created by chain termination by hydrogen. The quasi steady state assumption was applied and the average molecular weight was modeled assuming single site behavior. The model can accurately describe both initial reaction rate and average molecular weight simultaneously.

This model is limited to the catalyst system used in the research and to operational conditions near T = 70 ^{0}C and p = 25 bar. Of course, general concepts such as a slow first monomer insertion and the model derivation can be used for other catalytic systems and other operational conditions as well.

The problem of modeling of the molecular weight distribution of multi-site catalysts still remains unsolved, because of the large number of model parameters. In the present work the number of model parameters has been reduced dramatically compared to multi site models, but still the confidence intervals are relatively large.

5 Notation

C_1	Active site with one monomer attached	[-]
C_j	Growing polymer chain containing j monomers	[-]
C_{max}	Maximum concentration of active sites	[kg/g_{cat}]
D_j	Terminated (dead) chain containing j monomers	[-]
k_1, k_2, k_3	Ratios of kinetic constants	[-]
K_1, K_2	Expressions of kinetic constants	[-]
k_d"	Gas phase deactivation rate constant (GP first order model)	[1/hr]
k_h	Chain transfer to hydrogen rate constant	[1/hr]
k_m	Chain transfer to monomer rate constant	[1/hr]
k_p	Propagation rate constant	[1/hr]
k_{reh}	Dormant site reactivation by hydrogen rate constant	[1/hr]
k_{rem}	Dormant site reactivation rate constant	[1/hr]
k_{st}	First monomer insertion rate constant for 1,2 insertion	[1/hr]
k_{ts}	First monomer insertion rate constant for 2,1 insertion	[1/hr]
M	Concentration of monomer	[mol/l]
M_m	Molecular weight of monomer	[g/mol]
M_w	Molecular weight of polymer	[g/mol]
p	Chain propagation probability	[-]
q	Chain termination probability	[-]
R_p	Polymerization rate	[kg/g_{cat}hr]
$R_{p,0}$"	Pseudo initial polymerization rate gas phase (GP first order model)	[kg/g_{cat}hr]
S_1	Dormant site with 1 monomer attached	[-]
S_j	Dormant site containing j monomers	[-]
t	time	[sec]
T_0	Ti-H active site after reaction with hydrogen	[-]
X	H_2/M ratio	[-]

6 Literature

Bukatov, G. D., V. S. Goncharov, V.A. Zakharov, V.K. Dudchenko, S.A. Sergeev (1994); Kinet. Catal. **35**(3): 358

Chadwick, J. C., A. Miedema, O. Sudmeijer (1994); "Hydrogen activation in propene polymerization with MgCl2-supported Ziegler-Natta catalysts: the effect of the external donor." Macromol. Chem. Phys. **195**: 167-172

Chadwick, J. C., G. M. M. van Kessel, O. Sudmeijer (1995); "Regio-and stereospecificity in propene polymerization with MgCl2-supported Ziegler-Natta catalysts: effects of hydrogen and the external donor." Macromol. Chem. Phys. **196**: 1431-1437

Chadwick, J. C., J. J. R. Heere, O. Sudmeijer (2000); "Factors influencing chain transfer with monomer and with hydrogen in propene polymerization using MgCl2-supported Ziegler-Natta catalysts." Macromol. Chem. Phys. **201**: 1846-1852

Chien, J. C. W. and C.-I. Kuo (1986); "Magnesium chloride supported High-mileage catalysts for olefin polymerization. X. Effect of hydrogen and catalytic site deactivation." Journal of polymer Science: Part A: Polymer chemistry **24**: 2707-2727

Chien, J. C. W. and T. Nozaki (1991); "High activity magnesium chloride supported catalysts for olefin polymerization. XXIX. Molecular basis of hydrogen activation of magnesium chloride supported Ziegler-Natta catalysts." Journal of polymer Science: Part A: Polymer chemistry **29**: 505-514

Fait, A., L. Resconi, G. Guerra, P. Corradini (1999); "A possible interpretation of the nonlinear propagation rate laws for insertion polymerizations: a kinetic model based on a single-center, two-state catalyst." Macromolecules **32**: 2104-2109

Guastalla, G. and U. Giannini (1983); "The influence of hydrogen on the polymerization of propylene and ethylene with an MgCl2 supported catalyst." Makromol. Chem. rapid commun. **4**: 519-527

Han-Adebekun, G. C., M. Hamba, W.H. Ray (1997); "Kinetic study of gas phase olefin polymerization with a TiCl4/MgCl2 catalyst I. Effect of polymerization conditions." Journal of Polymer Science **35**(10): 2063-2074

Keii, T. (1986) in: Studies in Surface Science & Catalysis, Vol. 25, Catalytic Polymerization of Olefins; T. Keii, K. Soga; Ed. Elsevier, New York, p. 1

Kioka, M. and N. Kashiwa (1991); "Study of the activity enhancement caused by the addition of hydrogen in olefin polymerization." Journal of macromol. sci.-chem.A **28**(9): 865-873

Liu, B., H. Matsuoka, M. Terano (2001); "Kinetic investigation of propylene polymerization with stopped-flow method." Macromolecular Symp. **165**: 3-10

Meier, G.B., G. Weickert, W.P.M. van Swaaij (2001); "Gas-phase polymerization of propylene: reaction kinetics ans molecular weight distribution." Journal of Polymer Science **39**(4): 500-513

Mori, H., M. Endo, K. Tashino, M. Terano (1999); "Study of activity enhanchement by hydrogen in propylene polymerization using stopped-flow and conventional methods." Journal of Molecular Catalysis A: Chemical **145**: 153-158

Mori, H., M. Endo, M. Terano (1999); "Deviation of hydrogen response during propylene polymerization with various Ziegler-Natta catalysts." Journal of Molecular Catalysis A: Chemical **145**: 211-220

Natta, G. (1959); Adv. Catal. **11**: 1

Pater, J.T.M., G. Weickert, J. Loos, W.P.M. van Swaaij (2001); "High precision prepolymerization of propylene at extremely low reaction rates - kinetics and morphology." Chemical Engineering Science **56**: 4107-4120.

Rishina, L. A., E. I. Vizen, L.N. Sosnovskaja, F.S. Dyachkovsky (1994); "Study of the effect of hydrogen in propylene polymerization with the MgCl2-supported Ziegler-Natta catalyst - Part I. Kinetics of polymerization." European Polym. J. **30**(11): 1309-1313

Samson, J. J. C., Weickert, G., Heerze, A. E., Westerterp, K. R.(1998); "Liquid-phase polymerization of propylene with a highly active catalyst." AIChE Journal **44(6)**, 1424-1437

Samson, J. J. C., P. J. Bosman, G. Weickert, K.R. Westerterp (1999); "Liquid-phase polymerization of propylene with a highly active Ziegler-Natta catalyst. Influence of hydrogen, cocatalyst, and electron donor on the reaction kinetics." Journal of polymer Science: Part A: Polymer chemistry **37**: 219-232

Schindler, A. (1965); J. Polym. Sci., Part B **3**: 793

Shimizu, F. (2001); PhD Thesis, University of Twente, Enschede, The Netherlands: 73

Shimizu, F., J.T.M. Pater, G. Weickert (2001); "Kinetic study of a highly active $MgCl_2$-supported Ziegler-Natta catalyst in liquid pool propylene polymerization II. The influence of alkyl Aluminum and alkoxysilane on catalyst activation and deactivation." Journal of Applied Polymer Science **81**(4): 1035-1047

Soares, J. B. P. and A. E. Hamielec (1996); "Effect of hydrogen and of catalyst prepolymerization with propylene on the polymerization kinetics of ethylene with a non-supported heterogeneous Ziegler-Natta catalyst." Polymer **37**(20): 4599-4605

Soares, J. B. P. and A. E. Hamielec (1996); "Kinetics of propylene polymerization with a non-supported heterogeneous Ziegler-Natta catalyst - effect of hydrogen on rate of polymerization, stereoregularity, and molecular weight." Polymer **37**(20): 4607-4614

Spitz, R., P. Masson, C. Bobichon, A. Guyot (1988); "Propene polymerization with MgCl2 supported Ziegler catalysts: activation by hydrogen and ethylene." Makromol. Chem. **189**: 1043-1050

Weickert, G. et al. (2002); EC project report GRD2-2000-30189 "Polyprop", Milan, Nov. 2002; 'Modeling of polymerization rate and molecular weight: H_2 response

Ystenes, M. (1991); "The trigger mechanism for polymerization of alpha-olefins with Ziegler-Natta catalysts: a new model based on interaction of two monomers at the transition state and monomer activation of the catalytic centers." Journal of catalysis **129**: 383-401

Chapter 6

A pilot plant of a circulating slugging fluidized bed reactor

Abstract

A pilot plant of a circulating slugging fluidized bed reactor was designed and built. The pilot plant was designed similar to the cold flow set-up that was used to measure hydrodynamic properties of the slugging fluidization. A reactor consisting of a riser and a downer part was combined with a gas recycle. In the gas recycle gases like nitrogen, hydrogen and propylene could be fed. A riser of 2.5 m resulted with a diameter of 102 mm and 55 mm. The total volume of the pilot plant was 125 l for the 102 mm riser and 112 l for the 55 mm riser.

Temperature control was possible in the reactor via jackets around the riser and downer and cooling of the centrifugal blower in the gas recycle. Pressure in the reactor as well as pressure differences over the riser, blower and distribution plate for the gas could be measured. Temperature measurements were at 10 places in the riser.

With the pressure difference over the riser at minimum fluidization velocity of powder in the riser the powder hold up in the riser could be determined. Analysis of pressure difference data over the riser showed if the fluidization in the riser was in bubbling or in slugging fluidization.

It was possible to circulate powder through the reactor and this movement could be observed via pressure difference measurements.

1 Introduction

In the present work research was done on propylene polymerization in a circulating slugging fluidized bed reactor operated in the gas phase. Goal was to be able to describe the polymerization reaction in such a reactor system. To study the different subjects into detail, the research was split into a study of the hydrodynamic behavior of the slugging fluidization (chapters 2 and 3) and a study of the polymerization reaction of propylene in the gas phase (chapters 4 and 5). Heat transfer in the reactor with the very exothermic polymerization reaction was not studied experimentally, but instead relations taken from the open literature would be used. Sorption of monomer into the polymer was not studied into detail although it was an integral part of the polymerization reaction. The work of others in the same research group could be used.

By splitting up the research areas the influence of hydrodynamics and polymerization on each other was however neglected. Also the influence of high pressure and thus high gas density on hydrodynamics and polymerization was studied only scarcely in the separate works.

Next to that, with the results from the study of these separate parts ultimately a mathematical model of the reactor system was to be constructed that could describe and predict the polymerization in such a reactor concept. Experimental results to verify the model would however strengthen the model results.

Therefore, a pilot plant scale of the slugging polymerization reactor was designed and constructed.

2 Pilot plant design

The pilot plant should combine the separate studies. Propylene polymerizations in semi-continuous operation (typically 5 hours) had to be possible. Comparison between the results from the pilot plant and the cold flow set-up and between the pilot plant and the polymerization experiments had to be possible. This resulted in the following design parameters:

- Configuration of the reactor similar to the cold flow set-up, thus a circulating reactor with a cyclone on top of the downer for separation of gas and solids and a re-entry of powder at the bottom of the riser with possibilities for restriction of the maximum solids flows.
- The riser should be as large as possible within the confines of the laboratory.

- The downer should be as small as possible to prevent a large production of polymer in the downer.
- Possibilities for extra cooling of the riser and the downer.
- Modular design of the reactor system for easy replacement of parts of the system.
- Different riser diameters: 5 cm and 10 cm risers.
- Opening for feed of powder to the closed reactor.
- Propylene, hydrogen and nitrogen feed.
- Maximum pressure of 30 bar, maximum temperature of 120 °C.
- Recycle for the gas stream.
- Temperature control of the gas.
- Possibilities for the injection of catalyst during operation.
- Possibilities for removal of product during operation.
- Control of the circulation rate of solids.
- Smooth inner surface of the reactor without horizontal surfaces or dead places to prevent wall sheeting.
- Possibility to measure temperature, pressure, pressure difference in the riser, gas concentrations and to be able to detect the occurrence and properties of slugging fluidization in the riser.
- Design for a safe operation of the reactor system in all situations.

Without analysis of the general safety of the reactor system, it was clear that the potential dangers of the reactor system were so high because of the amounts of propylene that would be used, that beforehand it was decided to place the system in a Box in the High Pressure Lab of the University of Twente.

Such a Box is constructed of walls of 50 cm of concrete, with a loose ceiling to prevent pressure build up in case of an explosion. The atmosphere in the Box is controlled and the contents of the Box are refreshed 6 times per hour. The pressure inside the Box is slightly lower than atmospheric to create an under pressure and thus prevent gases from leaking out of the Box. Detection of several gases including propylene, hydrogen and oxygen is present. Remote control of the reactor system from outside the Box is possible; in fact no electricity is available in the Box to prevent sources of ignition for burnable or explosive gases.

2.1 Reactor system design

The reactor was designed for a maximum pressure of 30 bar and a maximum temperature of 120 °C. The reactor was made of RVS 316 and the insides of the reactor were electrolytically polished. The volume of the total pilot plant is 98 l plus the volume of the riser tube.
Since propylene is used in the system and the system is designed for higher pressures, the reactor was designed according to the rules of the “Stoomwezen” for high pressure vessels.

2.1.1 Reactor

The circulating fluidized bed reactor was designed for a maximum total possible length of the riser of 2.5 m (figure 1). The riser section was divided into three sections.
The bottom section (A in figure 1) contains a coupling to the downer, a connection for the feed of monomer gas, a connection for the injection system for the catalyst and a connection to the riser tube. The diameter of the bottom section is 102 mm. For the 5-cm diameter riser an adjustment to 5 cm is made in the middle section. In this way both diameters can be used in the same configuration. At the entrance of the gas flow to the riser a distributor plate is placed (Siperm R) with a thickness of 3 mm. At the bottom and at the top of the section a connection is made for temperature or pressure measurements.
In the top of the bottom zone the injection system for the catalyst is connected. The injection system was a copy of the design of the injection system for catalyst in the Fluid Bed Reactor of Gerben Meier (Meier et al.(2002)) (figure 2). The catalyst was introduced with a vessel prepared and filled in the glovebox under a nitrogen atmosphere to prevent contaminations from killing the catalyst. The catalyst was allowed to flow into a ball
valve. The valve could be turned and then a nitrogen flow carried the catalyst into the riser. The opening to the riser was closed by a plunger to prevent clogging of the tube to the riser by polymer powder and active and polymerizing catalyst particles. With injection of the catalyst the plunger was shortly pulled back.
The middle section (B in figure 1) is the actual riser tube. Two tubes of different inner diameter were constructed (102 mm and 55 mm), each having a cooling jacket around it. Their respective volumes are 27.5 and 14.5 l. In the riser tube at different heights 6 connections are made to enable temperature or pressure measurements or to enable taking gas samples. For the 5 cm tube at the top and at the bottom of the tube an adjustment to a 5 cm diameter was made.

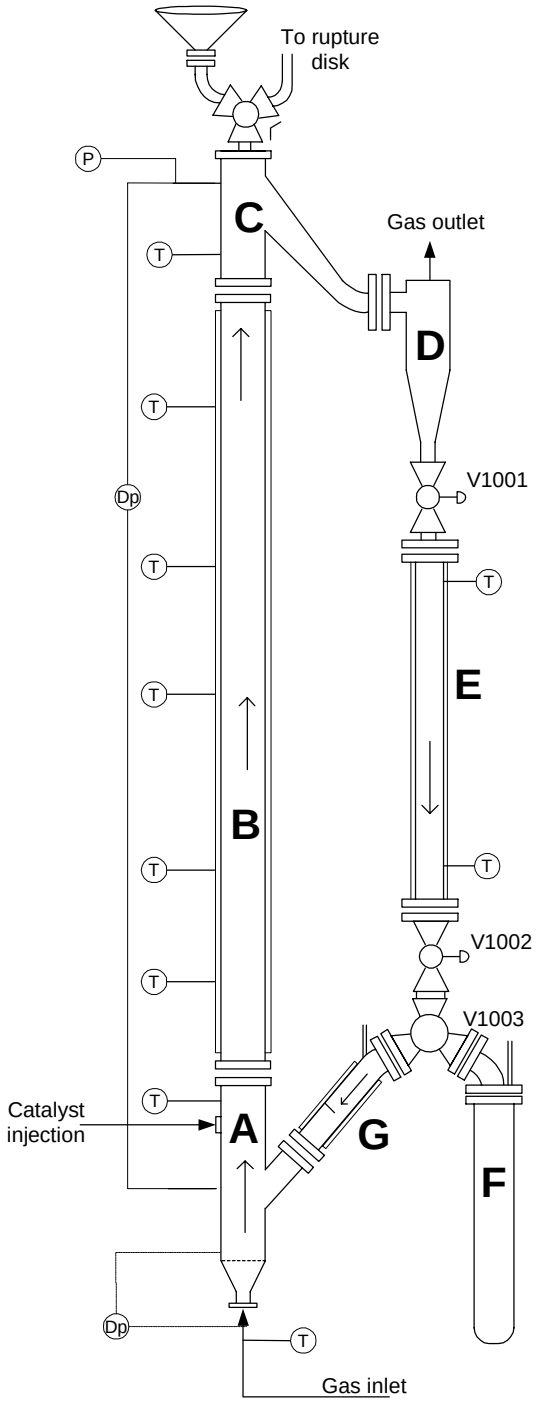

Figure 1: schematic of high-pressure circulating fluidized bed reactor pilot plant for propylene polymerization

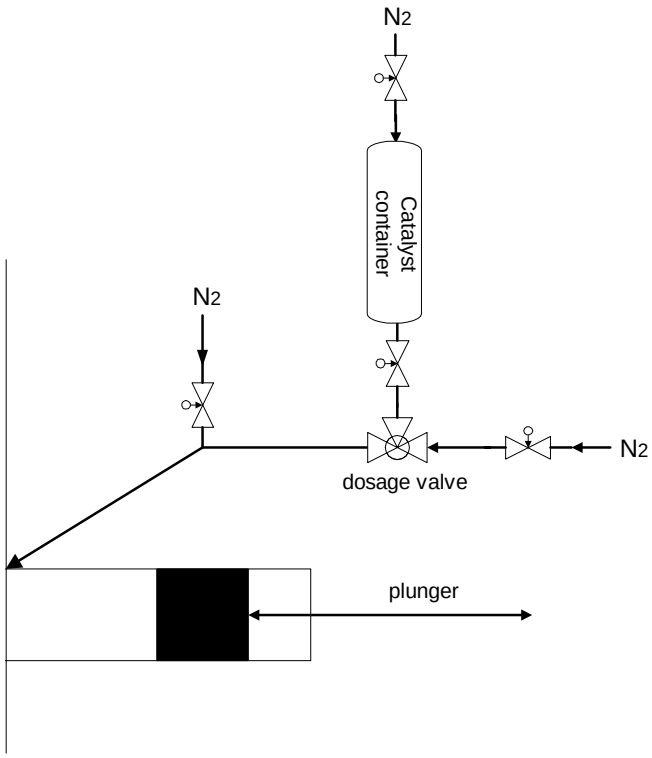

Figure 2: catalyst injection system

The top section (C in figure 1) contains a coupling to the riser tube and a coupling to the cyclone. The top section has an inner diameter of 10 cm. At the top and the bottom of the zone connections are made to enable temperature and pressure measurements. The section at the top of the riser has a downward inclined exit that is narrowed to the end to facilitate a larger velocity of the mixture of gas and solids into the cyclone. The stream has to enter the cyclone horizontally, so the exit is curved from directed downwards to horizontal. This curving is done after the narrowing to prevent powder from settling down on the horizontal surface since the velocity of the emulsion is higher.

On top of the coupling different flanges can be connected, each containing at least an opening to the purge lining and the rupture disk. For the experiments a feed opening was connected. A 3-way valve was connected to the opening of the flange, which could be switched between the rupture disk exit and the feed opening. Feed of powder bed can only be done when the reactor is not pressurized. During an experiment the 3-way valve was always switched to the rupture disk.

The cyclone (D in figure 1) was designed for the separation of gas and solids in a stream containing large amounts of solids. Since powder is only transported over the top at discrete

intervals in plugs, the separation always involves large amounts of solids. Solids flow down out of the cyclone into the downer section.

In the downer section (E in figure 1) two ball valves are placed to prevent gas from flowing through the downer. By using the two valves as in a lock system, it is possible to transport solids through the downer. The downer has an internal diameter of 38 mm and is fitted with a cooling jacket around it. The length of the downer tube is 105 mm. This length is the result of the constructional design of the reactor. The volume of the downer is large enough to contain a full plug that comes out of the riser.

Beneath the downer a 3-way valve is located. With the 3-way valve the flow of solids can be redirected back into the riser, or can be directed to the product vessel. In this way product can be removed from the system when polymerization reactions are done. The valve cannot be switched to connect the entrance to the riser with the product vessel. When no product vessel is connected to the reactor, the valve cannot be switched to the product vessel. This would mean an opening of the reactor.

The product vessel (F in figure 1) can be removed manually and replaced by another product vessel. The product vessel can be purged and flushed with nitrogen.

In the jacketed entrance leading back to the riser (G in figure 1) different smaller openings can be inserted to control the maximum flow of solids back into the riser. An extra connection is made at the top of the re-entry section to be able to blow extra gas into this section in order to increase the maximum possible solids flow. The entrance enters the riser below the injection of catalyst. This means that the catalyst will be injected in a full powder flow and will thus mix up quickly with the powder bed.

2.1.2 Recycle

A recycle of gas is necessary because of the expected low conversion rate of propylene. The conversion in this type of gas phase polymerization reactors typically lies between 2 and 4 % per pass through the riser.

A centrifugal blower (Somef) is placed in the recycle section to pump the gas around and has a maximum allowable pressure of 30 bar. The maximum speed of the blower is 4000 rpm, and

can be adjusted via a frequency control on the electrical power supply. Depending on the total gas density the blower can generate a maximum pressure difference of 800 mbar.

The greasing of the blower is done with oil and is separated from the gas stream by a sealing. The pressure difference over the sealing should be kept small. Part of the heat produced by the blower is transferred to the oil. The oil is cooled with water in a heat exchanger. The remaining part of the heat produced by the blower is transferred to the gas.

The diameter of the tubes in the recycle section is 76 mm. Curves are bent with large bends to prevent large pressure drops in the recycle section. The pipes are not insulated, because extra cooling is advantageous.

The gas is separated from the solids in the cyclone and is redirected back to the blower. 2 Meters after the cyclone nitrogen and hydrogen are introduced from the gas panel. The gases are supplied from the central gas supply, in which the gases are purified. On the gas panel, inlet pressures of nitrogen and hydrogen can be adjusted and several connections are available to supply either nitrogen or hydrogen to the reactor system. The gases can be fed to the system directly or via a Mass Flow Controller. The maximum flows of the MFCs are 5 m3n/hr for nitrogen and 5.5 m3n/hr for hydrogen.

Before the gas enters the blower (60 cm), propylene is sprayed into the middle of the gas stream and is expected to vaporize immediately. The propylene will mix up with the gas in the blower. The propylene is fed to the system via a jacketed storage vessel of 16 l containing liquid propylene. The propylene is fed to the reactor by heating up the contents by the heating/cooling jacket and thus increasing the pressure to a level that is higher than the actual pressure in the reactor. The propylene is fed to the storage vessel from the central propylene supply that comprises a catalytic purification unit and several molecular sieve columns.

After the blower a heat exchanger is placed. Two manual valves are placed in the gas stream to be able to isolate the reactor from the recycle section for maintenance. The central purge of the system and a vacuum pump are connected to the recycle section between the blower and the heat exchanger.

In the gas feed to the reactor a flow meter is placed that can measure flows up to 2000 kg/hr propylene. The flow meter is a coriolis flow meter type, with two internal loops of 30 mm in series.

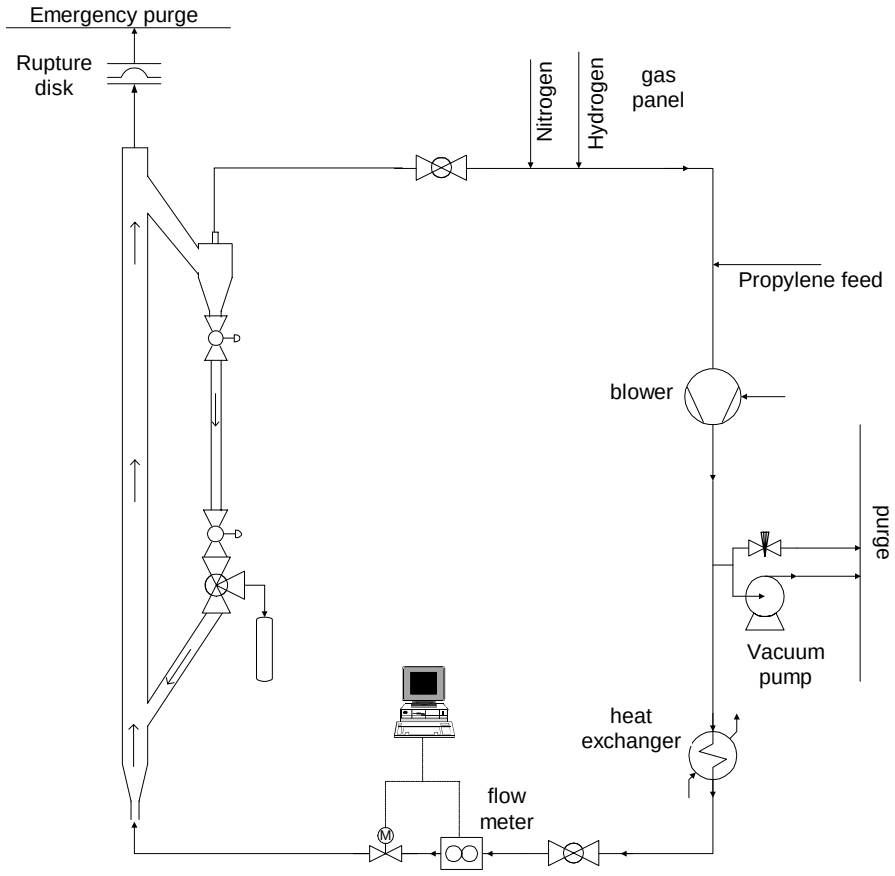

Figure 3: recycle section in pilot plant

2.1.3 Control

The reactor system is operated from outside the box. Valves are switched with a pressurized air control system from outside the box. Temperature, pressure, pressure difference and mass flow readings were done electronically. Feed and control of the blower in the gas recycle were placed outside the box. A computer program reads and interprets the measurement readings and controls the system. Temperatures and pressures are measured every 10 seconds. Pressure differences can be measured with a frequency of 3 Hz.

Data acquisition from the set-up and transfer of control signals to the set-up is done by a Data Acquisition and Control Unit from Hewlett-Packard. The DACU contains several cards for acquisition of measurement data, but also relay cards to for instance switch valves in the set-up.

For temperature control a Cryostat thermostat bath is used, that controls the temperature of the water in the cooling jackets. The cryostat can cool down and heat up the water, depending on the desired temperature in the jacket.

2.1.4 Safety measures

To prevent pressure built up in the reactor an alarm procedure was written in the computer control program. When the pressure came above 25 bar the purge was opened until the pressure dropped to below 25 bar. The temperature could also be lowered by pumping cold water through the jackets in the reactor system, thus lowering the pressure.

When the pressure was further increased the rupture disk would open. A lining of 38 mm was made from the top of the riser to the rupture disk, and after the rupture disk a purge line with a diameter of 38 mm went outside the Box. The lining to the rupture disk was always open.

Automated valves were connected to a pressurized air control system involving no electricity inside the Box. A safety relay was placed on the 3-way valve V1003 (see figure 1). When no product vessel was in place, the 3-way valve could not be switched to the product vessel to prevent a direct opening of the set-up.

2.2 Design of reactor control

2.2.1 Mass flow calibration

To determine a procedure for accurate control of the gas flow, the reactor was pressurized with nitrogen up to pressures of 20 bar. The operation of the blower has a large influence on the gas flow.

The mass flow of gas in the system at a given operation of the blower is a function of the pressure difference in the system. The blower in the recycle stream can generate a maximum pressure difference of up to 0.8 bar, depending on the total gas pressure in the system. This means that the mass flow in the system can be different at different bed heights of powder in the riser. For accurate measurements these fluctuations need to be minimized.

A mode of operation needs to be found in which the gas flow is almost constant for every given bed height at a certain controlled input value. Experiments with nitrogen at 20 bar showed that at maximum operation frequency of the blower the gas flow hardly changes. The blower can generate enough pressure difference at higher operation modes to dampen changes in pressure drop in the set-up.

2.2.2 Control of the gas flow

A blower is placed in the system that can be controlled with a frequency control. Additional mass flow control in the set-up might not be necessary, although the range of control of the

blower is only limited. With an additional control the gas flow can be restricted with for instance a valve, allowing control of the flow with the blower operating in a different power range. Thus, calibration of the blower at no restriction of the gas flow at different pressures is required as well as calibration of the flow at different restrictions by a control valve in the gas feed to the reactor. For the calibration of the flow with maximum opening pressures of 15 and 20 bar were chosen.

Figure 4 shows the measurements of the gas flow at 15 and 20 bar nitrogen for the case of no restriction of the gas flow. The power of the blower is given in percentage of the maximum frequency of the blower. This frequency is the frequency of the electrical feed; the maximum is 50 Hz. The frequency of the blower feed is increased with 10% increments with every step.

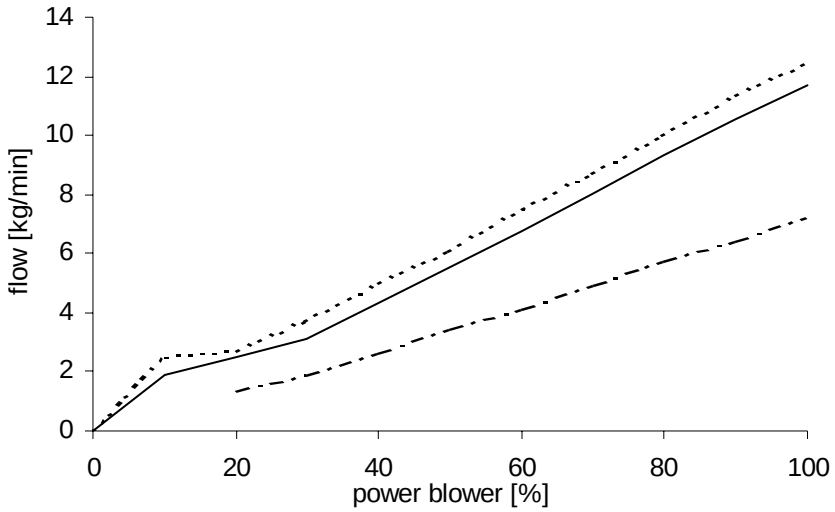

Figure 4: Nitrogen flow through reactor system as a function of the performance of the blower. ____ = 20 bar, no flow restriction; - - - - = 15 bar, no flow restriction; - · - · - = 20 bar, restriction in flow by manual valve.

Already at 10% of the operation of the blower a relatively large mass flow is generated, but the blower is not very reliable in the low operating range (figure 4).

The calibration is repeated with the control valve closed for approximately 60%. Experiments revealed that the maximum flow did not drop linearly with increasing restriction from the valve. Above a certain restriction the mass flow would suddenly drop to zero due to a too large pressure drop in the stream. At lower pressures the flow would drop to zero more easily since the blower can handle a lower pressure drop at lower pressures.

The calibration of the mass flow at increased restriction shows that the range of mass flows can be adjusted easily, although some trial-and-error is required. The restriction for the mass

flows in figure 4 is chosen such that the maximum resulting gas velocity in the 10-cm riser does not exceed 1.2 m/s. This velocity is about the maximum gas velocity for the slugging fluidization regime in the cold flow set-up.

The minimum fluidization velocity is an important parameter in fluidization measurements and is normally generated at low operating frequencies of the blower when no restriction is set in the gas flow. This causes fluctuations in the mass flow and unreliable mass flows at a given operation frequency. Accurate measurement of the mass flow is therefore required. But at low gas velocities near the minimum fluidization velocity, the gas flows are lower than the detection range of the mass flow controller. An alternative measurement of the mass flow is therefore necessary.

Simultaneously with calibration of the mass flow through the system, the pressure difference over the distributor plate was measured to monitor possible fouling of the plate. The pressure difference over the distributor plate was calibrated at different gas flows and at different pressures. This measurement could act as an alternative measure for the gas flow (figure 5), regardless of the pressure in the system or a restriction in the gas flow.

This pressure difference over the distributor plate could be translated to a gas velocity in the riser, see figure 6.

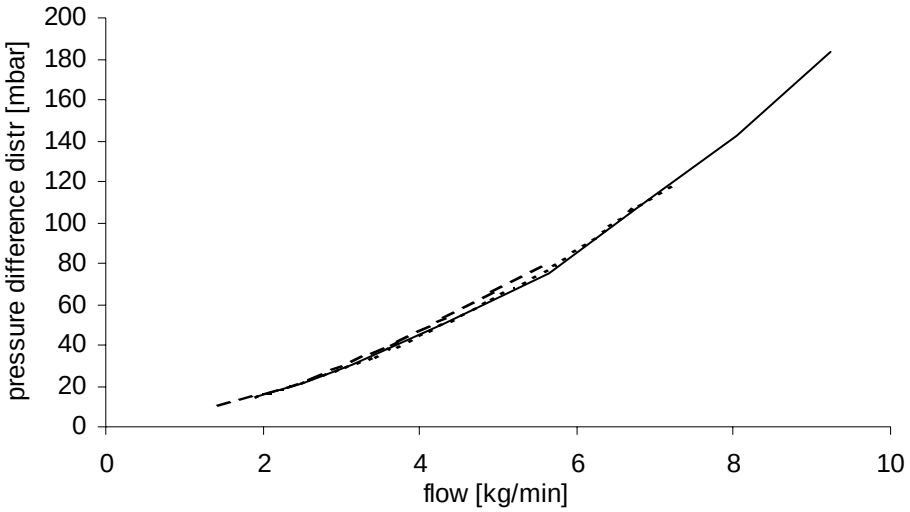

Figure 5: pressure difference over the distributor plate as a function of the gas flow.
___ = no restriction of the gas flow, 19.8 bar; - - - - = small restriction, 20.15 bar; __ __ = large restriction, 18.4 bar.

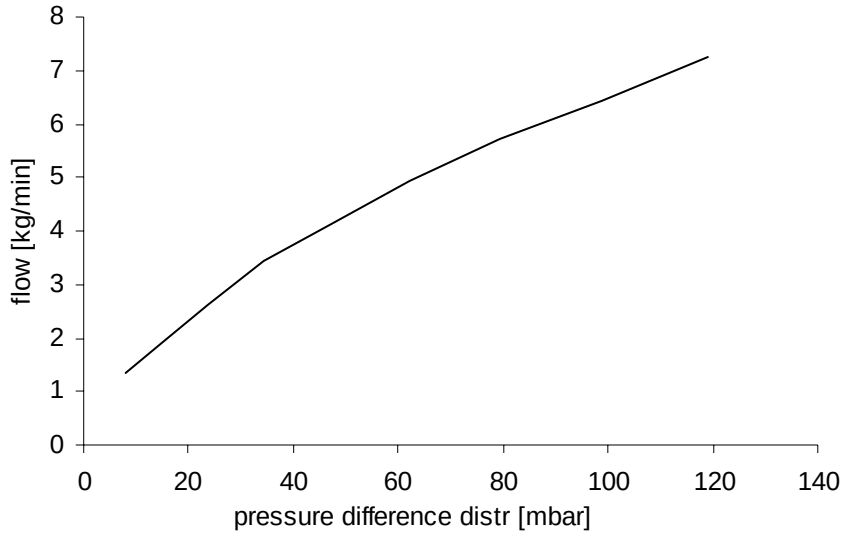

Figure 6: the pressure difference over the distributor plate is a measure for the gas velocity in the riser. Interpolation to lower pressure differences can help identify the gas velocity at low mass flows.

3 Results

3.1 Development of a method to determine the bed height

One of the important parameters in the polymerization process is the residence time of the particles in the riser. The residence time is dependent on the solids flux through the riser, and on the hold up of solids in the riser, as explained in chapter 2. In the cold-flow set-up measurement of the hold up was done by visually measuring the powder bed height after suddenly stopping the gas flow, but this cannot be done in the pilot plant. An alternative procedure must be developed for a reliable measurement method of the powder bed height in the riser.

In the cold-flow set-up the minimum fluidization velocity was determined by measuring the pressure difference over the bed while the gas velocity was increased in steps. The minimum fluidization velocity was the velocity at which the trend in pressure difference changed (Kunii and Levenspiel (1991)). The total pressure difference was different for different bed heights, but the gas velocity at which the powder was at minimum fluidization stayed the same.

The powder bed height in the pilot plant can thus be measured at or slightly above the minimum fluidization velocity of the gas. The accompanying pressure difference at that gas

velocity is then a direct measure for the bed height. In the experiments the minimum fluidization velocity was found to be 17.9 cm/s.

To overcome operational problems with the blower, the maximum gas flow is restricted, so as to have the blower operating at a higher frequency at these low gas velocities and assuring that the pressure drop does not exceed the possibilities of the blower. The pressure differences over the distributor plate should be the same for every bed height since in that case the gas velocity is the same and thus the bed is at minimum fluidization.

The pressure drops at different known heights of the bed (20, 40, 60, 80 and 100 cm) were determined at a pressure of 20 bar nitrogen (figure 7). The gas velocity was set at 27 cm/s, slightly above the minimum fluidization velocity (figure 8). A linear dependency results, as was expected. The deviations are small and the measurement of the pressure difference shows to be a good tool for measuring bed heights. The bed height was not increased to more than 100 cm since it was expected that the bed height would not be larger than 100 cm during the experiments, based on the results from experiments at low pressure.

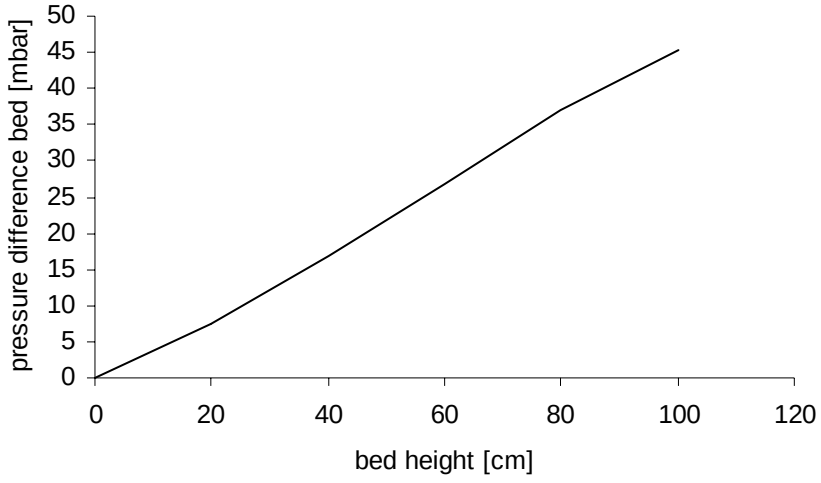

Figure 7: pressure difference measured over the riser measured at minimum fluidization velocity for different bed heights.

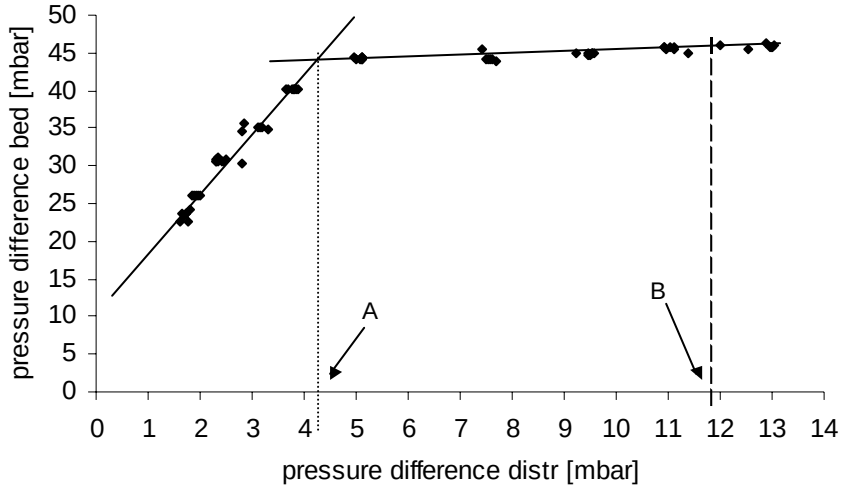

Figure 8: determination of the minimum fluidization velocity for the 100 cm bed. Pressure difference over the powder bed is measured as a function of the pressure difference over the distributor plate. A: minimum fluidization velocity; B: gas flow at which pressure drop is measured for calibration.

3.1.1 Detection of slugging fluidization

The next step was to see whether the fluidization regime in the riser was actually slugging fluidization. In the cold flow experiments, visual observation was enough to determine if slugging fluidization was obtained. In the pressurized set up, this determination could only be done with measurement and analysis of pressure difference measurements in time. Detailed analysis of pressure fluctuation measurements ha2 been done in literature (Cho et al. (2002), Drahos et al. (1988), Van der Schaaf et al. (2002)), but was not used in such detail in the current research. The measurement of the pressure difference was done at a frequency of 3 Hz. With the higher frequency it was possible to measure the pressure difference fluctuations with a frequency higher than the frequency of the fluctuations.

As soon as fluidization exceeds minimum fluidization at increasing gas velocity pressure difference fluctuations will occur due to the formation and migration of gas bubbles through the bed (Noordergraaf et al. (1987)). When the gas velocity is further increased slugs will start to appear and the pressure differences will become more vigorous but also more regular since the slugs are larger than bubbles but appear more regularly.

First bubbling fluidization was measured. It is known at which velocities bubbling fluidization occurs: at gas velocities just higher than the minimum fluidization velocity. Then the gas velocity was further increased to gas velocities up to 1 m/s.

Figure 9 shows the measurement results of pressure difference measurements in bubbling fluidization and in slugging fluidization. The respective gas velocities were 0.27 and 0.63 m/s.

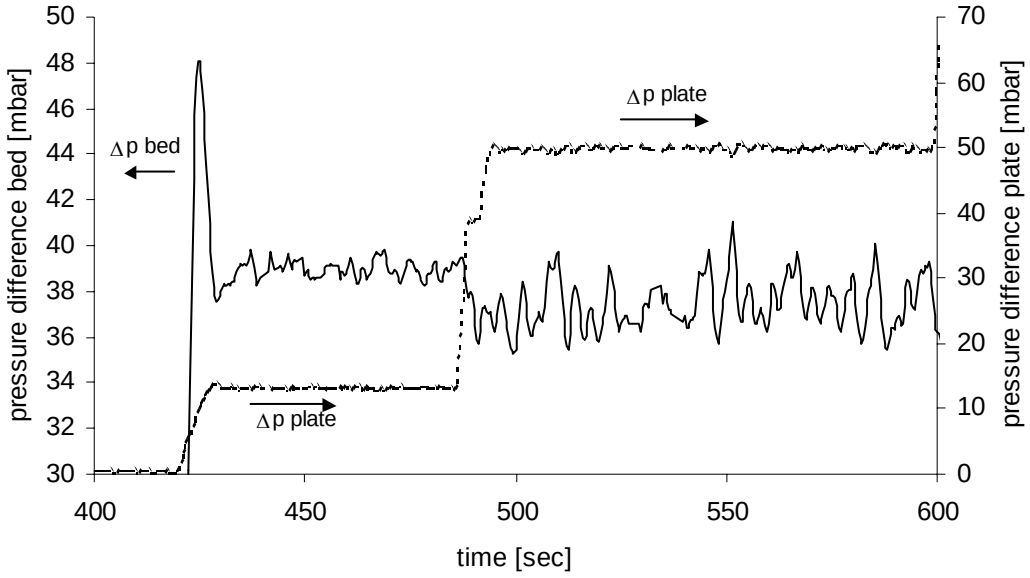

Figure 9: measurement of the pressure difference over the bed in bubbling fluidization (420-480 sec) and slugging fluidization (480-600 sec).

Comparison of the pressure difference fluctuations at the different gas velocities in the figure clearly shows the difference in fluidization regime. At the lower gas velocity, represented by a pressure drop over the distributor plate of 12 mbar, the fluctuations are approximately 2 mbar but can also be much less. At this gas velocity the bed is in bubbling fluidization. Then the gas velocity was increased to a value comparable to those that result in slugging fluidization in the cold-flow set up. At the higher gas velocity, represented by a pressure drop over the plate of 50 mbar, the amplitude of the fluctuations is approximately 4 mbar. The fluctuations are larger and more regular. The frequency of the fluctuations is around 13 fluctuations per 50 seconds, or 1 per 4 seconds.

When it is assumed that only one slug is present in the riser during such a fluctuation and that the slug travels over the whole riser length, then the slug can travel at maximum 2.5 m in 4 seconds. This means that the velocity of the slug is at minimum 0.63 m/s. This is comparable to the gas velocity, but this is only the minimum velocity of the slug, it can travel faster. From the experiments it can only be concluded that a slug appears every 4 seconds.

3.1.2 Hold up

After these calibrations a test experiment was done to study the hold up in the riser as a function of the gas velocity. This could help identify the similarities and differences between the high pressure fluidization and the low pressure fluidization.

An amount of powder was put into the reactor that resulted in a powder bed height of 100 cm in the riser, 7.85 liters of powder. The reactor system was pressurized to 20 bar of nitrogen pressure. Then the blower was started and a gas velocity of 0.9 m/s was set while the pressure difference over the bed was measured with a frequency of 3 Hz. Apparently the average hold up at this velocity was lower than 100 cm of powder bed, since powder was being blown over the top of the riser and actual circulation of powder was taking place.

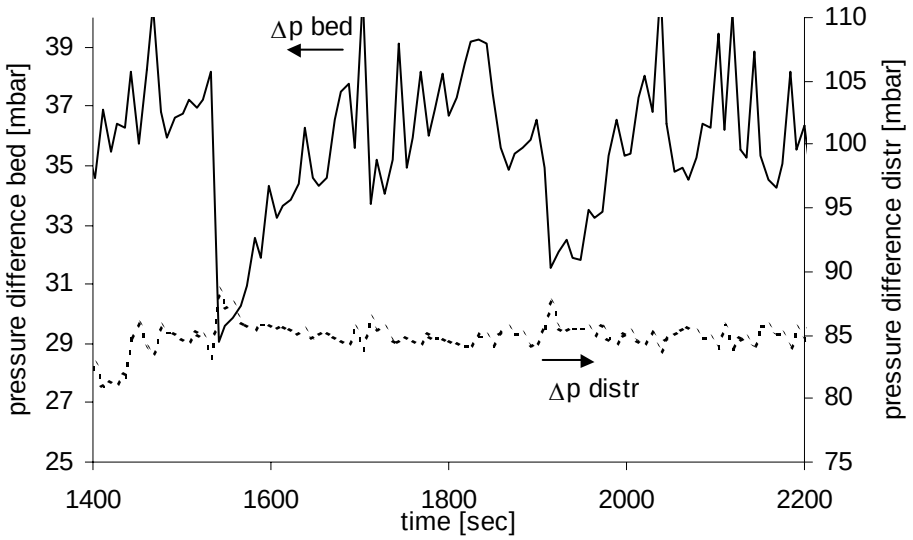

Figure 10: Pressure difference fluctuations in the riser at a gas velocity of 0.9 m/s. The original powder bed height in the riser was 100 cm. Measurement done at 20 bar nitrogen pressure

This is visible in figure 10: on the left axis is the pressure drop over the bed given and the pressure difference over the bed suddenly drops. Then the pressure difference increases again until it again suddenly drops. It is thought that the drop in pressure differences visualizes the lower hold up due to a plug of powder blown out of the riser. The powder from the plug is redirected back to the riser via the downer. The powder flows back into the riser at a lower rate till enough powder is present in the riser to get a plug to be carried over the top of the riser. From the increase in pressure difference over time the solids flux can be calculated, from the drop in pressure difference the length of a plug might be calculated and thus the amount of powder being carried over the top.

When the gas velocity is further increased, the average maximum pressure difference in the riser decreases and thus the average maximum hold up of powder decreases, see figure 11. After 3100 sec the gas velocity is increased (the pressure difference over the distributor plate increases) and the maximum pressure difference at 3400 sec and 3600 sec decreases from 38 mbar to 35 mbar respectively.

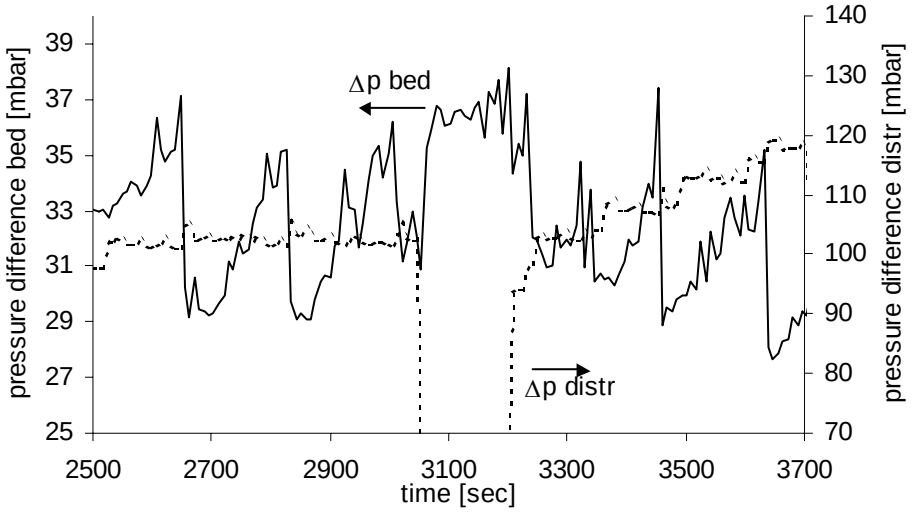

Figure 11: Pressure difference fluctuations in the riser at different gas velocities. The original powder bed height in the riser was 100 cm. Measurement done at 20 bar nitrogen pressure

To be able to measure the hold up accurately the gas flow should suddenly be stopped and the powder bed should be fluidized at minimum fluidization. This was done in the test experiment between 3050 sec and 3200 sec. As can be seen the pressure difference is higher then when the gas velocity is such that slugging fluidization occurs. This suggests that the powder that comes out of the downer still flows into the riser when the bed is at minimum fluidization. To overcome this problem the powder should be kept in the downer, but then no actual circulation of powder takes place. Stopping the powder flow only when the hold up does not increase anymore would result in measurements of only the maximum hold up n the riser. A relation between the hold up and the average pressure difference over the bed during slugging fluidization needs to be found. That was however not part of this research program.

4 Conclusions

A pilot plant of a circulating fluidized bed reactor was built. The reactor meets the different requirements set in the design parameters. Gas flow could be measured and controlled accurately without the use of a mass flow controller. The measurement of pressure difference over the distributor plate in the bottom of the riser was shown to accurately represent the gas flow into the riser.

The measurement of pressure difference over the riser could be used to measure powder hold up in the riser, as well as to identify the fluidization regime in the riser. It was possible to obtain slugging fluidization in the reactor and circulation of powder was observed.

No experiments could be done within the limits of the current project, but the set-up is configured in such a way, that fluidization experiments at higher pressures can be performed and the measurement data from these experiments can be analyzed and interpreted. With some minor changes, the reactor could be used for “hot” polymerization experiments.

5 Literature

Cho, H., Han, G., Ahn, G. (2002). "Characteristics of slug flow in a fluidized bed of polyethylene particles." Korean Journal of Chemical Engineering **19**(1): 183-189.

Draho[illegible], J., Pun[illegible]ochá[illegible], M., Slucký, K., [illegible]ermák, J. (1988). “The diagnostics of slugging in fluidized beds.” Powder Technology **54**(4): 285-287.

Kunii, D. and Levenspiel, O. (1991). Fluidization Engineering, 2nd ed. Butterworth-Heinemann, Boston: 68-72

Meier, G. B., Weickert, G. Van Swaaij, W.P.M. (2002). "FBR for catalytic propylene polymerization: controlled mixing and reactor modelling." AIChE journal **48**(6): 1268-1283.

Noordergraaf, I. W., Van Dijk, A., Van den Bleek, C.M. (1987). "Fluidization and slugging in Large-particle systems." Powder Technology **52**: 59-68.

Van der Schaaf, J., Schouten, J.C., Johnsson, F.Van den Bleek, C.M. (2002). "Non-intrusive determination of bubble and slug length scales in fluidized beds by decomposition of the power spectral density of pressure time series." International Journal of multiphase flow **28**: 865-880.

Chapter 7

Modeling the riser of a circulating slugging fluidized bed reactor for gas phase polymerization of propylene

---

Abstract

A model was constructed that could describe the polymerization process in the riser of a circulating slugging fluidized bed reactor. Hydrodynamic properties of the slugging fluidization regime and a description of the polymerization of propylene were combined in a cell model to predict polymerization at elevated pressures. The number of cells is a function of the degree of mixing in the reactor and is expressed as a function of gas velocity and solids flux.

The model could predict the hydrodynamic behavior of the slugging fluidization very well. The polymerization reaction changes due to the changes in hydrodynamic properties. The influence of the gas velocity on the production and on the yield is significant, as well as the influence of the solids flux. At very different mixing patterns in the riser the same production and the same yield could be established accepting a temperature rise of 10 K.

Changing the intensity of the circulating flow influences the degree of back-mixing. The window of operation with this type of reactor is large. The reactor could be operated as a well-mixed system or as a plug flow system and everything in between. Heat removal and heat production can be adjusted easily by changing the gas velocity and solids flux without changing the mixing pattern in the riser. This offers possibilities in applying different production rates.

1. Introduction

Gas phase reactors for olefin polymerization are used frequently in industry nowadays. They combine a number of advantages as compared to liquid phase or slurry phase reactors. Operation is simpler and less costly because only gas streams are involved, separation of monomer and product is easier. The range of product qualities that can be produced in one reactor has expanded. However, heat removal is more difficult because of the lower removal capacity of the gaseous monomer in gas phase reactors and monomer concentration is lower. This could lead to lower specific production rates.

Not always the possibilities and restrictions in the performance of a reactor are known. To explore the performance of an existing reactor or to explore the possibilities of new reactor concept a mathematical model was constructed. Aspects of the polymerization of propylene at conditions resembling those of industrial fluidized bed reactors as well as strongly deviating conditions were studied.

To the authors' knowledge no models combining hydrodynamic properties of slugging fluidization and olefin polymerization are described in the open literature.

2. Towards a novel reactor model

In this work a reactor model was developed that could describe propylene polymerization in a circulating slugging fluidized bed reactor, based on the constraints given by the hydrodynamics on solids mixing and solids loading in the reactor and influenced by the gas flow and the solids flow. Reaction rate of the polymerization reaction, heat production and heat removal are modeled as well as deactivation of the catalyst and calculation of the molecular weight of the produced polymer. The model should be able to describe the temperature and concentration gradients.
The model is set up in the programming environment gPROMS. as a cell-model in which each cell is considered well-mixed (figure 1). This construction offers the ability to incorporate certain constraints given by the hydrodynamics, which will be explained later.

The model uses the following input parameters: gas velocity and solids flux; reactor volume and reactor diameter; injected mass of catalyst and hydrogen concentration; temperatures of the jacket, inlet of monomer and inlet of solids; density of the gas to represent the pressure in the system.

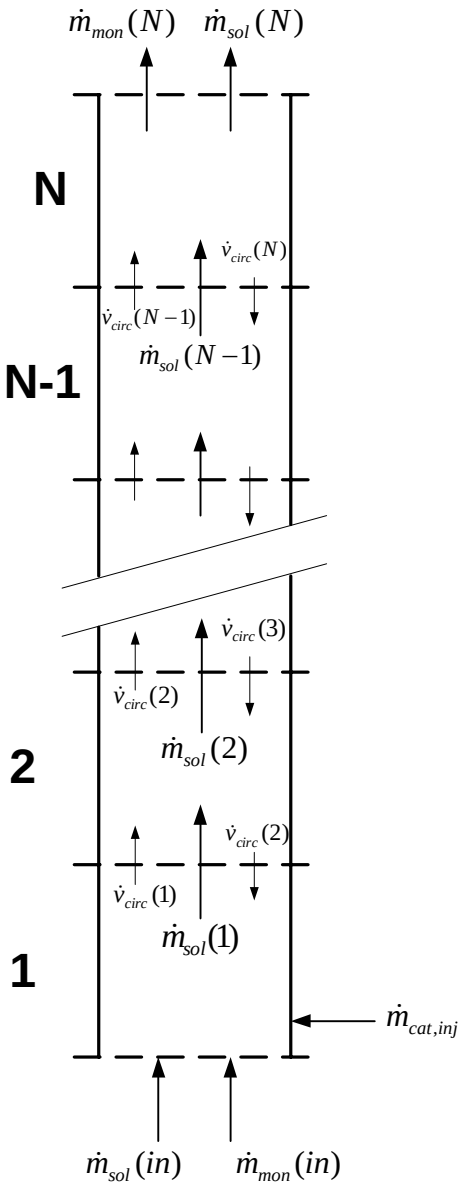

Figure 1: scheme of cell model

The hydrodynamic relations are derived from data by Van Putten et al (2004b). In the model a powder with the same properties as used in the study on hydrodynamics is described. The kinetic data on the catalyst system and the polymerization reaction are used from Van Putten et al. (2004a). The initial reaction rate is described as a function of hydrogen concentration at 70 °C and 25 bar total pressure. The deactivation constant k_d is described as a function of the hydrogen concentration and temperature. The density of the gas phase is a function of the temperature in the cell and is described according to a Peng-Robinson EOS.

The first and the last cell in the reactor are modeled separately, because of the different conditions. In the first cell all feeds come in. They can have different (independent) temperatures and the feeds also have to be mixed up. Also the circulating flow cannot flow back to the entrance of the reactor. In the slugging fluidized bed in reality a dense bubbling zone can be detected in the lowest part of the riser. In this dense zone complete mixing takes place. The first cell can simulate this dense bubbling zone as a well-mixed reactor.

In the last cell exit effects play a role. In the model these exit effects are not modeled completely, but the circulating flow is limited: the circulating flow only flows to the exit and no flow comes back from the exit. In reality exit effects are caused by a partial backflow of the convective flow of solids. Part of this flow is bounced back into the riser, its extent

dependent on the geometrical shape of the exit, Noordergraaf et al. (1987). This is not modeled. It is assumed that the exit causes negligible backflow effects.

To get a clear understanding of the model a detailed description of the relations to describe the hydrodynamics and the material and energy balances are given below.

2.1. Assumptions

The major assumptions for the model are as follows:

1) The ratio of volume of solids per volume of reactor is constant for every cell and is given by the fluidization model.
2) The Peclet number determines the number of cells.
3) The circulating flow is constant for every cell.
4) The rate of segregation determines the ratio of convective to circulating flow of solids.
5) The volume and mass of catalyst is not taken into account for the calculation of the volume and mass of solids.
6) Hydrogen is not consumed.
7) The resistance to mass and heat transfer to gas and solids in each cell is negligible Particles moving through the reactor are absorbing and desorbing propylene due to temperature gradients in the system. Equilibrium is assumed in each cell.
8) Energy effects due to absorption and desorption are neglected.
9) Sorption and desorption of monomer from the circulating flows compensate each other; there is no net effect.
10) No monomer is sorbed in the solids flow into cell 1. Thus $\dot{m}_s(0) = \dot{m}_{pol}(0)$.
11) The dynamics of the slugging fluidization is not modeled in detail. Particles move through the column in slugs or gas bubbles and plugs, packets of solids on top of a slug. A particle moves up through the column in a plug and falls down again through a slug. During the residence time of a solid in the riser column (typically 60-600 s) a solid moves through several plugs and slugs with an average residence time in a plug of up to 4 to 5 seconds and a residence time in a slug of less than 0.5 seconds. This behavior is averaged into a migration through the column in a bed of the same bulk density as a plug and with a particle velocity through the column that is dependent on the solids flux at the entrance and the polymer.

12) It is assumed that changes in the composition of solids due to polymer production during the residence time of the solids are negligible.

2.2. Parameters

2.2.1. Hold up of solids in reactor

The nature of the fluidization dictates that the hold up of solids in the reactor is a function of the gas velocity and geometry of the reactor (Van Putten et al. (2004b)). The data on hold up of solids in the reactor was analyzed and a fit was made through the results (figure 1). Gas density and solids density are not taken into account.

$$H_b = 0.5u_g^{-3.9\sqrt{D}} \qquad 1.$$

The hold up is measured as volume of solids. It is assumed that the density of the solids does not change, so also the mass of solids changes with changing volume of solids. The mass of solids per cell can then be calculated as:

$$m_{sol} = \frac{H_b}{3.54} V_r \rho_{bulk} \qquad 2.$$

2.2.2. Mixing behavior: number of cells in model

The number of cells is a function of the degree of mixing, expressed in a calculated Peclet number. The Peclet number is calculated from experimental data as function of gas velocity and solids flux through the riser.

$$Pe = \frac{2.46G_s^{1.74}}{8.35u_g^{5.18}} \qquad 3.$$

$$N = Pe/2 \qquad 4.$$

2.2.3. Convective and circulating flow of solids

Both a convective and a circulating flow of solids are incorporated in the model. The convective flow is the solids flux through the reactor. The circulating flow is a flow between

the different cells in the model and is a function of the degree and velocity of segregation. The circulating flow can thus be used as a mixing flow to express differences in the residence time between particles of different size, next to the number of cells. The circulating flow takes care of forward and back mixing of catalyst particles. These particles are normally very small and small particles have a broader residence time distribution, hence the mixing effects. The circulating flow is typically very small as compared to the convective flow but still contributes to the mixing in a reactor with solids flux.

$$\dot{v}_{circ} = \frac{G_s A}{\frac{a \cdot H_b}{3.54}\rho_{bulk}} \qquad 5.$$

With *a* is a constant representing the percentage of the convective flow.

These elements form the hydrodynamic basis of the model. These elements can be calculated from parameters that can be measured in simple experiments. The number of cells is a parameter in the model that needs to be calculated before the simulation starts, so the Peclet number is calculated first from the gas velocity and solids flux.

Next to these essential hydrodynamic parameters, the model has to be filled in with variables describing the polymerization process and relations to describe the heat transfer to the monomer gas and to the wall of the reactor.

2.2.4. Polymerization

The polymerization is modeled with the polymerization model as explained in Van Putten et al. (2004). This model describes the pseudo initial reaction rate in the gas phase as a function of the concentration of hydrogen in the gas phase and the average molecular weight as function of the concentration of hydrogen. The propagation constant was found by analysis of polymerization experiments in liquid phase with the same catalyst. It is used here with the assumption that the character of the behavior according to the propagation constant is the same in liquid phase as in gas phase polymerization.

$$R_p(i) = \frac{k_p(i)\rho_{g,calc}(i)\left(1+378.5X_{H_2}\right)}{1+40.49X_{H_2}(i)+2641X_{H_2}^{2}} \cdot \left(\frac{m_{cat}(i)}{3.6}\right) \quad 6.$$

With:

$$k_p(i) = 8.82\left(6.4065\cdot 10^{8} e^{\frac{-67.22451\cdot 10^{3}}{RT_{cell}(i)}}\right) \quad 7.$$

The activation energy in equation (7) is taken from Al-haj Ali et al. (2005).

2.2.5. Catalyst

For the polymerization the deactivation of the catalyst is important. The deactivation is expressed in the mass balance for the catalyst as first order decay $k_{d,cat}*m_{cat}$. The deactivation constant is also dependent on the hydrogen concentration (chapter 5, figure 5). The value of the deactivation constant was derived as a function of the concentration of hydrogen at 70 °C

The deactivation of the catalyst as function of temperature was not studied, but a representative dependency was found by analysis of polymerization experiments in liquid phase with the same catalyst, studied by Al-haj Ali et al. (2005). It is used here with the assumption that the character of the behavior according to the temperature dependency is the same in liquid phase as in gas phase polymerization, although the numerical values may be different.

$$k_{d,cat}(i) = \frac{\left(1.88\cdot 10^{10} e^{\frac{-69836}{RT_{cell}(i)}} + 0.8\left(1-e^{-26X_{H_2}(i)}\right)\right)}{3600} \quad 8.$$

The deactivation of the catalyst is modeled in the mass balance as:

$$m_{cat}(i)k_{d,cat}(i) \quad 9.$$

2.2.6. Hydrogen concentration

The fraction of hydrogen in the reactor is necessary for the calculation of the reaction rate, the deactivation of the catalyst and the average molecular weight. It is assumed that hydrogen is

not consumed. The change in hydrogen fraction is therefore only due to changes in the monomer concentration.

$$X_{H_2}(i) = \frac{X_{H_2}(i-1)m_{mon,g}(i-1)}{m_{mon,g}(i)} \qquad 10.$$

2.2.7. Monomer sorption

The monomer sorption is taken constant in the model. The sorption is taken as a factor αm_{pol} in the mass balances. The sorption is dependent on the temperature in reality, but this dependency is neglected. For calculation of the reaction rate the bulk density of monomer is necessary and not the concentration of monomer at the active site. The sorption of monomer can however be important for the calculation of the mass of polymer in a cell but this influence is thought to be insignificant.

$$\alpha = constant \qquad 11.$$

2.3. Mass balances

With the relations describing the hydrodynamics and the polymerization mass balances can be calculated. Mass balances for monomer, polymer and catalyst are set up. The mass balances are calculated over cell 2 to cell N-1.

2.3.1. Catalyst

The mass of catalyst changes in time due to deactivation and washing out of catalyst via convective and circulating flow. Mass balance for catalyst in cell i:

$$\frac{\partial m_{cat}(i)}{\partial t} = \dot{m}_{sol}(i-1)y_{cat}(i-1) - \dot{m}_{sol}(i)y_{cat}(i) - k_{d,cat}(i)m_{cat}(i) + \dot{v}_{circ}\rho_{bulk}\left(y_{cat}(i-1) - 2y_{cat}(i) + y_{cat}(i+1)\right) \qquad 12.$$

Fraction of catalyst in the solids:

$$y_{cat}(i) = \frac{m_{cat}(i)N}{m_{sol}} \qquad 13.$$

With an expression for the fraction of catalyst in cell N the fraction of catalyst in cell (*i*+1) is known (see further).

2.3.2. Polymer

The mass of polymer per cell can change due to reaction and sorption effects and thus temperature. The circulating flow has no net effect since the flow is always the same. Sorption effects are assumed to counterbalance each other for the different contributing flows of the circulating flow in a cell. Mass balance for polymer:

$$\frac{\partial m_{pol}(i)}{\partial t} = \dot{m}_{pol}(i-1) - \dot{m}_{pol}(i) + R_p(i) \qquad 14.$$

Flow of polymer from cell *i*:

$$\dot{m}_{pol}(i) = \dot{m}_{pol}(i-1) + R_p(i) - \dot{m}_{pol}(i-1)\big(\alpha(i-1) - \alpha(i)\big) \qquad 15.$$

2.3.3. Solids

The mass of solids in a cell is constant, given by the hydrodynamics. Thus only the flow of solids is needed for calculation. The mass of solids contains also monomer that is sorbed into the polymer material.

The flow of solids increases per cell when polymerization takes place. The circulating flow does not have a net influence on the mass of solids in a cell since the circulating flow does not change in size.

Flow of solids from cell *i*:

$$\dot{m}_{sol}(i) = \dot{m}_{pol}(i-1)\big(1+\alpha(i-1)\big) + R_p(i)\big(1+\alpha(i)\big) \qquad 16.$$

2.3.4. Monomer

For the calculation of the mass of monomer in cell *i* the density of the monomer needs to be calculated from the temperature, pressure and pressure difference due to the bed of solids. Data from simulations using a Peng-Robinson model were fitted. The fit is used in the model

for temperatures between 50 and 100 °C and pressures between 19 and 30. The pressure (at the outlet of the reactor) is an input parameter but is at the bottom of the reactor different than at the top:

$$p(i) = p_{input} + \frac{\frac{H_b}{3.54}\rho_{bulk} L_{tube} g(N-1)}{10^5 N} \quad 17.$$

Then the gas density in cell i is calculated with::

$$\rho_{g,calc}(i) = a_\rho (T_{cell}(i))^2 - b_\rho T_{cell}(i) + c_\rho \quad 18.$$

with:

$$\begin{aligned} a_\rho &= 5.19\cdot 10^{-6} p(i)^3 - 3.63\cdot 10^{-4} p(i)^2 + 8.66\cdot 10^{-3} p(i) - 6.76\cdot 10^{-2} \\ b_\rho &= 1.23\cdot 10^{-3} p(i)^3 - 8.65\cdot 10^{-2} p(i)^2 + 2.08 p(i) - 16.3 \\ c_\rho &= 7.35\cdot 10^{-2} p(i)^3 - 5.16 p(i)^2 + 126 p(i) - 988 \end{aligned} \quad 19.$$

The mass of monomer in cell *i* then becomes:

$$m_{mon}(i) = V_{cell}\rho_{g,calc}(i) \quad 20.$$

And the flow of monomer from cell *i*:

$$\begin{aligned} &\dot{m}_{mon}(i) = \dot{m}_{mon}(i-1) - R_p(i)(1+\alpha(i)) + \\ &m_{pol}(i-1)(\alpha(i-1) - \alpha(i)) + (m_{mon}(i-1) - m_{mon}(i)) \end{aligned} \quad 21.$$

With the last term contributing for the density effects in each cell.

2.4. Energy balance

The energy balance calculates the temperature in each cell. Heat production is taken into account, as well as heat transfer to each of the flows through the cells and heat transfer to the wall. For the heat transfer from the solids to the monomer gas it is assumed that there are no heat transfer limitations. All the heat that is produced in the solids is divided over the solids, the monomer gas and to the wall. The convective heat transfer from the circulating flow is taken into account.

$$\begin{aligned}&\left(m_{sol}C_{p,sol}+m_{mon}(i)C_{p,gas}\right)\frac{\partial T_{cell}}{\partial t}=\dot{m}_{sol}(i-1)C_{p,sol}T_{cell}(i-1)+\dot{m}_{mon,g}(i-1)C_{p,gas}T_{cell}(i-1)\\&-R_p\Delta H_r+\dot{v}_{circ}\rho_{bulk}\frac{H_b}{3.54}C_{p,sol}\left(T_{cell}(i-1)-2T_{cell}(i)+T_{cell}(i+1)\right)\\&-\dot{m}_{sol}(i)C_{p,sol}T_{cell}(i)-\dot{m}_{mon}(i)C_{p,gas}T_{cell}(i)-U(i)A_h\left(T_{cell}(i)-T_{jac}(i)\right)\end{aligned}\qquad 22.$$

2.4.1. Heat transfer

The heat transfer to the wall is modeled with the basic equation

$$Q=U(i)\frac{A_h}{N}\left(T_{cell}(i)-T_{jac}(i)\right)\qquad 23.$$

The temperature of the wall is kept constant by a cooling medium, in this case water. For the heat transfer coefficient the heat transfer model for fluidized beds of Molerus and Wirth (1997) is used:

$$\begin{aligned}\frac{hL_l}{k_g}=&\frac{0.125\left(1-\varepsilon_{mf}\right)\left\{1+33.3\left(\sqrt[3]{\frac{u-u_{mf}}{u_{mf}}}\sqrt[3]{\frac{\rho_p c_p}{k_g g}\left(u-u_{mf}\right)}\right)^{-1}\right\}^{-1}}{1+\frac{k_g}{2c_p\mu}\left\{1+0.28\left(1-\varepsilon_{mf}\right)^2\left(\frac{\rho_{g,calc}(i)}{\rho_p-\rho_{g,calc}(i)}\right)^{0.5}\left(\sqrt[3]{\frac{\rho_p c_p}{k_g g}}\left(u-u_{mf}\right)\right)^2\frac{u_{mf}}{u-u_{mf}}\right\}}\\&+0.165\,\mathrm{Pr}^{1/3}\left(\frac{\rho_{g,calc}(i)}{\rho_p-\rho_{g,calc}(i)}\right)^{1/3}\left\{1+0.05\left(\frac{u-u_{mf}}{u_{mf}}\right)^{-1}\right\}^{-1}\end{aligned}\qquad 24.$$

With:

$$L_l\equiv\left[\frac{\mu}{\sqrt{g}\left(\rho_p-\rho_g\right)}\right]^{2/3}\qquad 25.$$

And:

$$\mathrm{Pr}\equiv\frac{c_g\mu}{k_g}\qquad 26.$$

Also a heat balance over the jacket is made, because the cooling medium in the jacket will warm up along the length of the riser when the cooling medium flows in cocurrent flow. The heat balance for the jacket is constructed with the quasi steady state assumption as:

$$0 = U(i)\frac{A_h}{N}\left(T_{cell}(i) - T_{jac}(i)\right) + \dot{m}_{wat,jac} C_{p,wat}\left(T_{jac}(i-1) - T_{jac}(i)\right) \quad 27.$$

The QSSA is valid for the cooling medium in the jacket because it is expected that the flow of medium, water in these simulations, is large and the residence time of the water in the jacket is very short compared to the processes in the reactor.

2.5. Cell 1

For cell 1 some mass balances are different and a number of parameters are given initial values. Only the changes are given below.

- mass of catalyst: in cell 1 the catalyst is introduced in the reactor. The circulating flow can only flow to and from cell 2. The mass balance for the catalyst in cell 1 thus becomes:

$$\frac{\partial m_{cat}(1)}{\partial t} = m_{cat,inj} - \dot{m}_{sol}(1) y_{cat}(1) - k_{d,cat}(1) m_{cat}(1) + \dot{m}_{circ}\left(-y_{cat}(1) + y_{cat}(2)\right) \quad 28.$$

- mass of polymer: in cell 1 a certain mass of polymer is introduced with the backflow of solids from the downer of the circulating fluidized bed. Since it is assumed that no monomer is sorbed into this polymer, the mass of polymer in cell 1 is equal to the mass of solids in cell 1:

$$\frac{\partial m_{pol}(1)}{\partial t} = 0 \quad 29.$$

The mass flow of polymer from cell 1 is taken equal to the solids flux plus the production:

$$\dot{m}_{pol}(1) = G_s A + R_p(1) \quad 30.$$

- mass flow of solids in cell 1: the mass flow of solids in cell 1 is equal to the polymer flow plus monomer sorbed:

$$\dot{m}_{sol}(1) = \dot{m}_{pol}\left(1+\alpha(1)\right) \tag{31.}$$

- mass flow of monomer: in cell 1 the monomer flow is given by the gas velocity and the given monomer density.

$$\dot{m}_{mon}(1) = u_g A \rho_{g,calc}(1) \tag{32.}$$

- the concentration of hydrogen in cell 1 is an input parameter for the model. For cell 1 this value is given, for the other cells the hydrogen concentration is calculated.

- the energy balance for the reactor in cell 1 differs from the other cells, because in cell 1 the monomer and polymer can flow in with a different temperature. The resulting temperature in cell 1 needs to be calculated from these differences. Also the circulating flow is different since the circulating flows only go to and from cell 2. The energy balance for cell 1 is thus constructed as:

$$\begin{aligned}&\left(m_{sol}C_{p,sol} + m_{mon}(1)C_{p,gas}\right)\frac{\partial T_{cell}(1)}{\partial t} = \dot{m}_{sol}(1)C_{p,sol}\left(T_{in,sol} - T_{cell}(1)\right)\\&+\dot{m}_{mon}(1)C_{p,gas}\left(T_{in,mon} - T_{cell}(1)\right)+\dot{v}_{circ}\frac{H_b}{3.54}\rho_{bulk}\left(T_{cell}(2)-T_{cell}(1)\right)\\&-R_p(1)\Delta H_r - U(1)A_h\left(T_{cell}(1)-T_{jac}(1)\right)\end{aligned} \tag{33.}$$

The inlet temperature of the solids and the inlet temperature of the monomer are input parameters.

- energy balance for the jacket in cell 1 is calculated as:

$$0 = U(i)\frac{A_h}{N}\left(T_{cell}(1)-T_{jac}(1)\right) \tag{34.}$$

2.6. Cell N

There is no circulating flow at the exit of the reactor. Thus the mass balances and the energy balance in cell N are different from those in cells 2 to N-1.

- mass balance for catalyst in cell N:

$$\frac{\partial m_{cat}(N)}{\partial t} = \dot{m}_{sol}(N-1)y_{cat}(N-1) - \dot{m}_{sol}(N)y_{cat}(N) - k_{d,cat}(N)m_{cat}(N) + \dot{v}_{circ}\rho_{bulk}\left(y_{cat}(N-1) - y_{cat}(N)\right) \quad 35.$$

- fraction of catalyst in cell N:

$$y_{cat}(N) = \frac{m_{cat}(N)N}{m_{sol}} \quad 36.$$

- mass of monomer in cell N:

$$m_{mon}(N) = V_{cell}\rho_{mon} \quad 37.$$

- energy balance for the reactor in cell N:

$$\begin{aligned}\left(m_{sol}C_{p,sol} + m_{mon}(N)C_{p,gas}\right)\frac{\partial T_{cell}(N)}{\partial t} &= \dot{m}_{sol}(N-1)C_{p,sol}T_{cell}(N-1) \\ &+ \dot{m}_{mon}(N-1)C_{p,gas}T_{cell}(N-1) - R_p(N) - \Delta H_r \\ &+ \dot{v}_{circ}\rho_{bulk}\frac{H_b}{3.54}C_{p,sol}\left(T_{cell}(N-1) - T_{cell}(N)\right) \\ &- \dot{m}_{sol}(N)C_{p,sol}T_{cell}(N) - \dot{m}_{mon}(N)C_{p,gas}T_{cell}(N) - U(N)A_h\left(T_{cell}(N) - T_{jac}(N)\right)\end{aligned} \quad 38.$$

2.7. Molecular weight of the polymer

The molecular weight of the polymer determines the product quality. It is a function of the hydrogen concentration. The hydrogen response model used for the calculation of the reaction rate also predicts the molecular weight of the polymer, in the form of a termination probability:

$$q(i) = 7.5 \cdot 10^{-5} + 0.00418 X_{H_2}(i) + 0.9 \cdot 10^{-4} \cdot \frac{378.53 X_{H_2}(i)}{1 + 378.53 X_{H_2}(i)} \quad 39.$$

The termination probability is changed into the so-called instantaneous weight average molecular weight by:

$$\overline{M}_w(i) = \frac{2M_{prop}}{q(i)} \quad 40.$$

The average molecular weight produced in the reactor over all cells is then calculated as:

$$\overline{M}_{w,reactor}(i) = \frac{\sum R_p(i)\overline{M}_w(i)}{\sum R_p(i)} \quad 41.$$

3. Results

Simulations were done for several situations. In all simulations a base case was used for the input parameters:

D	0.1	[m]
L_{tube}	3.54	[m]
$T_{in,\,mon}$	343.15	[m]
$T_{in,sol}$	343.15	[m]
P	25	[bar]
X_{H2}	0.011	[-]
a	100	[-]

At this hydrogen fraction the pseudo initial reaction rate in the gas phase is 45 kg/g_{cat}hr and that is the maximum reaction rate with this catalyst (see chapter 4). Gas velocities were chosen between 0.4 and 0.95 m/s and solids fluxes between 2 and 12 kg/m^2s.

Initial conditions were:

$m_{pol}(i)$	m_{sol}/N	[kg]
$m_{cat}(i)$	$10^{-8}/N$	[kg]
$T_{cell}(i)$	343.15	[K]

First simulations were done of a batch mode reactor; a reactor without solids flux into the riser with catalyst present in the riser. Pressure and temperature were similar to those in the polymerization experiments as explained in chapter 3 and 4. Goals were to see if the model predicts the polymerization reaction accurately. These simulations were done for several different reaction conditions.

Table 1: input parameters and results of simulations

Simulation	u_g [m/s]	G_s [kg/m^{2}s]	# of cells [#]	$m_{cat,inj}$ [mg/s]	X_{H2} [-]	ΔT [K]	Production [g/s]	Yield [g/g$_{cat}$s	τ [s]
0	0.7	-	4	-	0.011	-	-	-	-
1	0.7	-	4	-	0.011	3	-	-	-
2	0.7	-	4	0.1	0.011	>>	-	-	-
3	0.7	3	6	1	0.011	3	1.5	-	116
4	0.7	3	6	2	0.011	6	3.5	-	110.2
5	0.7	3	6	3	0.011	11	6	19	103.5
6	0.7	6	21	3	0.011	5	2.9	16.5	58.7
7	0.7	9	43	3	0.011	4	1.9	15.8	39.7
8	0.7	9	43	7	0.011	11	5.5	20.5	38.8
9	0.6	6	45	3	0.011	9	4	19.2	69.9
10	0.9	6	5	3	0.011	2.1	1.7	12.9	42.3
11	0.9	6	5	9	0.011	8.2	6.7	18.9	40.5
12*	0.9	6	5	3	0.011	2.1	1.7	12.9	42.3
13	0.7	6	21	3	-	-	-	-	-
14	0.7	6	21	-	0.011	-	-	-	-
15	0.7	6	21	-	0.011	-	-	-	-

*: in simulation 12 $a = 2$.

Then simulations of the reactor with solids flux into the riser were done. This allowed for an explorative study of the possibilities of such a slugging fluidized bed riser. Several input parameters were varied and their influences on the performance of the reactor were studied. The details of all simulations are given in table 1.

3.1. Simulation of batch polymerization

The gas velocity was set to 0.7 m/s. Initially in the reactor of 28 L 10 mg of catalyst was present. The number of cells was set to 4, because the model needs at least 4 cells to work properly.

In simulation 0 (table 1) the heat exchange coefficient U was set to 10000, so as to simulate an isothermal reaction. The temperature profile showed that the reaction was indeed isothermal. The presence of the catalyst made production of polymer possible and because of this production a polymer flow occurred, see figure 2.

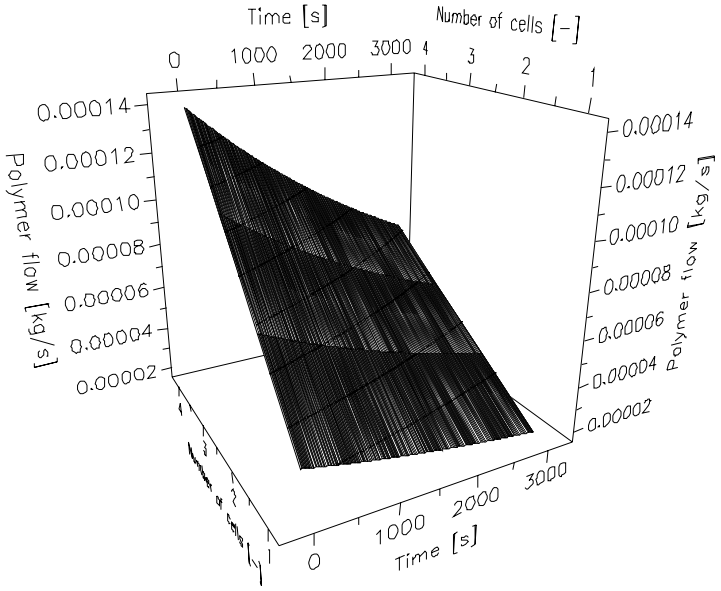

Figure 2: flow of polymer in reactor in simulation 1.

A polymer production in cell 1 exists, but decreases over time due to deactivation of the catalyst and outflow of catalyst. Because polymer is produced, a solids flow starts and thus a flow of catalyst through the reactor starts. The catalyst is taken with the solids and is partly flushed out of cell 1.

The total production of polymer is found at the outlet: initially approximately 140 mg/s, or a yield of 14 $g/g_{cat}s$ or 50 $kg/g_{cat}hr$. This value is slightly higher than found in the experiments done in chapter 4, but the propagation constant that is used causes this deviation. The production drops to 7.4 mg/s. The mass of active catalyst drops from 10 mg initially to 5.27 mg (figure 3). The catalyst is shifted to higher cells or out of the reactor.

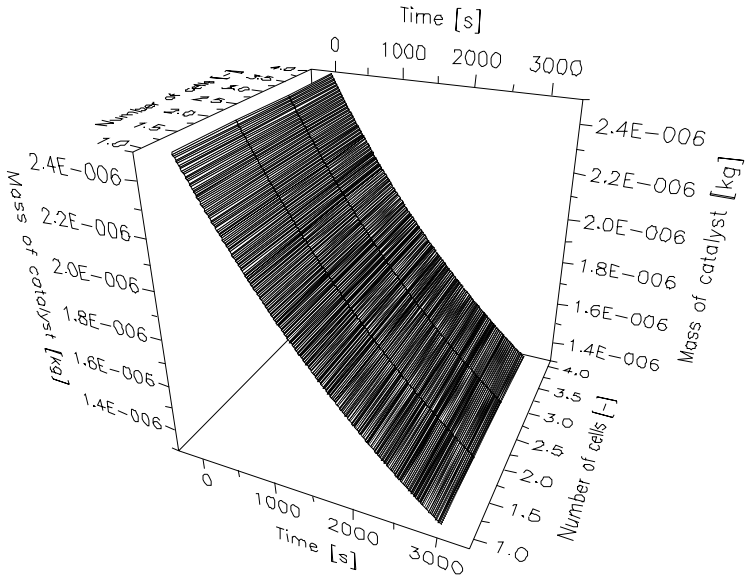

Figure 3: mass of catalyst in simulation 1.

Simulation 1 was run semi adiabatically: the heat exchange coefficient to the wall was set to zero, but convective heat removal takes place by the gas flowing through the reactor. This cannot be prevented: the model is designed for a fluidized bed and cannot run without gas flow.

The resulting temperature profile (figure 4) shows that the maximum temperature rise is low. The polymer production is almost the same as in simulation 1, because the temperature rise is minimal and thus the reaction rate is increased only slightly. The produced heat is at maximum 350 W. The gas flow removes approximately 630 W/K. The polymer flow is negligible compared to the gas flow. The polymer also needs to be warmed up. The temperature rise that results is 0.35 K.

In simulation 2 the batch mode is changed by constant addition of 0.1 mg/s of catalyst to the system. The reactor is still run adiabatically. A runaway should occur when enough catalyst is added and the heat produced becomes larger than the convective heat removal. The temperature profile in figure 5 shows this runaway. The temperature is increased enormous and with it the deactivation constant of the catalysts is increased to values higher than the

propagation constant of the polymerization reaction at the highest temperature. Rapid deactivation of the catalyst takes place and a steady state results in which almost no active catalyst is present.

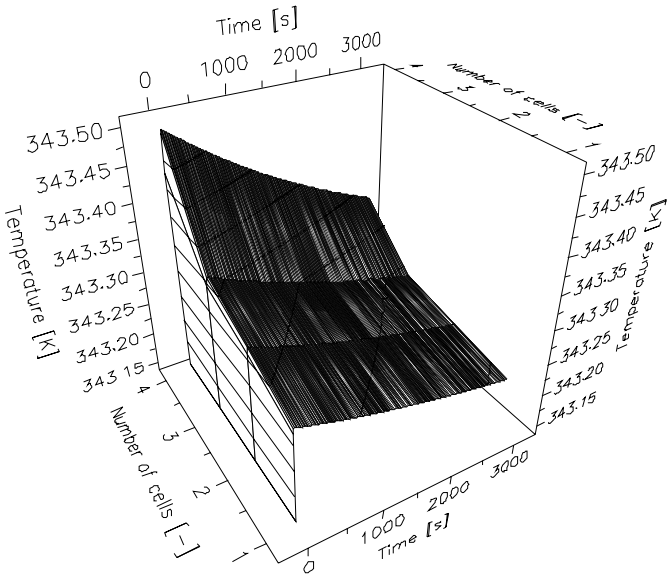

Figure 4: temperature profile in simulation 1.

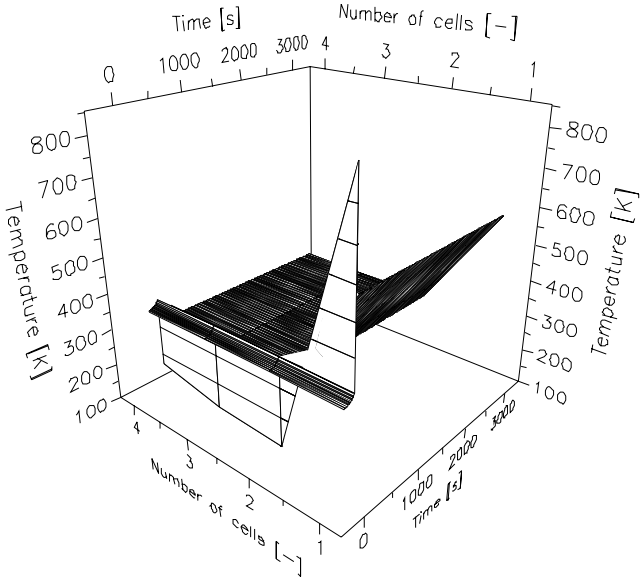

Figure 5: Temperature profile for simulation 2.

3.2. Simulation of continuous polymerization in a riser with solids flow into the riser

3.2.1. Influence of catalyst addition

After the batch simulations a solids flux was added to the simulation and the calculation of the number of cells was allowed. The heat exchange coefficient was calculated according to equation 24 and the heat balance for the jacket water was introduced (equation 27). Initially a tiny total amount of 0.1 mg of catalyst was present in the reactor for all experiments. For the simulations it was chosen to have a maximum allowable temperature increase over the reactor of 10 K. Goal was to find the maximum production at given solids flux and gas velocity.

First the amount of catalyst added continuously was increased until a temperature rise of around 10 K resulted. Simulations were done at a gas velocity of 0.7 m/s and a solids flux of 3 kg/m^{2}s. In simulations 3, 4 and 5 the addition of catalyst was increased from 1 mg/s in simulation 3 via 2 mg/s in simulation 4 to 3 mg/s in simulation 5. The temperature profiles at 3000 seconds, when steady state was well established, are given in figure 6.

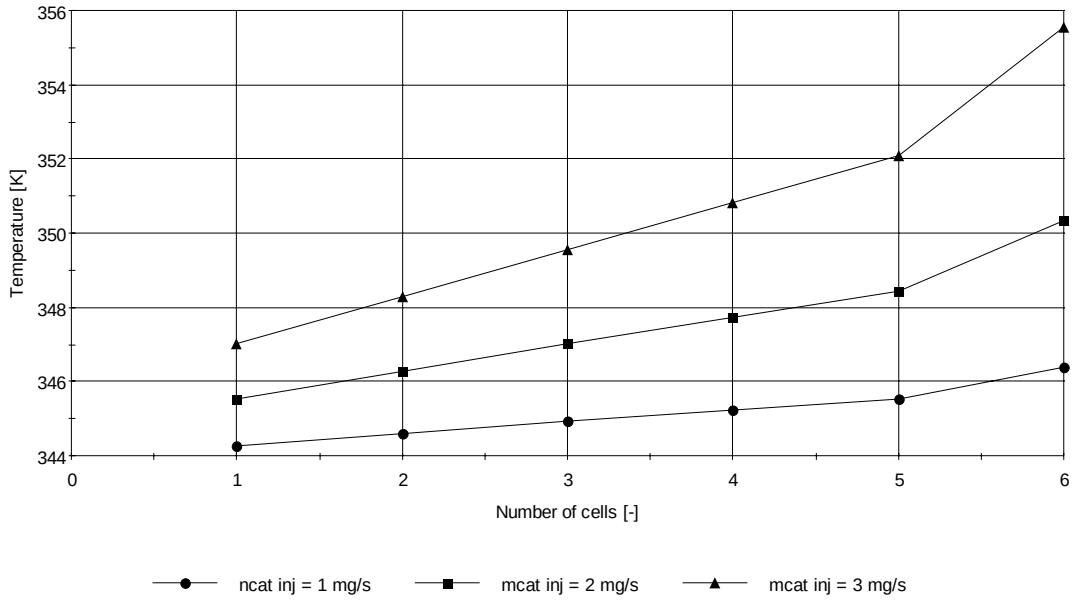

Figure 6: temperature profiles at 3000 s: ●: simulation 3 (1 mg/s catalyst addition), ▲: simulation 4 (2 mg/s catalyst addition); ■: simulation 5 (3 mg/s catalyst addition).

The polymer flow increases accordingly to the temperature rise when more catalyst is added (figure 7). The production is increased from 1.5 g/s to 6 g/s and is calculated by abstracting the outflow from the inflow of polymer; the solids flux is incorporated in the polymer flow. The production is expected to rise more than proportional to the temperature because of the

Arrhenius effect of the temperature, but with the higher production the flow of catalyst is also increased. Catalyst is washed out of the system (figure 8).

Due to the higher polymer flow because of the extra production the residence time of the solids and thus the catalyst decreases (figure 9).

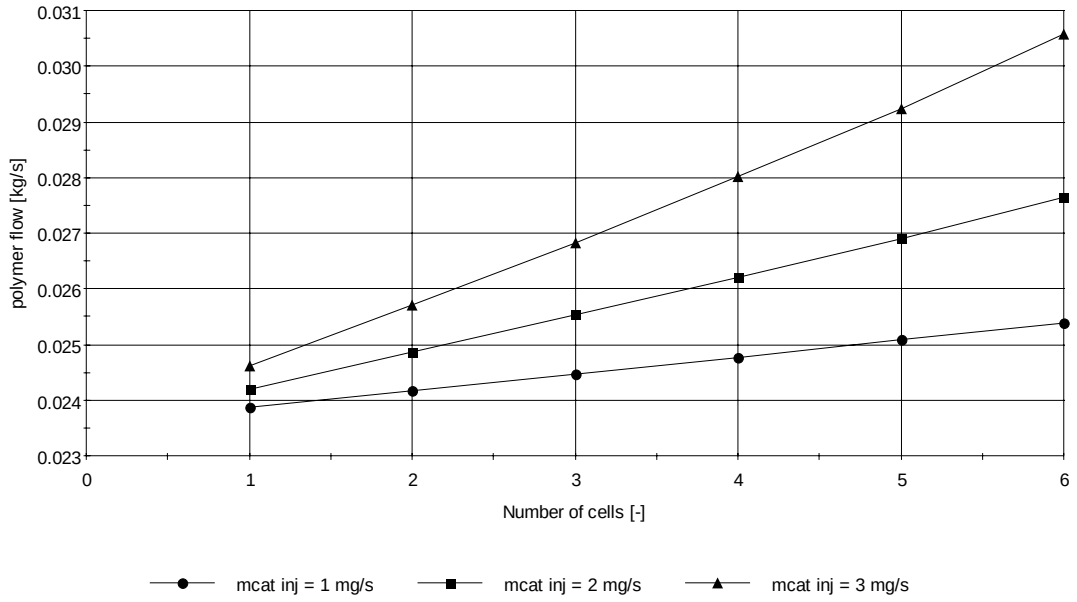

Figure 7: Polymer flows at 3000 s: ●: simulation 3 (1 mg/s catalyst addition), ▲: simulation 4 (2 mg/s catalyst addition); ■: simulation 5 (3 mg/s catalyst addition).

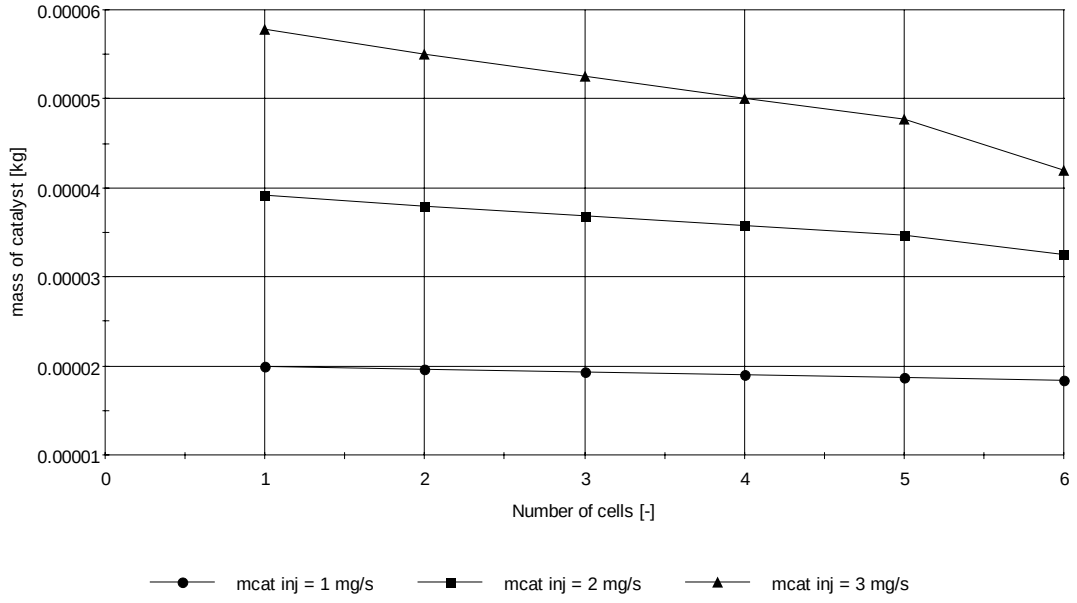

Figure 8: mass of catalyst in cells at 3000 s. ●: simulation 3 (1 mg/s catalyst addition), ▲: simulation 4 (2 mg/s catalyst addition); ■: simulation 5 (3 mg/s catalyst addition).

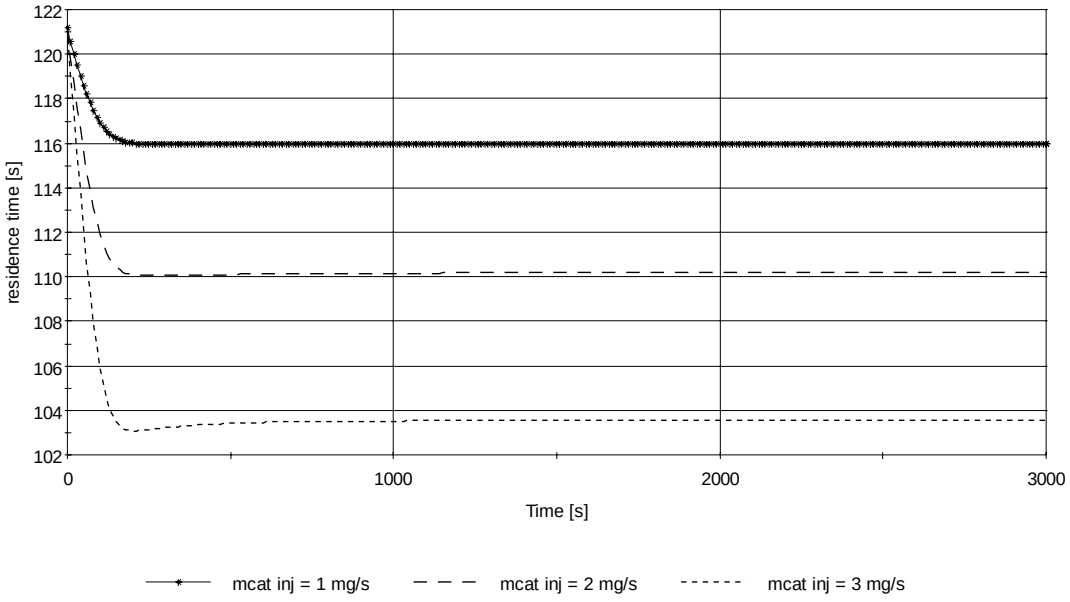

Figure 9: residence time of solids and catalyst in riser. -x-: simulation 3; __ __: simulation 4; - - -: simulation 5.

The resulting temperature rise in simulation 5 was 8 K, slightly lower than 10 K. With this restriction, more than 20 kg/h (0.16 kt/a) polymer can be produced in such a small single tube. This catalyst inflow was chosen to run the other simulations with.

3.2.2. Influence of solids flux

With the addition of catalyst set to 3 mg/s, the solids flux was increased in simulations 6 (G_s = 6 kg/m^{2}s) and 7 (G_s = 9 kg/m^{2}s). The increase in the solids flux caused an increase in the number of cells. With the increase in the solids flux the mass of catalyst per cell decreased (figure 10), because the catalyst was washed out more by the higher solids flux. This caused a decrease in the production per cell and a lower temperature rise (figure 11). Also the higher solids flux meant a higher convective heat removal and thus a decrease of the temperature rise. The residence time of solids and catalyst was decreased, see table 1.

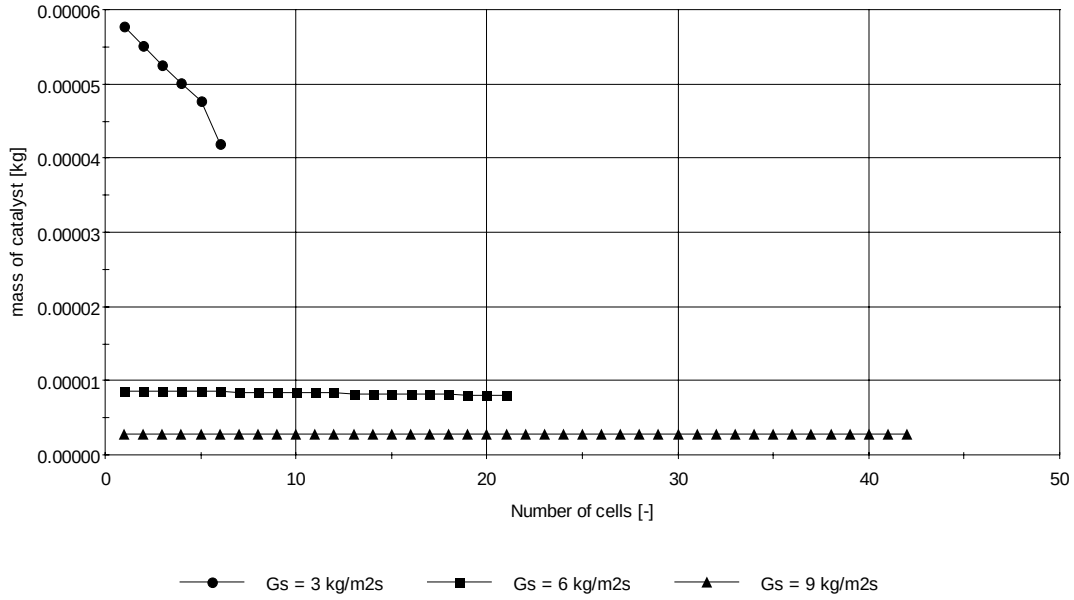

Figure 10: mass of catalyst per cell at 3000 s. . ●: simulation 5 (Gs = 3 kg/m^{2}s); ■: simulation 6 (Gs = 6 kg/ m^{2}s); ▲: simulation 7 (Gs = 9 kg/ m^{2}s)

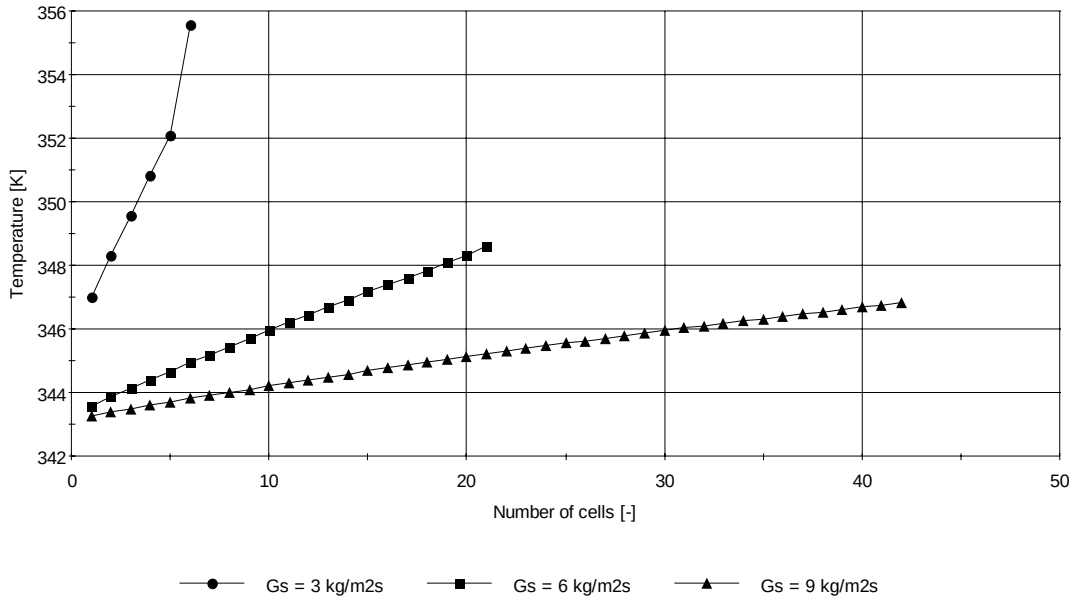

Figure 11: temperature profile in the reactor at 3000 s. ●: simulation 5 (Gs = 3 kg/m^{2}s); ■: simulation 6 (Gs = 6 kg/ m^{2}s); ▲: simulation 7 (Gs = 9 kg/ m^{2}s)

All these factors caused a change in the polymer production in the reactor (figure 12) and in the yield. In simulation 5 the yield was highest: 19 g/g_{cat}s. At the highest solids flux (simulation 7) the yield was lowest: 15.7 kg/ g_{cat}s (table 1).

The lowering of the yield may have been caused by the lower temperature rise. Then it is not "kinetically correct" to compare the results of these simulations with each other in terms of yield. When the added amount of catalyst is increased until the temperature increase is around 10 K, the comparison can be made.

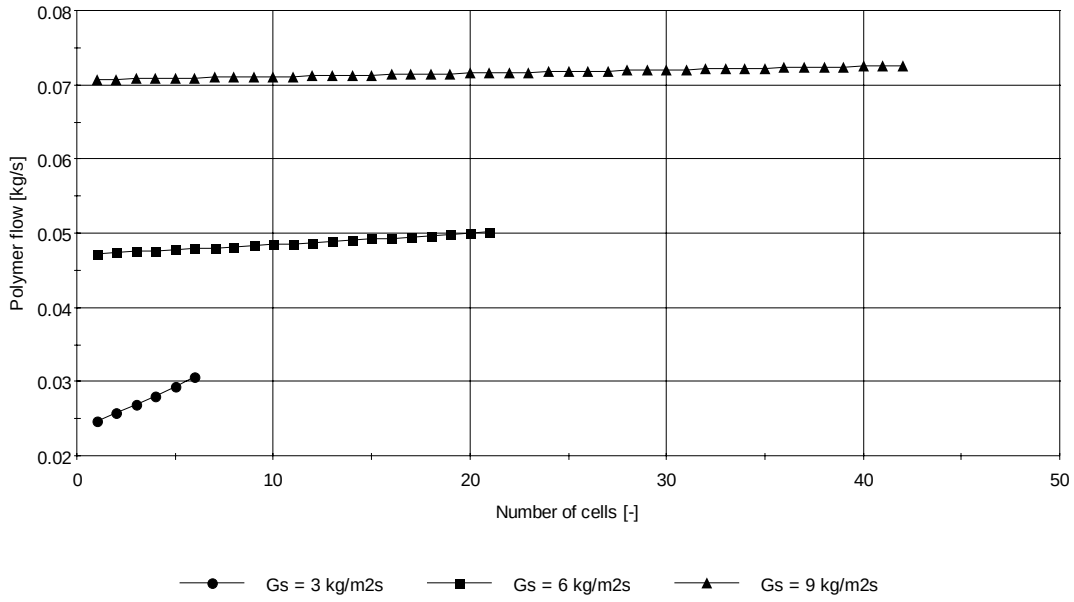

Figure 12: polymer flow in the reactor at 3000 s. ●: simulation 5 (Gs = 3 kg/m^{2}s); ■: simulation 6 (Gs = 6 kg/ m^{2}s); ▲: simulation 7 (Gs = 9 kg/ m^{2}s)

In simulation 8 the added catalyst amount is increased to 7 mg/s. With this amount of solids the temperature difference becomes 11 K. Comparison of the simulations shows that not only the absolute polymer production is increased, but also the yield (table 1): the yield becomes 20.5 g/g_{cat}s, slightly higher than the yield in simulation 5, but with an absolute production that is much higher. The yield compared to simulation 7 is increased by more than 20%.

3.2.3. Influence of the gas velocity

To determine the influence of the gas velocity on the residence time, on the production of polymer and on the temperature profile, the solids flux was kept constant at a value of 6 kg/m^{2}s (simulation 6) while the gas velocity was varied. The number of cells changed due to the change in gas velocity according to the fluidization model.

The gas velocity was chosen at 3 values that resulted, together with the solids flux of 6 kg/m^{2}s in about the same number of cells as in simulations 5, 6 and 7 (table 1). The results of simulation 6 were compared with a lower (0.6 m/s, simulation 9) and a higher (0.9 m/s,

simulation 10) gas velocity. At a decrease of the gas velocity, the hold up in the riser increases as well as the temperature rise (figure 13). The convective heat removal is lowered because of the lower gas velocity, while the residence time of the solids and the catalyst increases (table 1). Also the reaction rate increases because of the higher temperature in the higher cells of the riser. The yield becomes19.2 $g/g_{cat}s$ at a temperature rise of 9 K

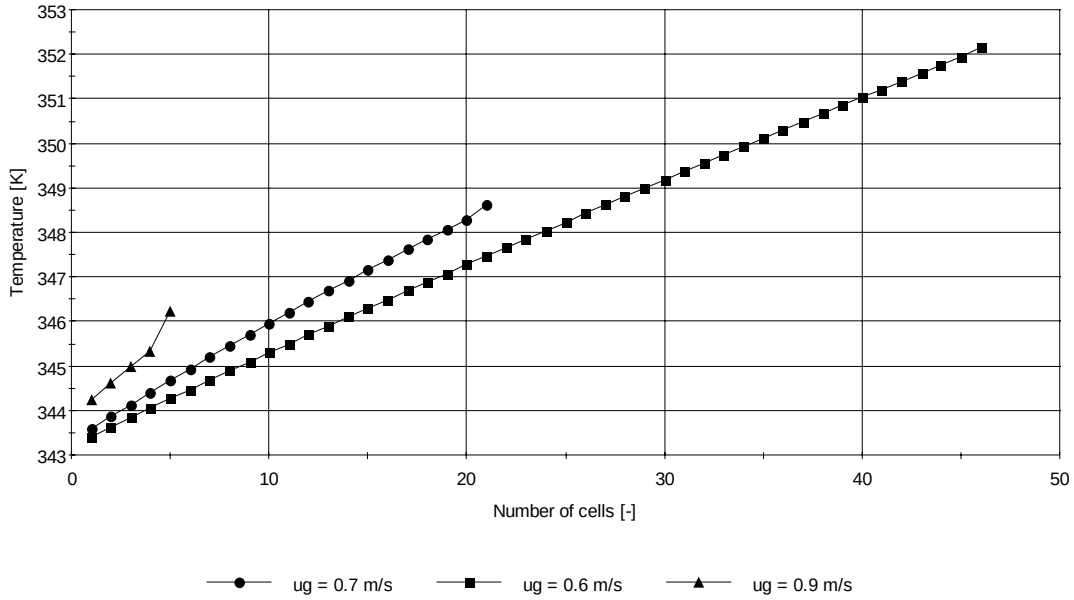

Figure 13: influence of gas velocity on temperature profiles at 3000 s. ■: simulation 9 (ug = 0.6m/s); •: simulation 6 (ug = 0.7m/s);▲: simulation 10 (ug = 0.9m/s)

The polymer production is proportional to the temperature rise: the polymer flow increases more at a higher temperature rise (figure 14). The mass of catalyst decreases more in the system with higher gas velocity or lower number of cells. The mass of catalyst in the system with low solids flux and thus low number of cells was also decreased more rapidly.

In simulation 10 the temperature rise is only 2 K. As was done with simulations 7 and 8, more catalyst was added in the system described in simulation 10 to reach a temperature rise of about 10 K. In simulation 11, an amount of 9 mg/s of catalyst was added, resulting in a temperature rise of 8 K (table 1). The yield in simulation 10 was only 12.9 $g/g_{cat}s$, whereas the yield in simulation 11 became 18.9 $g/ g_{cat}s$.

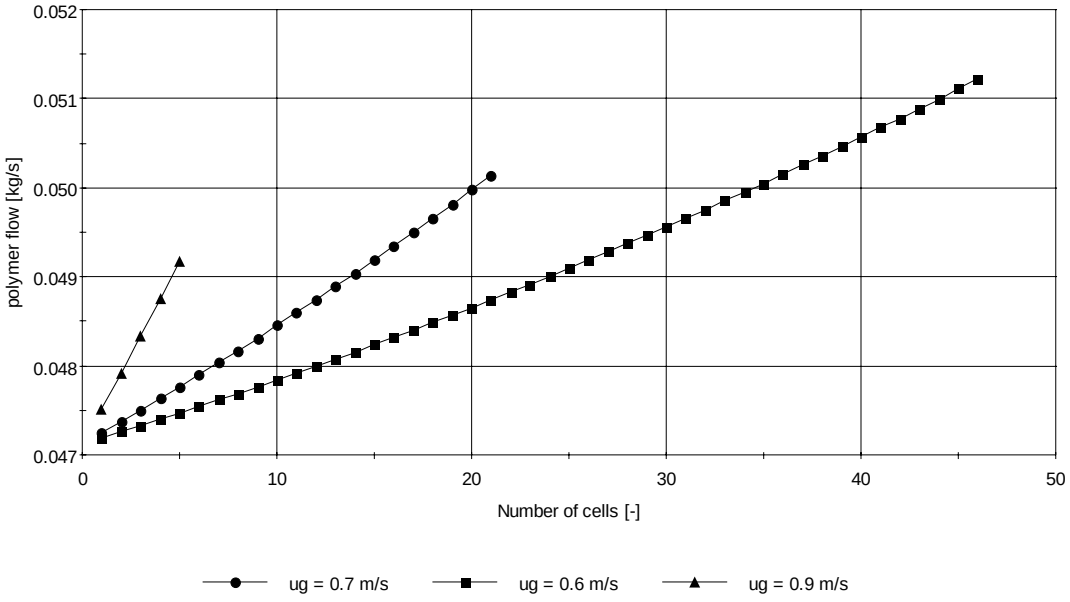

Figure 14: influence of the gas velocity on the polymer flow, taken at 3000 s. ■: simulation 9 (ug = 0.6m/s); ●: simulation 6 (ug = 0.7m/s); ▲: simulation 10 (ug = 0.9m/s)

3.2.4. Influence of the degree of mixing

The gas velocity and the solids flux both determine the number of cells in the model. Different combinations of gas velocity and solids flux result in the same Peclet number, in the same number of cells and thus the mixing behavior in these different systems can be the same. This means that the window of operation with such a reactor is very wide from the fluidization point of view. However, only the gas velocity influences the hold up whereas both the gas velocity and the solids flux influence the residence time of the solids.

Simulations 5 and 10 both have a low Peclet number. In simulation 10 both the solids flux and the gas velocity are higher, causing a lower residence time, but the yield and the absolute production are lower than in simulation 5, see figure 15. In fact a lot of gas and “dead” solids are pumped around without effect. Increasing the amount of catalyst added in simulation 9 leads to a higher production (simulation 11) but both the absolute production and the yield are still lower than in simulation 5.

Simulations 7 and 9 both have a high Peclet number. In simulation 9 both the gas velocity and the solids flux are lower, but the absolute production and the yield are higher than in simulation 7, see figure 16. Increasing the amount of added catalyst added (simulation 8) helps in increasing the productivity and the yield, more than in a more well-mixed system.

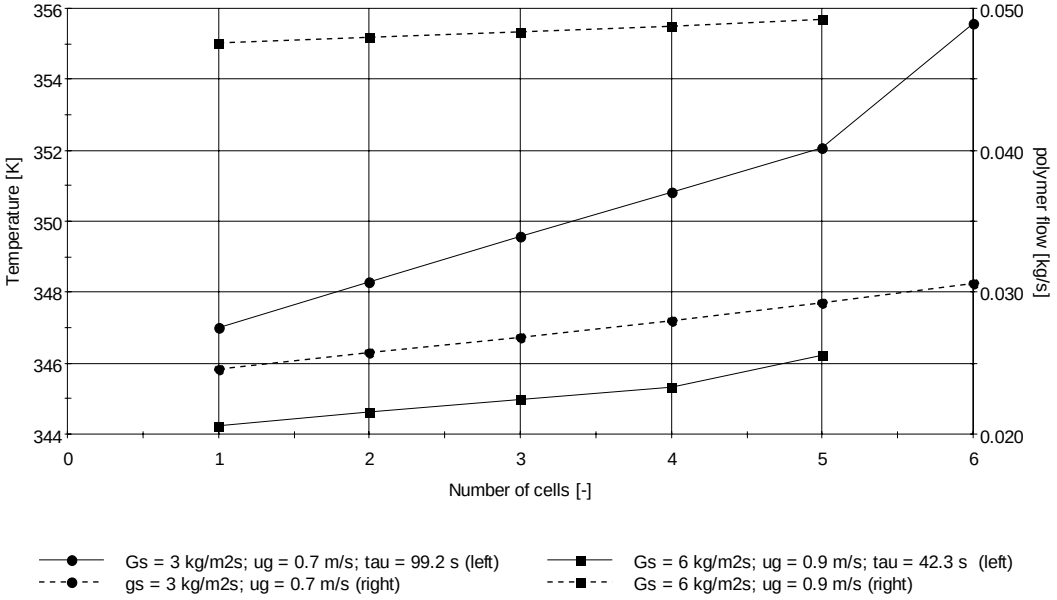

Figure 15: Comparison of simulations 5 and 10 that both have a low Peclet number.
Temperature and polymer flow are compared: •: simulation 5; ■: simulation 10;
___ = temperature; - - - - polymer flow.

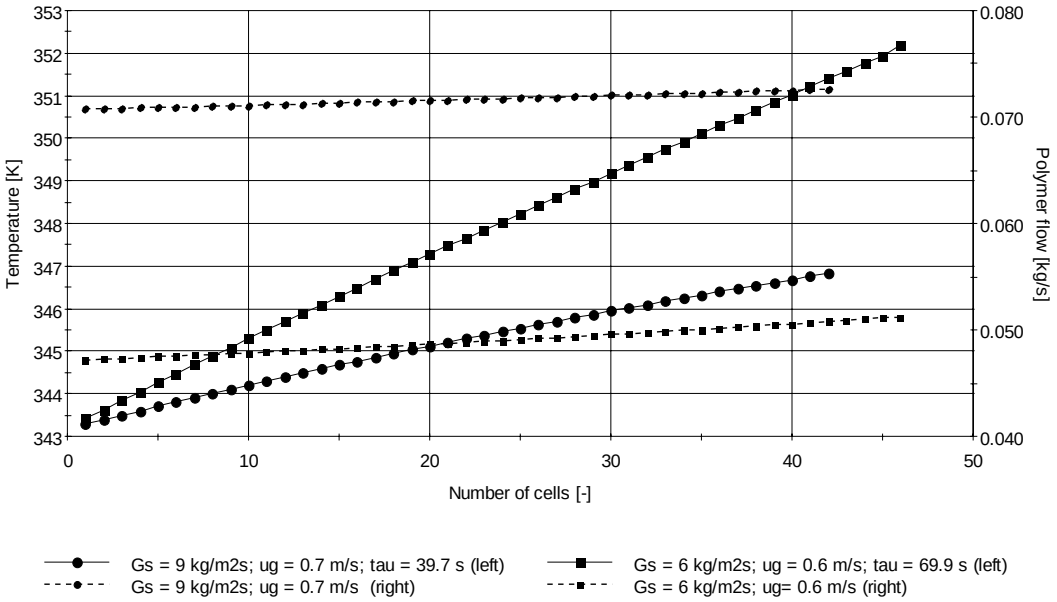

Figure 16: Comparison of simulations 7 and 9 that both have a high Peclet number.
Temperature and polymer flow are compared: •: simulation 7; ■: simulation 9;
___ = temperature; - - - - polymer flow.

Both at low and at high Peclet number it is favorable to keep the gas and solids flow relatively low when using the same amount of catalyst.

When comparing the simulations that are most productive in the well-mixed and in the plug flow systems, simulations 5 and 9, it is visible that the temperature increase is higher in the well-mixed system. The higher overall temperature in the reactor and thus a higher reaction rate might cause this. In the well-mixed system the absolute production is higher, but the residence time is too.
Comparison of the least productive systems (simulations 7 and 10) shows that in the well-mixed system productivity and yield respond more to changes in the gas velocity and solids flux than the plug flow system.

Comparison between simulations 5, 8, 9and 11, all having a high yield but different Peclet numbers, shows that although gas velocity and solids flux can be very different, the yield can be about the same. The production rate can however be very different, as well as the mixing behavior in the riser.
Simulations 5 and 11 have almost the same number of cells, thus also about the same Pe number. Both behave as a relatively well-mixed system. The residence times of the solids and catalyst however are very different: in simulation 5 the residence time is much longer but the added amount of catalyst is much lower than in simulation 11 to reach the same yield. The absolute polymer production in both simulations is approximately the same, around 7 kg/s.
Simulations 8 and 9 also have almost the same number of cells, but the number much higher: respectively 43 and 45. The system behaves much more as plug flow. The absolute production in both simulations is similar and around 4 to 5 kg/s. but the added amount of catalyst in simulation 8 is higher. The respective residence times are 39 and 70 s.

Summarizing the results of these simulations, the absolute production is higher in a more well-mixed system, but the required amounts of catalyst added to get a certain production are lower in a plug flow system. On the other hand, residence times vary more in more well-mixed systems. This makes operation more difficult, since with different residence times the hold up of solids will be very different, however the thermal control of the reactor is relatively easy this way.

3.2.5. Circulating flow

The circulating flow is used to describe the segregation between large and small particles, but since in these simulations an average particle size is chosen, the circulating flow does not

have an effect in that sense. However, the influence of the circulating flow on the back mixing in the system in general can be studied. Although the number of cells determines the mixing behavior in general in the reactor, with the circulating flow fine-tuning can be done. One should keep in mind that the use of both mixing parameters in principal leads to an over-dimensioned system.

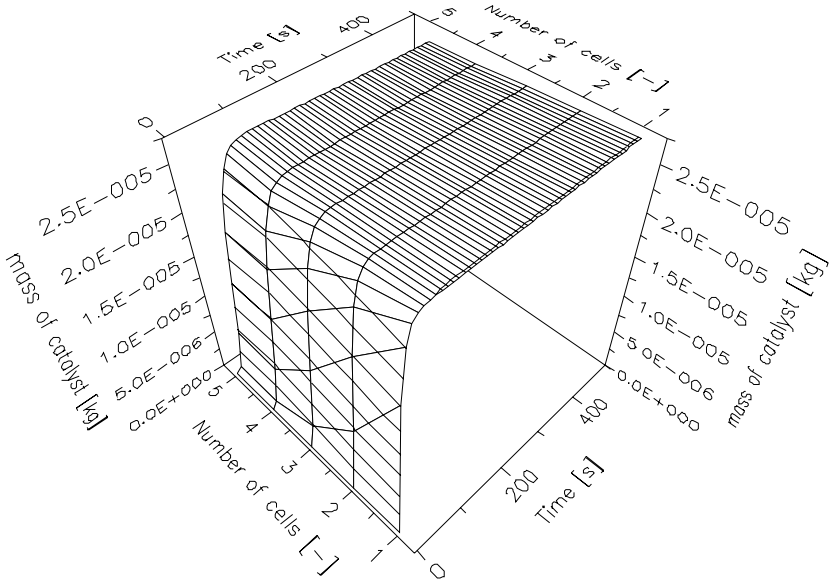

Figure 17: mass of catalyst per cell in simulation 10.

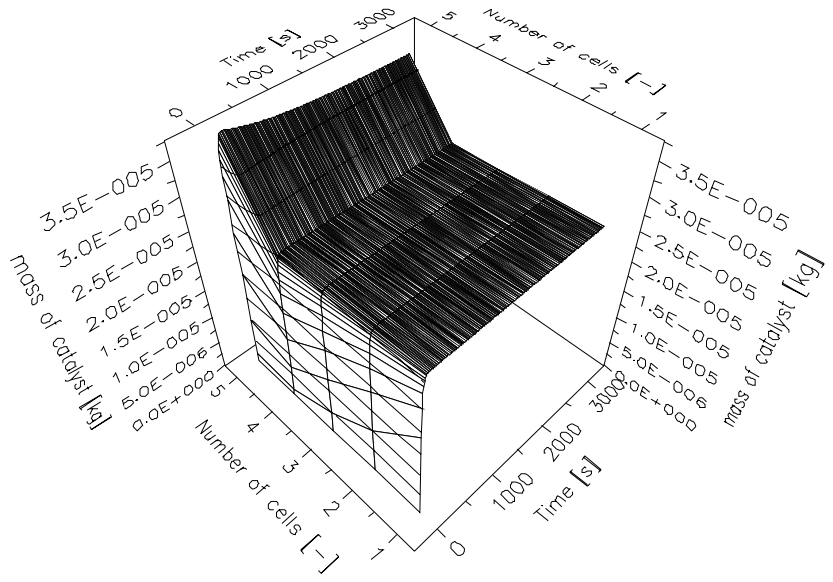

Figure 18: mass of catalyst per cell in simulation 12.

For the comparison simulation 12 was done. This simulation resembled simulation 10, but the circulating flow was half the size of the convective flow (a = 2) instead of one hundredth as in simulation 10 (a = 100). The mass of catalyst visualizes the changes best, since the mass of

catalyst in a cell is influenced by the circulating flows. Comparison of figures 17 and 18 shows that mostly for the last cell the circulating flow has influence. This increase in the mass of catalyst in the last cell is caused by the different description of the mass balance for catalyst in the last cell. The circulating flows can only interact with the before last cell. When powder flows out of cell N, it leaves the riser. In reality the last cell is exposed to exit effects that are dependent on the geometry of the exit.

3.2.6. Hydrogen concentration

From the polymerization model presented in chapter 5 and used in the reactor model it is known that the reaction rate increases with increasing hydrogen concentration to a maximum at a hydrogen mole fraction of 0.0110 and then drops again. The molecular weight is lower at higher hydrogen concentration and drops dramatically in the lower hydrogen concentration range.

Since it is assumed that hydrogen is not consumed, the concentration of hydrogen increases along the length of the riser, because the monomer density gets lower along the length of the riser due to the lower pressure from the bed of powder and some propylene is consumed by polymerization.

In simulation 13 the hydrogen fraction at the inlet is 0.0018. In cell 10 the hydrogen fraction is increased to 0.011. When extra hydrogen is added halfway into the reactor, the polymer molecular weight produced in the higher cells is lower and the average molecular weight drops to an outlet value that is comparable with the molecular weight that is measured afterwards (figure 19). The difference in reaction rate at different hydrogen concentration can also be found back in the calculation of the average molecular weight: the production of polymer with a low molecular weight is higher than the production of high molecular weight. The average at the outlet is closer to the low molecular weight polymer.

Because the reaction rate changes due to the different hydrogen concentration (figure 20), the temperature increase changes and the polymer flow increases more as well. More monomer is consumed, but the monomer is also warmed up and this leads to an expansion of the gas in a cell and thus an increase in the monomer flow. In figure 21 from cells 10 to 11 the monomer flow increases, from cell 12 onwards the higher consumption rate of monomer is visible. The sudden drop in monomer flow in the last cell is not realistic. This is due to the definition of the circulating flows in the last cell. The exit effects are not modeled into detail.

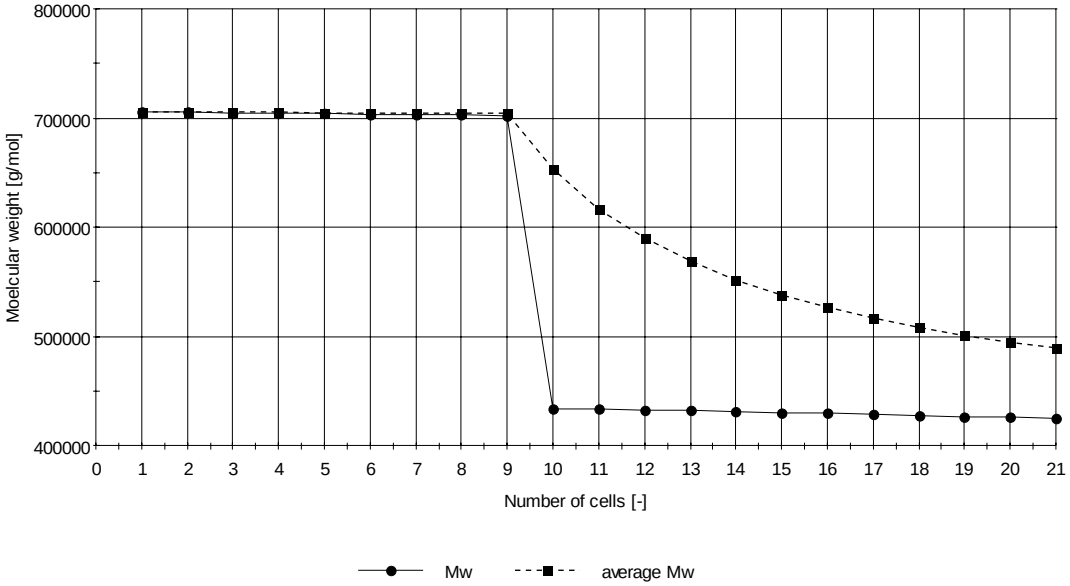

Figure 19: molecular weight per cell and average molecular weight per cell for simulation 13. Addition of extra hydrogen in cell 10 in the reactor. ___ = molecular weight per cell; - - - = average molecular weight

In reality back mixing of gas does exist. Not only can gas mix back in the gas phase, but due to sorption in the polymer particles it is also possible that hydrogen is transported downwards in the reactor by polymer particles being back mixed. No backflow of hydrogen is present in this simulation because back mixing of gas and sorption of hydrogen in the polymer was not programmed in the model.

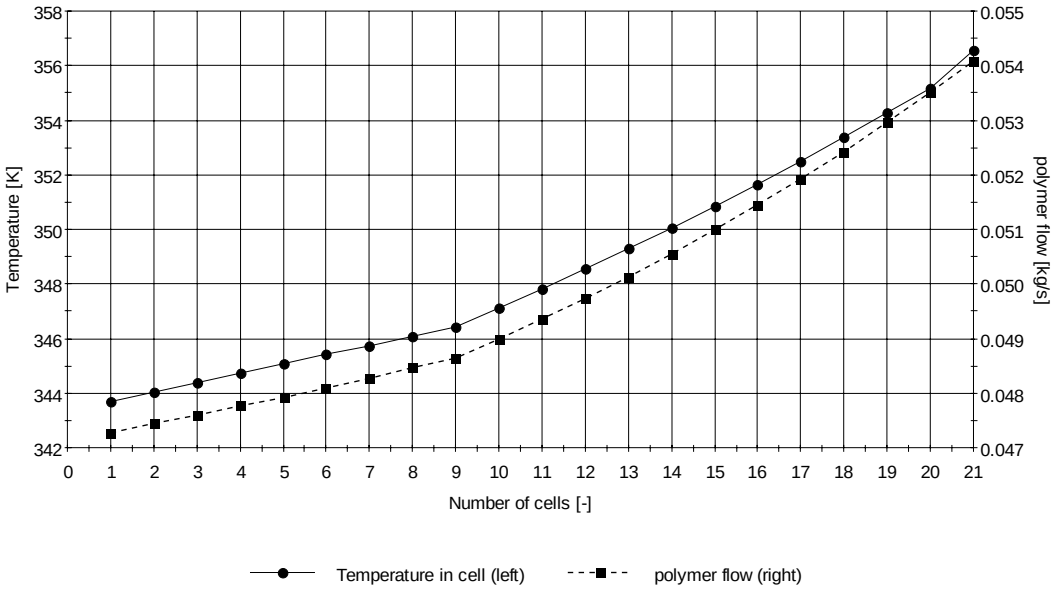

Figure 20: Temperature and polymer flow at 3000 s for simulation 13. At cell 10 extra hydrogen is added. ___ = temperature; - - - = polymer flow.

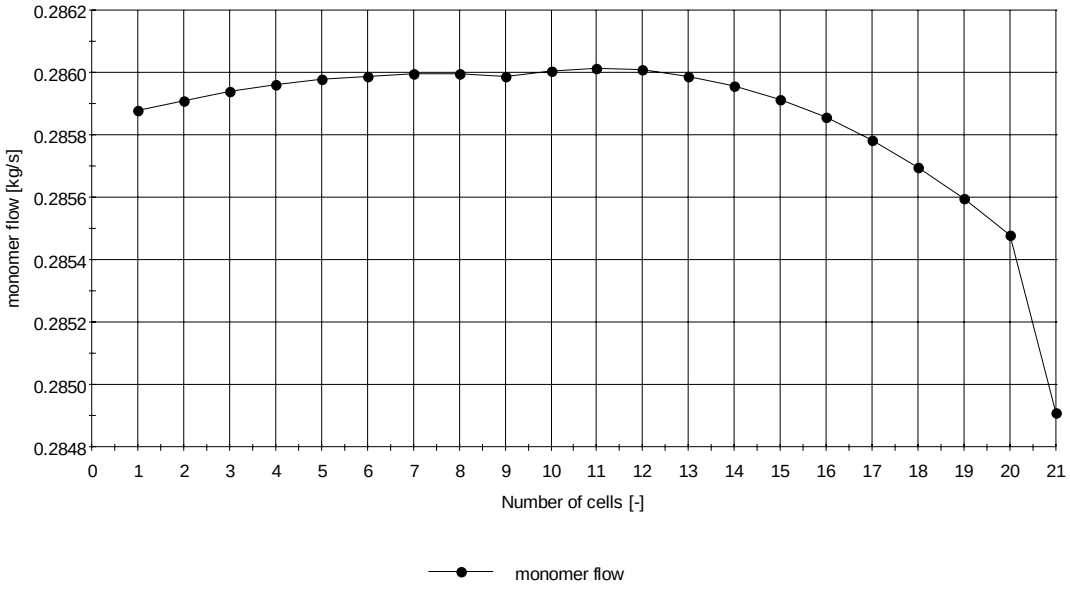

Figure 21: monomer flow at 3000 s in simulation 13.

3.2.7. Influence of the circulating flow

The circulating flow was incorporated in the model to model segregation between small and large particles by having small particles slightly back mixed in the reactor and large particles slightly forward mixed. Particles of average size should not be effected by the circulating flows. Since no distinction is made in the model between particle sizes, the circulating flow is useless in this sense. However, the circulating flow still causes back mixing and forward mixing of solids and catalyst irrespective of particle size. This could lead to an over-dimensioned system in terms of mixing, because the mixing behavior in the riser is basically determined by the number of cells, but for the sake of analysis of the performance of the model this is still done. To analyze these abilities two simulations were done.

The circulating flow is modeled as having the size of a fraction of the convective flow. To study its influence on back mixing of solids and catalyst, extra catalyst addition halfway up the reactor was simulated. With this extra addition the degree of back mixing can be easily visualized. In simulation 14 the size of the circulating flows is $1/100^{th}$, in simulation 15 the size of the circulating flows was half of the size of the convective flow. In both simulations the inlet mass flow of catalyst was 0.1 mg/s, and the addition of catalyst in cell 10 was 2.9 mg/s.

In figure 22 the mass of catalyst is given for both simulations. It is clear that at the higher circulating flow the back mixing of catalyst is much more pronounced. Up to four cells down extra catalyst is found. Also the temperature changes; the temperature increases more in the case of large back mixing. In simulation 15 the temperature rises already in cell 8 and 9 due to the presence of more catalyst and thus more production of polymer in those cells. This increase causes the slightly higher outlet temperature in simulation 15. The trend in the temperature increase in both simulations is the same because the amount of catalyst is about the same.

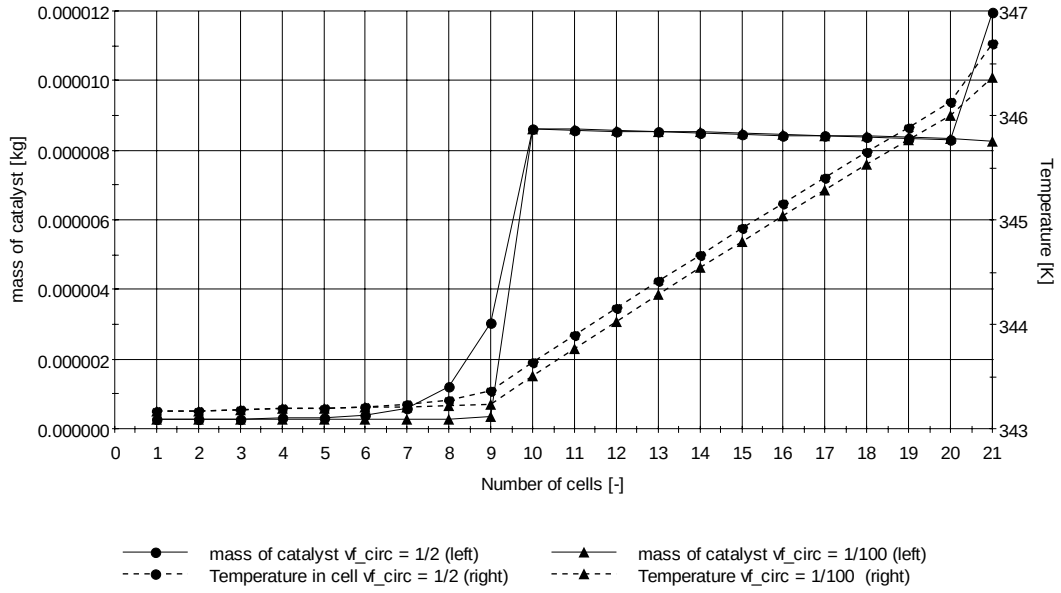

Figure 22: mass of catalyst per cell and temperature per cell at 3000 s. ●: simulation 14;▲: simulation 15; ___ = mass of catalyst; - - - = temperature.

The larger production is visible from the increased polymer flow in simulation 15 (figure 23). The back mixing of catalyst also causes a slightly higher consumption of monomer in the cells below cell 10. The expansion of the monomer flow after cell 10 is primarily caused by expansion of the monomer in the cells and thus a larger outflow of monomer from these cells. Note that the increase in the monomer flow is only approximately 1 g/s. From cell 15 onwards the consumption of monomer is larger than the expansion and the monomer flow decreases again. Exit effects were not modeled in detail and this causes the unrealistic values in the last cell.

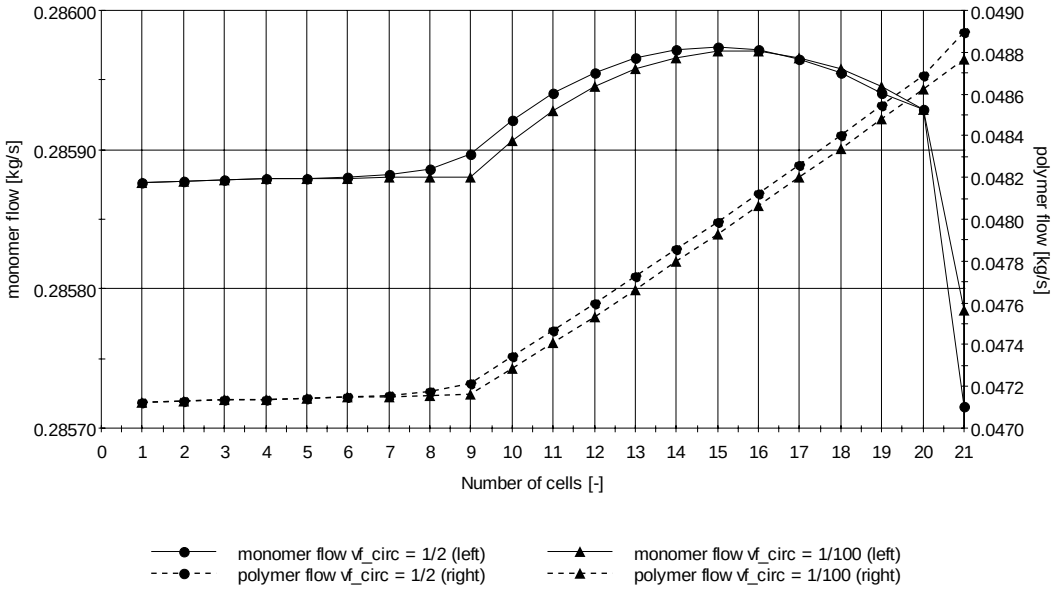

Figure 23: monomer and polymer flow at 3000 s in simulations 14 and 15. ●: simulation 14;▲: simulation 15; ___ = monomer flow; - - - = polymer flow.

4. Discussion

The results of the model are what can be expected. It predicts differences in production due to differences in the mode of operation and temperature profiles tell us more about the production rate along the length of the riser. But this behavior in the riser should be combined with a production of polymer in the downer of the circulating fluidized bed. And that changes circumstances for the production in the riser.

The solids that flow into the riser have a certain molecular weight and contain a certain amount of catalyst in different stages of deactivation due to circulation of the solids and due to possible production of polymer in the downer. This is not simulated in this work. Also the flow of solids cannot be set independently of the production in the riser and the downer as is assumed in the model in this chapter.

The desired production rate and molecular weight of the product in the downer can influence the operation of the riser. For instance in the case of a bimodal product with a certain fixed mass ratio between both polymers in the product the production rate and residence time in the riser and the downer are fixed. The production rate in the downer then directly influences the production in the riser.

These constraints narrow the window of operation for the riser. Knowledge of the possibilities in terms of production and product quality in the riser should be combined with knowledge of

the operational possibilities in the downer to complete a reactor model for the entire circulating fluidized bed.

5. Conclusions

A model was constructed that could describe the polymerization process in the riser of a circulating slugging fluidized bed reactor. Hydrodynamic properties of the slugging fluidization regime analyzed in chapters 2 and 3 and a description of the polymerization of propylene as given in chapter 5 were combined in a cell model to predict polymerization in a polymerization reactor at elevated pressures. The number of cells in the model is a function of the degree of mixing in the reactor and expressed as a function of gas velocity and solids flux.
The model that was constructed could predict the hydrodynamic behavior of the slugging fluidization very well. The polymerization reaction changes due to the changes in hydrodynamic properties. The influence of the gas velocity on the production and on the yield is significant, as well as the influence of the solids flux. At very different mixing patterns in the riser the same production and the same yield could be established with a temperature rise of 10 K.
Changing the size of the circulating flow could influence the degree of back-mixing. Although the system seems to be over-dimensioned, the circulating flows can cause significant back-mixing of the catalyst.
The window of operation with this type of reactor is large. The reactor could be operated as a well-mixed system or as a plug flow system and everything in between. Heat removal can be adjusted easily by changing the gas velocity and solids flux without changing the mixing pattern in the riser. This offers possibilities in applying different production rates.
Interpretation of the model results for a complete riser-downer system must be done carefully. The simulations done in this chapter were only done for a riser with the same size as the cold flow set up described in chapters 2 and 3 and the pilot plant described in chapter 6. Scaling up requires additional information on scaling up parameters. Also the polymerization behavior in the riser should be combined with polymerization in a downer to complete a model of a circulating fluidized bed reactor for olefin polymerization.

6. Notation

a	Constant relating the size of the circulating flow to the convective flow	[-]
A	Cross sectional area of riser	[m^2]
A_h	Heat exchange area of riser	[m^2]
a_ρ	Pressure dependent parameter for density calculation	[-]
b_ρ	Pressure dependent parameter for density calculation	[-]
c_p	Pressure dependent parameter for density calculation	[-]
$C_{p,gas}$	Heat capacity of the gas	[kJ/kgK]
$C_{p,sol}$	Heat capacity of the solids	[kJ/kgK]
c_ρ	Heat capacity of the solids	[kJ/kgK]
D	Diameter of the riser	[m]
g	Acceleration of gravity	[m/s^2]
G_s	Solids flux	[kg/m^2s]
h	Heat exhange coefficient	[W/m^2K]
H_b	Bed height of solids in the riser	[m]
ΔH_r	Reaction heat	[kJ/kg]
$k_{d,cat}(i)$	Deactivation constant for the catalyst	[1/hr]
k_g	Thermal conductivity of the gas	[W/mK]
$k_p(i)$	Propagation constant for polymerization reaction	[$m^3/g_{cat}hr$]
L_l	Laminar flow length scale	[m]
L_{tube}	Length of the riser tube	[m]
$m_{cat}(i)$	Mass of catalyst in cell i	[kg]
$\dot{m}_{circ}$	Circulating mass flow	[kg/s]
$m_{mon,g}(i)$	Mass of monomer in cell i	[kg]
$\dot{m}_{mon,g}(i)$	Mass flow of monomer from cell i	[kg/s]
$m_{pol}(i)$	Mass of polymer in cell o	[kg]
$\dot{m}_{pol}(i)$	Mass flow of polymer from cell i	[kg/s]
m_{sol}	Mass of solids in the riser	[kg]
$\dot{m}_{sol}(i)$	Mass flow of solids from cell i	[kg/s]
$p(i)$	Pressure in cell i	[bar]

p_{input}	Pressure setpoint	[bar]
Pe	Peclet number	[-]
Pr	Prandtl number	[-]
$R_p(i)$	Reaction rate of polymerization reaction in cell i	[kg/s]
$T_{cell}(i)$	Temperature in cell i	[K]
u	Gas velocity	[m/s]
U	Heat exchange coefficient	[W/m^{2}K]
u_g	Gas velocity	[m/s]
u_{mf}	Minimum fluidization velocity	[m/s]
V_{cell}	Volume of cell	[m^3]
$\dot{v}_{circ}$	Volumetric circulating flow	[m^3/s]
V_r	Reactor volume	[m^3]
$X_{H2}(i)$	Hydrogen fraction	[-]
$y_{cat}(i)$	Fraction of catalyst	[-]
$\alpha(i)$	Constant representing degree of sorption	[-]
ε_{mf}	Porosity at minimum fluidization	[-]
μ	Viscosity	[Pa.s]
ρ_{bulk}	Bulk density	[kg/m^3]
$\rho_{g,calc}(i)$	Calculated gas density in cell i	[kg/m^3]
ρ_p	Particle density	[kg/m^3]
τ	Residence time	[s]

7. Literature

Al-haj Ali, M., Roffel, B., Weickert, G. (2005). “Liquid-pool polymerization of propylene in a full-filled reactor with a highly active Ziegler-Natta catalyst. II. Determination of kinetic constants” *to be published*

Molerus, O., Wirth, K.-E. (1997). Heat transfer in fluidized beds, Chapman & Hall, London

Dankwoord

Mijn promotie begon met het in de gang tegen Günter Weickert oplopen die vervolgens zei: “He, je bent er weer eens ! Hoe gaat het bij de luchtmacht ? Vlieg je al ?” Waarop ik moest antwoorden dat ik niet vloog, omdat ik net de week daarvoor besloten had dat dat toch niet iets voor mij was.

Op dat moment sloop ik door de gangen van het CT-gebouw op weg naar een vriendin, in de hoop Günter te ontlopen. Ik had namelijk al tijdens mijn afstudeeropdracht interesse in promoveren, maar was tegelijkertijd bezig met de keuring voor de luchtmacht. Toen ik goedgekeurd bleek te zijn had ik het aanbod voor een promotieopdracht afgeslagen maar dat was niet lang meer voor de opdracht zou beginnen en ik was in de veronderstelling dat Günter daar kwaad over zou zijn.

Dat bleek niet zo te zijn. Sterker nog, zijn volgende vraag was: “Enne, promoveren ?” waarop ik nog een middag heb nagedacht. De volgende dag belde ik op en binnen twee weken was ik begonnen als AIO. En tot mijn grote genoegen. Ik heb mij tijdens mijn promotie als een vis in het water gevoeld. Goed de tijd hebben om zaken uit te denken, te bediscussiëren, je interesses te volgen en uiteindelijk met een mooi resultaat te komen. Ik had een brede opdracht met veel afwisseling en dat is mij wel op het lijf geschreven.

Ik wil Günter dan ook bijzonder bedanken voor de geboden mogelijkheid om dit werk te kunnen doen en voor de vele discussies over problemen en oplossingen. Zijn aanstekelijke passie voor het vak en de geestdrift waarmee hij te werk ging gaven het vak een extra glans. Ook heb ik een deel van zijn stijl van denken overgenomen: snel iets kunnen uitrekenen of inschatten hoe het wordt en altijd blijven denken dat er een oplossing is. Ik hoor hem nog zeggen (met een Duits accent) dat je een ingenieur bent en dat ingenieurs dat en dat moeten kunnen. Dank u wel !

Verder heb ik natuurlijk al dat werk niet helemaal alleen gedaan. In het Hoge Druk Laboratorium heb ik altijd de hulp gehad van de technici, zowel voor technische zaken als voor deskundig advies over hoe ik mijn kapsel zou moeten veranderen. In het HDL heb ik gebruik gemaakt van 3 verschillende opstellingen: de cold flow opstelling waar Geert Monnink mij bij hielp, de autoclaaf opstelling in Box 2, waar Karst van Bree mij bij hielp en Rob Emonds voor ons de experimenten uitvoerde. De circulerend gefluidiseerd bed opstelling in Box 9 is uitgedacht door Karst, Fred ter Borg en Gert Banis en gebouwd door Karst. Bij Fred kon ik altijd aankloppen voor elektronische zaken en hij heeft onder anderen de detectoren uitgedacht die gebruikt zijn bij de cold flow opstelling. Bedankt voor alle hulp en de gezelligheid !

Naast technici hebben een aantal afstudeerders mij geholpen met het meer inhoudelijke en experimentele werk middels doctoraal opdrachten. Bas Kooij heeft mij geholpen met het pionierwerk in de cold flow opstelling. Zijn handigheid en praktisch inzicht maakten dat we een goede start konden maken met het onderzoek naar fluidisatiegedrag. Anne Peter Lindeboom heeft het ondanks zijn uitgesproken afkeer ervan het meeste ‘domme handwerk’ voor mij gedaan voor de cold flow opstelling: de vele metingen met gekleurde tracerdeeltjes, het in elkaar zetten van de detectoren en vele van de metingen aan plugs en slugs met deze detectoren. Robin Bouwman heeft de opstelling omgebouwd van 5 cm diameter naar 10 cm diameter en vervolgens daar vergelijkende metingen uitgevoerd. Ook is hij serieus begonnen met denkwerk over hoe dit fluidisatiegedrag te modelleren. Jos Frusch heeft als laatste afstudeerder op de cold flow opstelling gekeken naar vallende deeltjes en heeft verschillende gassen door de opstelling heen gejaagd. Daarnaast ben ik met hem begonnen aan een hydrodynamica model dat u echter helaas niet in dit werk kunt terugvinden.
Muriel Heijnen heeft mij geholpen bij het zoeken en testen van een geschikte katalysator en daarna het vaststellen van een experimenteel recept. Vele experimenten zijn gedaan waarbij in meerdere of mindere mate plastic is gemaakt. Haar werk heeft het mogelijk gemaakt dat Rob Senden een experimenteel programma kon uitvoeren waar uiteindelijk het waterstof respons model uit is gekomen dat u in hoofdstuk 5 kunt lezen. Al deze

studenten wil ik hartelijk bedanken voor hun werk en voor het plezier tijdens het werk en in de pauzes.

Voor het meer inhoudelijke werk en het werk aan het modelleren van fluidisatie gedrag heb ik vele discussies gevoerd met Martin van Sint Annaland. Een deel van de inzichten die hier uit naar voren zijn gekomen zijn verwerkt in het reactormodel dat u kunt vinden in hoofdstuk 7. Helaas is er in een promotiewerk geen ruimte om twee grote onderwerpen tot op het bot uit te zoeken, want de interessante discussies met Martin waren meer uitwerking in de richting van beschrijving van fluidisatiegedrag zeker waard geweest.

Voor bestellingen, gezelligheid in mijn eerste jaar op de begane grond en hulp met zaken waar ik weinig verstand van had kon ik rekenen op de mensen van het TechnoCenter CT. Wim Platvoet, Nelly Voss en Ineke Klinkenberg waren altijd aanspreekbaar over zaken die besteld waren of moesten worden, en de mensen van SGA waaronder Joachim, Jan en Guilbert hadden genoeg geduld om steeds weer mijn vragen te beantwoorden en mij te helpen als ik weer eens ruzie had met mijn computer.

Verder heb ik met diverse mensen binnen de faculteit van tijd tot tijd discussies gehad over meer of mindere serieuze zaken. Aangezien ik graag met mensen praat zijn dat er veel en ik zou al deze mensen hartelijk willen bedanken voor hun bereidheid met mij te praten over allerlei inhoudelijke moeilijkheden in mijn promotie.

Voor de niet-inhoudelijke discussies die echter wel interessant waren, en voor het nodige administratieve werk wil ik Wies Elfers en Yvonne Bruggert graag bedanken. Het was altijd moeilijk om me weer los te trekken van het secretariaat als mijn mok leeg was na de koffiepauze. Het wel en wee van de faculteit, van jullie en van de wereld in het algemeen zal ik nooit vergeten. Ook de luisterende oren en geruststellende woorden die er altijd waren als ik mij weer eens ergens druk over maakte zal ik onthouden.

De verschillende leden van de vakgroep Industriële Polymerisatie Processen hebben mij erg geholpen en voor vele vruchtbare discussies gezorgd. Ook mijn kijk op de wereld en

het gevoel wereldburger te zijn heb ik aan hen te danken. Makarand, Ravi, Parasu, Shankara, Yahya, Mohammed, Michiel, Gerben en Jochem en alle anderen, dank jullie wel voor de goede tijd. Thank you for the good times we had !

De paranimfen Nathalie en Muriel hebben voor leuke maar ook vermoeiende winkeldagen gezorgd. Helaas was het vinden van geschikte kleding niet gelukt, maar we hebben wel grote delen van commercieel Amsterdam en Amersfoort gezien. Verder bedank ik hen voor de bereidheid paranimfen te zijn. Ik kwam er echter pas achter wat paranimfen eigenlijk geacht worden te doen toen ik mijn concept al ingeleverd had en ik mijn promotiedag ongeveer al geheel had geregeld. Maar toch, bedankt voor het paranimf willen zijn !

Ik wil bij deze graag ook mijn ouders, familie en vrienden bedanken voor de getoonde interesse en steun. Ook als het soms onbegrijpelijk was waar ik mee bezig was, deden jullie toch je best om op de hoogte te blijven van wat ik nu eigenlijk deed. En als laatste wil ik Bart bedanken voor zijn niet aflatende steun en begrip in de afgelopen jaren.

Inge

Levensloop

Inge van Putten werd op 6 januari 1975 geboren in Medemblik. Na de lagere school op ’t Vierkantje heeft ze in 1993 haar VWO diploma gehaald aan de R.S.G. Wiringherlant te Wieringerwerf. In augustus van dat jaar begon ze aan de studie Chemische Technologie aan de Universiteit Twente. In het tweede jaar besloot ze de richting Informatica binnen de Chemische Technologie te volgen. Tijdens deze studie liep ze stage bij Purac Biochem BV in Gorinchem. In februari 1999 sloot ze haar studie af met een opdracht binnen de vakgroep Industriële Processen en Producten om een opstelling voor onderzoek naar kinetiek van olefine polmerisaties in het Hoge druk Lab te automatiseren.

Na een korte uitstap naar de officiersopleiding van de Koninklijke Luchtmacht begon Inge in november 1999 als assistent in opleiding in de vakgroep Industriële Polymerisatie Processen. Ze verrichtte onder leiding van professor Weickert en in samenwerking met het Dutch Polymer Institute het onderzoek dat in dit proefschrift staat beschreven.

Vanaf 1 juli 2004 werkt Inge bij Sabic EuroPetrochemicals in Geleen.